Eidgenössische Technische Hochschule Zürich
Swiss Federal Institute of Technology Zurich

Design and Implementation of Multi-sensory Fabric as Deformable Musical Interface

by

Irmandy Wicaksono

B.Eng. Electronic Engineering, University of Southampton (2014)

Submitted to the Department of Electrical Engineering and Information Technology,
in partial fulfilment of the requirements for the degree of

Master of Science in Electrical Engineering and Information Technology
Areas of Specialisation: Electronics and Photonics

at the

EIDGENÖSSISCHE TECHNISCHE HOCHSCHULE ZÜRICH
SWISS FEDERAL INSTITUTE OF TECHNOLOGY ZURICH

November 2016

Certified by,

signature redacted

Prof. Joseph A. Paradiso
Alexander W. Dreyfoos (1954) Professor, Media Arts and Sciences
Responsive Environments, Media Laboratory, MIT

Accepted by,

signature redacted

Prof. Gerhard Tröster
Professor, Department of Electrical Engineering and Information Technology
Wearable Computing, D-ITET, ETH Zurich

The following person served as a reader of this thesis,

signature redacted

Nan-Wei Gong, PhD
Research Affiliate
Responsive Environments, Media Laboratory, MIT

Abstract

This work presents *StretchyKeyboard*: a multi-modal fabric sensate surface as a deformable musical interface. Multi-layer fabric sensors that detect touch, proximity, electric field, pressure, and stretch were machine-sewn in a keyboard pattern on a stretchable substrate. The result is a fabric-based musical controller that combines both the discrete control of a keyboard and various continuous controls from the fabric sensors. This enables new tactile experiences and novel interactions both with physical and non-contact gestures: physical by pressing, pulling, stretching, and twisting the fabric and non-physical by hovering and waving towards/against the keyboard and a field source. We also developed other fabric interfaces such as ribbon-controller and trackpad allowing performer to add more expressive, position sensing controls. The multi-modal fabric sensate surface demonstrates an effort towards seamless, self-aware, and washable media.

Supervisor

Prof. Joseph A Paradiso, Responsive Environments, MIT Media Lab

Co-supervisor

Prof. Gerhard Tröster, Wearable Computing Lab, ETH Zürich

Thesis Reader

Dr. Nan-Wei Gong, Responsive Environments, MIT Media Lab


The Perfect Gift Idea!
Surprise and delight the organists and pianists on your gift list with this Super-Size Keyboard© Scarf. This 6-foot 88-note keyboard is precision knit in beautiful black and white acrylic and trimmed with an attractive black fringe. The scarf is warm, soft and lots of fun to wear! Never out of fashion, this novel gift is sure to make a big hit with that special musician.
Just $19.95 plus $1.50 for shipping and handling. Order an extra one for yourself, and we'll ship them both for free! Money back guarantee of satisfaction.
Clip and send this coupon with your check or money order to Catalog Music Supply, P.O. Box 641 Wayne, New Jersey 07470.
☐ Send me one scarf for $19.95 plus $1.50 shipping and handling.
☐ I want one too! Send me two scarves for just $39.90!
Name
Address
City/State/Zip
Please allow 2-4 weeks delivery.
NJ residents please add 6% sales tax.
AB-09-87

Acknowledgments

In this opportunity, I would like to sincerely thank Prof. Joe Paradiso for giving me the opportunity to be a part of Responsive Environments, for his continuous support, guidance, and patience. Electronics and Music have always been the two, separate, big chunks of my life; I could barely find the connections between them, until I met Prof. Joe. His admirable attitude and his work have inspired me and changed my perspectives about what's possible and the future. Media Lab is such an interesting place. These past six months, have definitely been the most challenging and enjoyable time throughout my academic journey -- I've never thought that I'd be able to make my own musical controller!

I would also like to express my gratitude to Prof. Gerhard Tröster. For inspiring me with his visions, motivating me to pursue them, and shaping me with his teachings. I gained a lot of knowledge and insights from his lectures and my time at the Wearable Computing Lab, and I am very thankful for that.

Thank you to Dr. Nan-Wei Gong for spending her time in reading my thesis and for the initial discussions of this project, to John DiFrancesco and Sam Calisch from Centre of Bits and Atoms for the help with laser cutting and Instron, to Amna and Keira for making everything possible, and to the Zeno Karl Schindler Foundation for supporting me throughout my time here at MIT.

To Responsive Environments crew, thank you for being the superstars, for being kind and supportive from the first day, for all of the deep conversations, for making it feels right, for everything.

To all my new and old friends that I've met these past two years of my Master study, either at ETH, KAUST, or MIT, either in Zurich, Jeddah, Boston, or back home, you guys have made me realize how tiny this world is, encouraging me to further explore it, and that there is no such thing as goodbye. Finally, to my family and my girlfriend, thank you for being patience, for always understanding me, and believing in me. I miss you and I'll see you soon.

I would like to end my thesis by quoting my favourite writer, who reminds me to always look forward to the future, to always imagine all of the possibilities. Looking back, I'd never have thought that the textiles I was seeing back then could be the textiles that I am seeing today.

> "And above all, watch with glittering eyes the whole world around you because the greatest secrets are always hidden in the most unlikely places. Those who don't believe in magic will never find it."
>
> **Roald Dahl (1991)** ***The Minpins***

Irmandy Wicaksono
Cambridge, MA 27/11/2016

Contents

List of Figures

List of Tables

List of Abbreviations

AC	Alternate Current
ADC	Analog Digital Converter
BLE	Bluetooth Low Energy
BPF	Band Pass Filter
CAD	Computer Aided Design
CC	Control Change
CLR	Carbon Loaded Rubber
CVD	Chemical Vapour Deposition
DIY	Do-it Yourself
DMI	Digital Musical Interface
EMI	Electromagnetic Interference
FFC	Flat Flexible Connector
FSR	Force-sensing Resistor
GUI	Graphical User Interface
HCI	Human-Computer Interaction
I2C	Inter-Integrated Circuit
IC	Integrated Circuit
IPA	Isopropanol
MIDI	Musical Instrument Digital Interface
OSC	Open Sound Control
PCB	Printed Circuit Board
PD	Pure Data
PDMS	Polydimethylsiloxane
PPy	Polypyrrole
PS	Polystyrene
PVA	Polyvinyl Alcohol
PVDF	Polyvinylidene Fluoride
PZT	Lead Zirconate Titanate
Q	Quality Factor
RRAM	Resistive Random-access Memory
UART	Universal Asynchronous Receiver Transmitter
USB	Universal Serial Bus

Chapter 1:
Introduction

Around the 90s, when miniaturized electronic systems were well-advanced, evoking the start of wearable computing era, there were several explorations to develop novel instruments for musical expression using smart-textiles and surfaces. Specific examples of works involving these include the Media Lab's Musical Jacket, Embroidered Musical Ball, and Magic Carpet that respectively utilize conductive threads, pressure sensors, and piezoelectric wires to detect gestural inputs such as touches, squeezes or pressure, and positions [1,2]. The development of smart-textile materials and integration also resulted in Imogen Heap's Musical Gloves [3], Zstretch, a stretchy fabric musical controller [4], and other works involving multi-touch and pressure sensing for fabric-based musical controllers [5]. There has also been a tremendous amount of work done on using diverse sensors as keyboard inputs or to complement it either to record and recreate performance [6], improve the performance of piano player by providing feedback, augment acoustic instruments [7], or give a more expressive control of sound to each key by adding continuous controls or transforming the keyboard's surface as demonstrated recently by TouchKeys and Seaboard, respectively [8,9].

Pianos and keyboards are one of the most prominent musical instruments that most people play, particularly when it comes to performing and composing music. Inspired by electronic textiles, we envision a fully-stitched keyboard with fabric-based multi-sensory control in a stretchable surface. This will allow keyboardist to not only play and compose music in a physically novel and deformable instrument, but also experience a new dimension of sound synthesis by applying different gestural inputs such as pressing, pulling, squeezing, stretching, and twisting. A keyboard and synthesizer controller made out of fabric, besides being a very unique musical instrument, it can be worn and easily folded and rolled up and packed in luggage like a pair of socks or a scarf [10]. To our knowledge, there has not been an interesting keyboard made out of a fabric yet. Japanese textile maker Gunze has just released a textile piano this year; however, the keys only work as a touch input [11]. In this thesis, we will start by initially looking into the past and current keyboard instruments and electronic musical controllers as well as the state-of-the-art smart textile materials and integrations before presenting our contribution (Chapter 2). We will then propose the multi-sensory fabric keyboard design and briefly go through its development process (Chapter 3).

We will also look deeper into the design and characterization of each fabric sensor modality (Chapter 4) and its corresponding circuitry (Chapter 5). After that, we will cover several approaches in interfacing sensor data to a computer and map them into sound (Chapter 6). At the end, we will propose several interaction possibilities and evaluate the performance of this fabric controller quantitative and qualitatively (Chapter 7). The development of this multi-sensate fabric surface is relevant not only for novel and expressive musical controllers, but also for other physical interaction media involving smart objects or surfaces.

Chapter 2:
Background Research and Related Work

2.1 Keyboard Instruments: from Acoustical to Digital

The keyboard is one of the most prominent musical instruments. Its interface has become standardized in today's musical controllers, as it is easy to use it to control acoustic or mechanical sound. Some of the earliest acoustic instruments involving keyboards are pipe-organ, harpsichord and clavichord. At that time, the plucks or hammers in these instruments could only emit sound in only one volume. Briefly after that, around the 1700s, pianoforte, a new style of acoustical instrument that can play note softly and loudly by hammering of a string depending on key force was introduced. Piano then became one of the most enduring instruments ever because of its expressive controls and rich sounds, creating emotional experience to both performers and audience. Overtime, features and modifications to the piano such as felt hammers, sound boards, and pedals, gave an even more expressive control to it.

As time went by and technology rapidly advanced, new keyboard instruments involving electrical components started to appear around the early 20th century. These include many keyboards to control electronic sound, such as Elisha Gray's Musical Telegraph (1876), Thaddeus Cahill's Massive Telharmonium (1906), and Lee DeForest's Audion (1915) which were built from self-oscillating reeds, dynamo wheels, and heterodyne oscillators respectively [81]. After that, the electric piano, which is a type of hybrid acoustical-electrical instruments, was introduced around the 30s. In this instrument, the vibrations generated by the hammer-strike are converted into electrical signals and fed to circuits with amplifiers and loudspeakers.

In the 60s, when integrated circuits were well miniaturized and commercialized, analog synthesizers such as the *Minimoog s*tarted to flood the market with its expressive capability to generate and manipulate sound with an electronic keyboard and an array of switches, sliders, and knobs. Further growths in transistor shrinkage and performance, along with the deployment of MIDI standard steadily substituted the sound processing from purely analog to digital. The big musical instrument companies began to develop integrated systems with sound-cards to perform sound recording and processing with built-in software, substituting the role of analogue circuitry in the old-time synthesizer; however, the keyboard still stood there as the main interface [12].

As the commercial computers and even embedded processors now have sufficient processing power, sound generation and manipulation can easily be done digitally through audio synthesis environments pioneered by Max Matthews in Bell Labs. This shift in the sound synthesis paradigm allowed people to synthesise any sound, generate any sequence, *et cetera* but with the static computer GUI, expression controls especially in live performance, could be limited and cumbersome [13]. This is where the interfacing involves, to bridge the gap between the physical (gestures) and digital component (sound) of electronic music. This chapter will cover the past development of electronic musical controllers involving keyboards and the state-of-the-art research in integrating these instruments with various sensing capabilities to add a new dimension of expressiveness and functionality. We will also look into modern electronic musical controllers and their design principles.

2.1.1 Early Electronic Musical Controllers

The Theremin (1920) is one of the earliest electronic musical controllers. This instrument works by using sensing antennas that can modulate oscillator's base frequency and amplitude based on electric field coupling as the performer's hand moving around the antenna. Even though is hard to master, the free-hand movements in this instrument provide boundless possibilities of continuous sound production and control capability to the performers, inspiring the developments of new and expressive electronic musical controllers until today. Paradiso reviewed different types of electronic musical controllers from keyboards, wind, to non-contact interfaces [13]. Focusing on keyboard controllers, Hugh Le Caine's Electronic Sackbut (1940) is a great example of early expressive keyboard instrument. It allows performers to play notes using right hand with the pressure-sensitive keys; its lateral and vertical pressure correspond to pitch and volume respectively. The left-hand controls, comprising movable pads as shown in Figure 2.1 below, can be expressively controlled to modulate the source waveforms in different ways thus changing the timbre of the sound. This illustrates the concept of "left-hand controller", which is a set of knobs, sliders, touchpads, joysticks, and others, normally positioned to the left of the keyboard, which the performer can use to articulate produced sound.

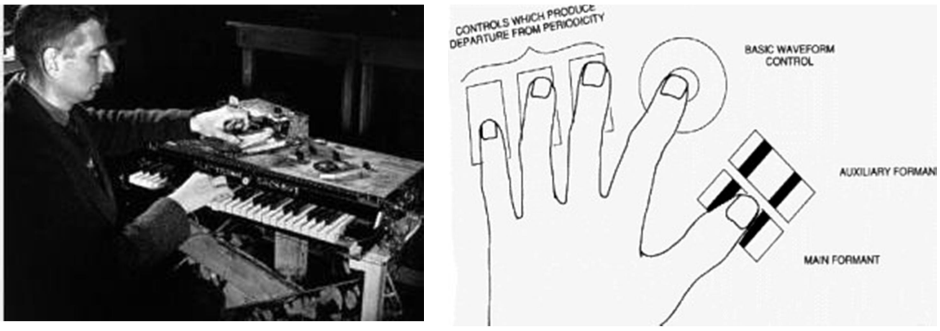

(a) (b)

Figure 2.1: Hugh Le Caine playing the Electronic Sackbut (a) and expressive left hand controls (b, reprinted [14])

In 1928, Maurice Martenot invented his own instrument, 'the Ondes Martenot' inspired by Theremin's work; the instrument also experienced multiple reconstructions through its time. As shown in Figure 2.2a below, the performer wears a ring that pulls a string to vary the pitch or vibrato of a sound continuously. The left hand pedal is used to control the volume. There is also an option to use the keyboard for discrete controls of pitch. The latter version (1940) allows additional lateral movement of the keyboard in millimeters for vibrato effects [15]. These keyboards and others that appeared around the same time however are monophonic, with the exception of electronic organs on early synthesizers, such as Gemsback's Pianorad and Bode's Organ [81]. Then, several decades after, polyphonic keyboards and synthesizers started to become common in the 70s. Another novel keyboard instrument is shown in Figure 2.2b. The Key Concepts Note Bender (1978) incorporates a longitudinal (back and forward) key displacement. The very first application of this displacement was to change colour of overall tone. After several improvements, the last prototype as shown in the figure could modulate the pitch of each key independently.

(a) (b)

Figure 2.2: a) Ondes Martenot with sliding ring
b) The Key Concepts Note Bender (reprinted [15,16])

Other electronic keyboards involve capacitive sensing techniques. Capacitive contact sensing has been embedded in synthesizers such as in EMS Sythin AKS or EDP Wasp from the early 70s [82]. Other influential examples are Buchla's Thunder and Moog's Multiply-Touch Sensitive Keyboards (1990) [7,13]. The thunder percussive controller consists of touch plates that can detect velocity, position, and pressure whereas Moog's MTS Keyboards were integrated with a new layer of sensors on the keyboard to detect finger gestures in X and Y with four corner-points current sensing as well as the Z or vertical position of the key by coupling a surface layer with a bottom aluminium layer. Furthermore, a force-sensor with resistive film is also combined in the design to measure pressure profile. Instead of turning knobs and sliders in synthesizers, these controllers allow expressive and fluid controls of the pitch and timbre of the sound generated by applying different gestural inputs right on the keyboard.

2.1.2 Integration of Discrete and Continuous Controls

After the development of Moog's MTS Keyboards, several new pieces of research emerged to incorporate continuous controls in a keyboard either by augmenting it or developing a slightly new interface. Using a capacitive multi-touch sensing PCB on every key's surface, TouchKeys allows performers to map their two dimensional finger positions and contact area to any sound parameter using the MIDI or OSC protocol [9]. Instead of using a capacitive technique, Grosshauser and Tröster designed a flexible PCB with a matrix of FSR to measure pressure and position of a finger on each key. This provides a technique to evaluate and possibly extend the performance of the player [8].

Haken *et al.* presented The Continuum [17]. An indiscrete keyboard controller that measures the X,Y positions and Z pressure of a finger on flat continuous surface and is able to accommodate up to ten simultaneous notes. The design of this instrument has evolved, from using a polarized light source to detect fingers with CCD camera, applying a thick carbon fibers rubber sheet that changes its impedance when compressed, to sensing proximity of magnets with hall-effect sensors. The instrument can control vibrato, tremolo, and timbre of notes by sliding and pressing our fingers in different directions across the sensing surface and is shown below in Figure 2.3.

Figure 2.3: Haken Continuum Fingerboard (reprinted [17])

Lamb and Robertson's Seaboard works similarly as the Continuum, but instead of an entirely flat surface, they designed a wavy keyboard pattern with silicone as a base, giving the surface an unique tactile feeling to touch, press, and slides [10]. By using this haptic pattern, unlike the Continuum, the discrete and continuous controls of the board can be physically and visually distinguished enabling a more accurate control of performance. All of the finger movements are sensed by a matrix of FSRs at the bottom of the silicone. Other efforts have also been made to design a microtonal keyboard to gain a greater control of pitch. One example, such as Snyderphonic Manta, is inspired by Buchla's Thunder and consists of 48 velocity-sensitive capacitive touch sensors in a hexagonal grid with two additional capacitive sliders [18].

2.1.3 Flexible and Deformable Musical Interface

The vast development of smart materials and sensor technologies has prompted a broad range of new interfaces for musical expressions, especially in flexible and deformable controllers as shown in Figure 2.4 below. The MIT Media Lab's Musical Jacket for example, consists of embroidered conductive threads that form a capacitive touch surface. These capacitive sensors are connected to a MIDI synthesizer. The Embroidered Ball, on the other hand, measures pressure exerted between the embroidered electrodes and grounds to produce particular sound [1]. Zstretch is a fabric with sewn stretch sensors on each side of to control sound parameters, such as tempo, volume, and speed by stretching [5] while the sonic banana is a MIDI instrument embedded and integrated with bend sensors and pushbuttons proposing new expressive gestures such as bending and twisting [19].

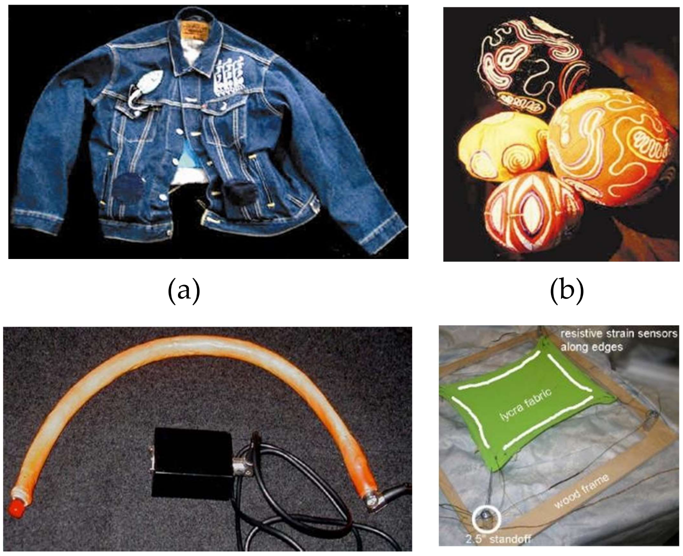

(a) (b) (c) (d)

Figure 2.4: a) The Musical Jacket b) Embroidered Musical Ball c) Sonic Banana d) Zstretch (reprinted [1,5,19])

Another soft instrument that is popular and still being refined until now is a musical glove, as it is very expressive and suitable for live performances. An early custom musical glove is Laetitia Sonami's "Lady's Glove" (1994) made at STEIM [20]. As new sensors are developed, especially in textile-forms, current musical glove is made out of fabric bend sensors with accelerometer sewn on top [35]. Most of the fabric interfaces mentioned here however are mostly played to shape or control sound; not many have capabilities of producing discrete sound like keyboard controllers.

2.1.4 Electronic Instrument Design and Parameter Mapping

The principle of electronic or digital instrument design is illustrated in Figure 2.5 below. For the inputs, Bongers classifies sensors for musical interfaces based on human output modalities that can be categorized as muscle action, blowing, voice, and others (blood pressure, heart rate, temperature, et cetera) [21]. In this work, we are interested in using muscle actuation as our inputs. This will involve isometric (pressure) and movement (both contact and contactless) sensors. The primary feedback is based on our physical interaction with the controller, such as the noise and tactile feedback we get from interacting with the instrument, while the secondary feedback is the sound and other features (such as visual, haptics) triggered and generated by the instrument. There is an interface gap between the controller and the sound processing component. This is the mapping layer between gesture and produced sound, taking a set of rules and transforms done by a processor or host computer to which the controller is attached.

Parameter mapping in instrument design is an important subject in music research, especially since it gives an instrument its own identity and influences how it should be played. There are several ways to approach this. One can use machine learning tools as a way to map certain parameters to a required output or another way, to explicitly define the parameters [12]. These decisions are mostly based on the performer's intention. As much as it has been a great research interest, it is however, still a mystery to generally evaluate what makes a good musical interface or mapping besides the qualitative, feeling of enjoyment (emotionally – expression and physically – feel) when playing it. It can be observed however, that the most successful electronic instruments, the ones that have gained popularity such as keyboard and electric guitar, mostly adapt their mappings from existing acoustic instruments.

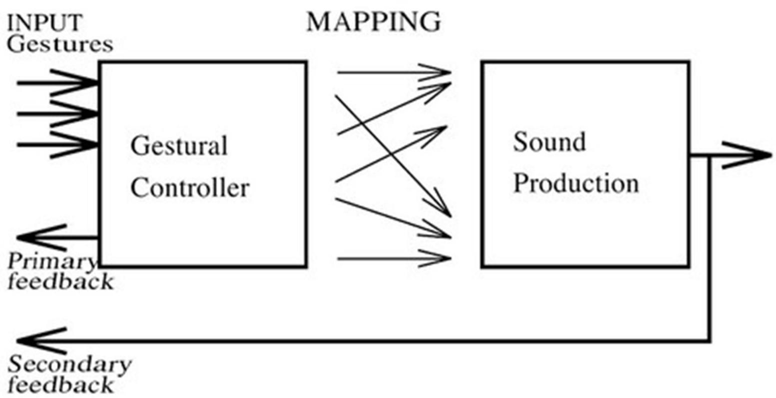

Figure 2.5: Digital Music Interface Model (reprinted [12])

2.2 Smart Textiles: from Manufacturing to Applications

The presence of textiles, garments, or fabrics in our lives is inarguably ubiquitous. From clothing to interior design, the comfortability and aesthetics of textiles have allowed us to keep our hygiene and warmth while also enable us to express ourselves. The advancement in materials and manufacturing technology has made textiles to be more adaptive. Some examples are moisture-repellent and phase-changing fabric that maintains comfortability and body temperature of the wearer, biometric knitting technique that improves athlete's performance in sports, and thermo-chromic fabric that can change colour when heated [23]. In the 90s, when electronic systems become much more advanced, visions started to appear in integrating electronics into textiles, to make them smarter and more functional; thus, the birth of textile-based computing. This section will cover the fundamental of e-textile materials and manufacturing techniques before looking deeper into its integrations and applications. Textile-based computing allows fabric to not only passively sense, but also to react and adapt its behaviour [1]; therefore, adding more functionality to textiles in areas such as physiological monitoring, activity recognition, physical interactions, and interactive media.

2.2.1 Textile Fibers and Manufacturing Techniques

Fibres are the fundamental components that produce a textile. There are two types of fibres: natural and artificial. Natural fibres come from animal (wool, hair, and silk) and plants (seed, bast, and leaf) whereas artificial fibres are made out of synthethic (polymers), regenerated (rayon), and inorganic materials (carbon, glass, ceramic, *et cetera*). The groupings of these fibres either by twisting or non-twisting in a long strand result in the development of yarns whereas the number of filaments and different techniques of twisting them define the yarns types and properties [24]. After the fibres or yarns are developed, different textile assemblies and treatments can be executed to produce fabrics. The different assembly techniques will define fabric properties, such as texture, appearance, drape, and feel, which correspondingly influence its performance, such as strength, durability, and comfort.

2.2.2 Textile-based Electronics

In this section, we will discuss current progresses of electronic textiles from fundamental materials to developing and deploying a system-on-textile. There have been many advances in textile-based electronics, including in circuits, energy harvesting, wireless transmission, and actuation [25]. However, since this research primarily focuses on smart-textiles as a media for physical interactions, we will limit our topics to textile interconnects, electrodes, and sensors.

2.2.2.1 Conductive Threads and Fabric

Conductive fabrics were mainly used for anti-static layers, electromagnetic interference shielding, and protective clothing in clean-room fabrication or military purposes before expanding its applications to wearables and ubiquitous computing. They are made either by weaving or knitting conductive threads. Some, such as metallic silk organza, were produced for traditional fashion in India, dating back to the mid 18th century [1].The conductive threads can consist of fully metal filaments (Cu, Ag, Au, Al, Steel) or a combination between metal filaments and base yarns or fibres (nylon, cotton, polyester, polyimide). The metal filaments are produced by a mechanical process called wire-drawing [26]. These filaments can be twisted together with the base fibres using a textile spinning machine; this spinning process will result in much more compatible threads for sewing due to improved flexibility. Another technique to make conductive threads is by metal-coating base yarns. This technique is less complex and develops a much softer conductive fabric. However, the threads cannot withstand heat unlike fully-metal filaments; therefore, they are unsuitable for soldering. Google's Project Jacquard's yarn is unique since instead of using metal fibres, they used insulated copper core twisted with common yarn making it easy to solder these yarns and customize their looks [27].

2.2.2.2 Textile-based Sensors

Different textile materials, sewing, and weaving techniques have been explored in order to create a textile that could electronically react to different stimuli and the environment. The following sections will discuss the fabrication process and properties of various existing textile-based sensors. Although there are some developments in inkjet-printing and screen printed smart materials on textiles, in this section, we will focus on purely fibre-based and textile-based sensors.

2.2.2.2.1 Muscle Actuated

2.2.2.2.1.1 Touch

Touch-sensing on textiles uses the principle of capacitive sensing where an area of conductive surface emits electric field that upon a presence of finger results in a change of capacitance [82,83]. Post *et al.* designs a musical jacket where they embroidered conductive threads as touch inputs on a fabric as shown previously in Musical Jacket [1]. The conductive surface was made sure to have good sensitivity to touch by parallel and multi-layer embroidering that reduces the impedance of the keypad. A plush game-controller was developed by Adafruit by using conductive fabrics as the input surfaces as shown in Figure 2.6. The fabric was cut into certain shapes then sewn onto a base fabric with the micro-controller embedded inside the plush to detect change in each input's capacitance. Conductive fabric can also be used for proximity sensing of fingers providing that the sensing circuit is sensitive enough to detect small change in capacitance as demonstrated by Freed and Matson with their interleaved conductive matrix fabric touch sensor [28].

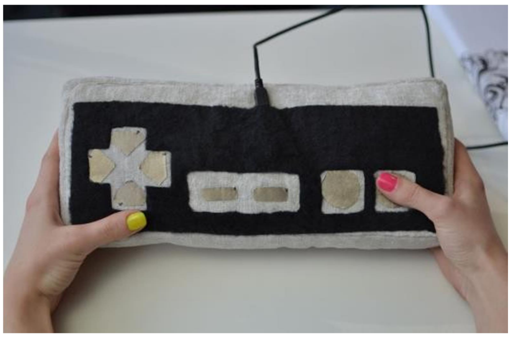

Figure 2.6: Adafruit's plush game-controller (reprinted [29]).

2.2.2.2.1.2 Pressure

There are two methods of pressure sensing: capacitive and resistive-based. Commonly, pressure sensing consists of a spacer in-between two conductive layers. Meyer *et al.* used a textile insulator in-between a common electrode fabric and an embroidered array of electrodes for activity detection (sitting postures) on a fabric surface [30]. The spacer is chosen to be squishy to improve comfortability of the pressure sensor. However, there are some challenges in that capacitive-sensing circuit is not only more complex to implement, but there is also hysteresis and fixed pattern noise behaviour observed requiring an adaptation algorithm for the measurements to work reliably. Resistive sensing uses a piezo-resistive fabric as a middle layer, where its resistance changes as a force is exerted. Even though hysteresis also exists in this case, the sensor is relatively easy to interface and gives a much higher and stable dynamic range.

A unique thin pressure sensor was demonstrated by Enokibori *et al.* Hollow conductive fibres were sewn in warp and weft fashion, and the intersections between these two lines acts as the sensing points [31]. As a pressure is exerted on these points, the distance between the fibres is reduced, increasing the capacitance at the sensing point and vice versa. This approach works with only one fabric layer; therefore, does not require a multi-layer design.

(a) (b)

Figure 2.7: a) Meyer's capacitive-based b) Bhattacharjee's resistive-based textile pressure sensor array (reprinted [30,32])

2.2.2.2.1.3 Position

Similar to how touchscreen works, position sensing can be realized by an interleaved matrix of connections as shown in Figure 2.8 below. Using piezo-resistive fabric, a matrix of machine-sewn conductive threads does not only detect position of multi-touch, but also the pressure profile on the fabric [6]. Recently, using a customized yarn and an industrial textile manufacturing process, Poupyrev *et al.* implement a woven fabric with gesture sensing capability [27]. The woven fabric also comprises matrix of conductive threads. The positioning mechanism is realized by applying projected capacitive sensing.

(a) (b)

Figure 2.8: a) Piezo-resistive fabric multi-touch pad b) Jacquard interactive fabric (reprinted [6,27])

2.2.2.2.1.4 Strain

Strain sensing in fabrics can be realized by several techniques. One way is to coat common fibres or threads with polymers that are either intrinsically or extrinsically conducting. It is usually made by uniformly-coating doped poly-pyrrole (PPy) which is an inherently conducting type of polymer or carbon-loaded rubber (CLR); the electrical property that changes due to strain in this case is resistance [33]. On the other hand, fabric stretch sensors by StretchSense are capacitively measured based on the geometry of deformation (expansion of fabric electrodes) [34].

Another way to develop fabric stretch sensors is by knitting piezo-resistive threads along with conductive and normal threads as demonstrated by Kobakant [35] or sewing conductive threads in certain patterns such as zig-zag and overlock patterns in a stretchy fabric [5,36]. The resistance of these fabrics will change based on the tension applied that could either compress the fabric to become more conductive or separate the thread structure from contacting each other to become more resistive. These techniques usually have a very low baseline resistance and limited dynamic range. They also do not have resilient structural stability, thus are poor in repeatability.

2.2.2.2.1.5 Stroke and Bend

Figure 2.9a illustrates a novel design of a textile sensor that responds to stroke. The fabric sensor consists of a large amount of conductive and non-conductive thread spikes, forming a sequence of bridges or switches. As the fabric is stroked, these spikes touch each other and form electrical connections between them that will be read by the electronics as a change in resistance. A mix between conductive and piezo-resistive threads on these spikes will also give a much more dynamic response [35].

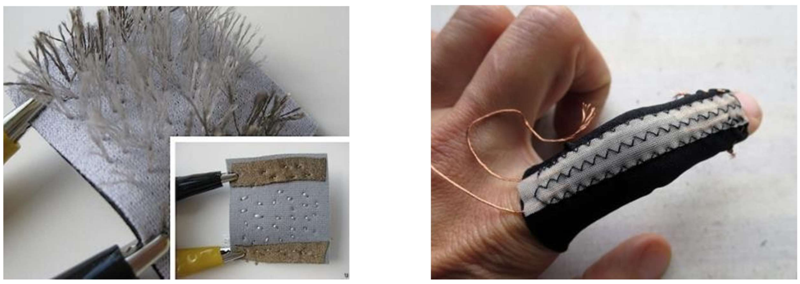

(a) (b)

Figure 2.9: a) Kobakant's one-directional stroke sensor b) Finger bend sensor (reprinted [35])

Fabric bend sensor is developed from a creative process of exploring different configurations of fabric sensors. Figure 2.9b shows an example of how piezo-resistive fabric interconnected with conductive threads can be used as a bend sensor in a smart-glove to detect finger movements. The fabric goes into stress and strain, depending on the angle of bend, changing its resistance accordingly.

2.2.2.2.2 Other types

2.2.2.2.2.1 Temperature

Some researchers have developed and studied the performance of metal fibres integrated into textile threads for temperature sensing purposes. Locher *et al.* realized a matrix of copper fibres embedded into a fabric to measure surface temperature profile [37]. However, the grid structure only allows the fabric to measure only one temperature hot-spot due to its spatial ambiguity. To be able to measure multiple hot-spots, pixelated sensors in interdigitated pattern are required as demonstrated by Hussain *et al.* in Figure 2.10 [38]. Their work also compares the sensitivity of different fibres material to temperature change and parasitic influence of strain and humidity.

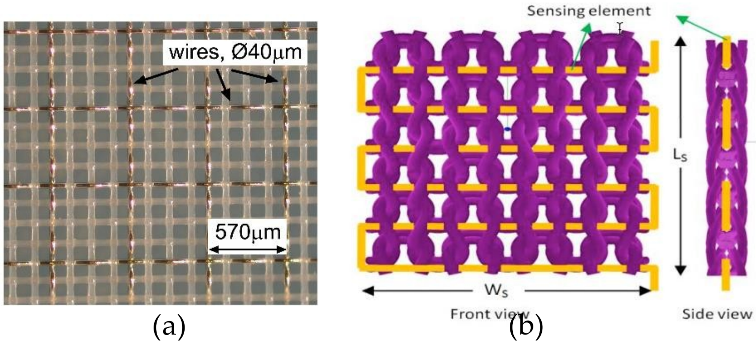

(a) (b)

Figure 2.10: a) Copper wires embedded in a fabric by Locher *et al.* b) Husain *et al.* interdigitated fibres embedded in a knitted fabric (reprinted [37,38])

2.2.2.2.2.2 Humidity

Pereira *et al.* developed a textile matrix sensor to measure the humidity profile by the change in conductivity of an absorbance layer as shown in Figure 2.11 [39]. The system can detect a difference in moisture level in the middle layer and also the outer absorbance layers separately by using an additional multiplexer. This allows the fabric to responsively react to perspiration. The challenge observed is that the absorbance layer needs to absorb and dry out quickly for more accurate and responsive readings. Pressure applied to the fabric can also alter the measurement since it also influences the conductivity. This can be solved by separately measuring the pressure profile, and then taking this result into account to neutralize parasitic pressure effects.

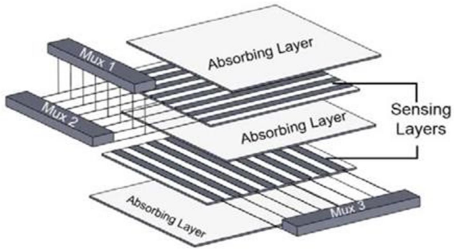

Figure 2.11: Multi-layer structure of a textile moisture sensor (reprinted [39])

2.2.2.2.2.3 pH

To continuously examine a wound treatment process, Nocke *et al.* fabricated a novel multi-layer miniaturised fibre sensor that could be woven into fabrics for pH detection [40]. The fibre, as shown in Figure 2.12 comprises an inner electrode gold wire coated with pH-responsive hydrogel (PVA/PAA) with sensitivity from 5 to 11. To complete the circuit, another gold wire is wound as the outer layer. The result shows an impedance change of up to 14% with respect to a change of pH (6 – 9) with 323kHz excitation frequency.

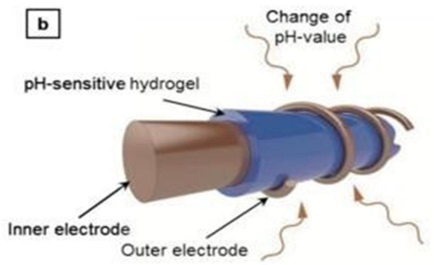

Figure 2.12: Fibre sensor structure for wound pH-detection (reprinted [40])

2.2.2.2.2.4 Chemical

Chemical sensing has attracted a large amount of recent studies, mostly in detecting odours or gasses (electronic nose). Seesaard *et al.* produced chemical gas sensors that can be coated in fabrics between the embroidered interdigitated electrodes [41]. Different polymers (PVC, PSMA, PSE, and PVP) are mixed with SWCNT to form several composites. Based on the resistive change of each composite in response to different odours, PCA discrimination is used for classification. Another approach, as suggested by Kinkeldei is to use a carbon black/polymer composite deposited on a flexible substrate. The substrate, can then be woven into fabrics. Using PCA, four different composites C-(PS, PIB, PVBU, PVP) can distinguish different types of solvent including Air, IPA, Methanol, Toluene, Acetone, as well as parasitic influence such as bending [42].

2.2.3 Systems-On-Textile Integration

The previous sections have covered various textile-based sensors and interconnects. In order to process the electrical change of each sensor, a circuit must be developed and integrated to the textiles. Several efforts have integrated fabrics with electronics in the form of individual ICs or the whole circuit board. As for the interconnects, many methods can be applied including sewing, embroidery, and weaving of conductive threads, or ink-jet printing, screen printing, fusing of conducting polymers.

Post *et al.* introduced the concept of e-broidery [43]. Due to the small adjacent distance and high density pins in current chip packaging for commercial PCBs, they designed packaging and integration techniques for system-on-textile using special carrier (PTCC), steel threads, and embroidery techniques. Another technique by Linz *et al.* is more straightforward in that the interconnects are sewn or embroidered directly onto a fabric and then looped into flexible PCB pads (Figure 2.13a) [44]. As an effort to create a much more seamless routing in e-textiles, Locher explored the possibility of creating a system-on-textile by developing wire-grid fabric called PETEX, consisting of threads embedded with metal wires (Figure 2.13b)[45]. Interconnects can be realized by cutting intersections by laser ablation and using conductive adhesive and encapsulation. Fusing interposers would then create a bridge to connect this wire-grid with IC pads.

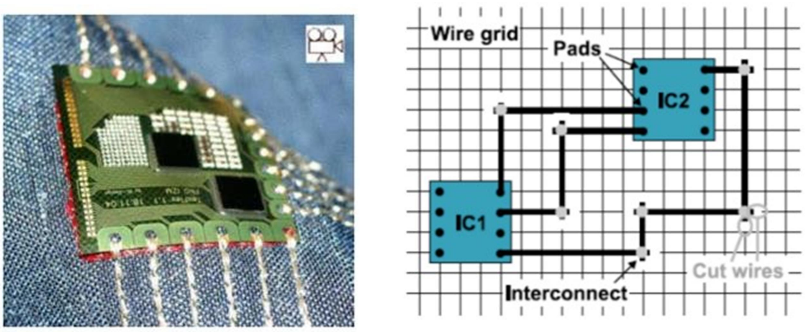

(a) (b)

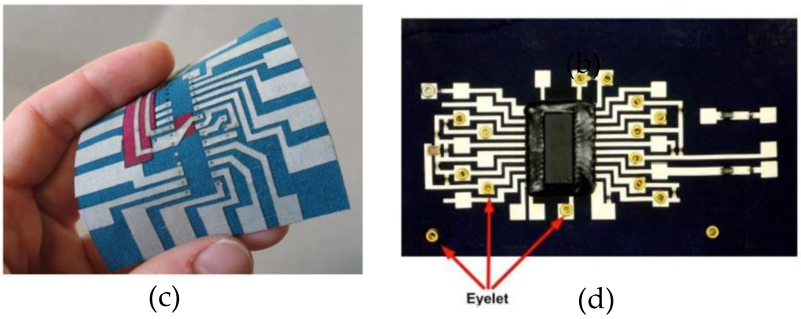

(c) (d)

Figure 2.13: a) Flexible PCB pads connected with embroidered conductive yarn (Linz *et al.*) b) Integrating circuits into fabrics with wire grids (Locher *et al.*) c) Multi-layer fabric PCB (Buechley and Eisenberg) d) Planar screen-printed fabric PCB with Eyelet (Lee *et al.*) (reprinted [44-47])

Buechley and Eisenberg demonstrated how to exploit an automated machine such as laser-cutter with CAD software to develop a multi-layer fabric PCB, as shown in Figure 2.13c [46]. The procedure requires a stack of conductive fabric, heat activated adhesive, and sacrificial paper. After cutting the design with laser, the patterned fabric is aligned and ironed to stick on to its fabric substrate. The chip can be then placed into the fabric PCB, carefully soldered with a flux, and finally encapsulated with epoxy. Lee *et al.* presented a planar fashionable circuit board by using screen-printing techniques [47]. This technique requires a mask development and annealing before and after the printing process. Metal beads and thin gold wires are attached and soldered to make contacts to the IC before encapsulation. They also further integrate their process and demonstrate a two-layer technique using an Eyelet which is a metal connector that can be used as a system-on-textile via, allowing two layers of screen-printed interconnects on a fabric PCB (Figure 2.13d).

The previously-discussed techniques to integrate electronics into fabric present some challenges in practice: the rigid electronics would defy the fabric-feel, wearability, and washability of the e-textile. This challenge has attracted some researchers to develop electronic systems that can be woven. Cherenack *et al.* develop electronic fibres with sensing and display functions woven in a fabric with conductive bus lines. They fabricated transistors on a strip of polyamides that communicates with sensors (temperature and humidity) and LEDs as shown in Figure 2.14a. The advance miniaturization of electronic devices and systems has enabled them to be attached on fibres and still retained functionality, even after multiple bending and washability tests [48].

Google's Project Jacquard (Figure 2.14b) showed a significant effort to commercialize intelligent textiles: from customizing their own yarns, weaving them into fabrics, connectorizing, to constructing all the components (textiles, connectors, and electronics) into a functional garment [27]. They implemented current electronics and textile manufacturing processes to develop interactive fabric surfaces in a large scale. Another emerging area in e-textiles is fibre electronics (fibretronics) where researchers explore methods to deposit organic transistors onto fibres so that in the future, electronics can be seamlessly fabricated on a fibre and woven into textiles in a low-cost and industrial fashion [49].

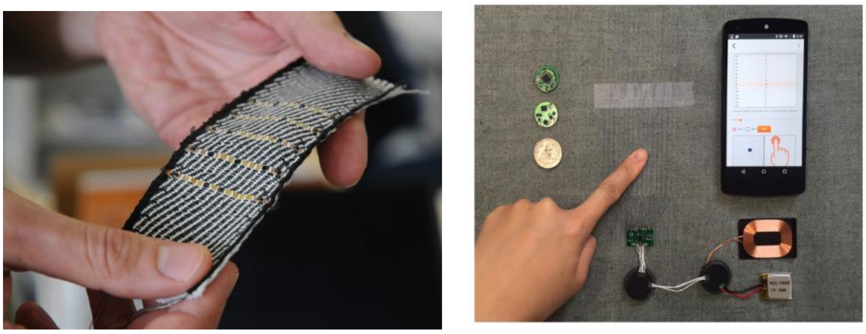

(a) (b)

Figure 2.14: a) Woven fabric with sensing and display function b) Full prototype of Jacquard's touch-sensitive fabric implemented with minimal electronic systems (reprinted [48,27])

2.2.4 Applications of Textile-based Computing

Textiles are soft, 3D-conformable materials, as opposed to standard electronics which has to be built on rigid structures or flexible substrate that can only be bent along one axis at a time. The fact that textiles are ubiquitous in our life and there has been a significant advance on making them more functional and intelligent present many interesting applications. We separate these applications into four main areas: activity recognition, health monitoring, physical interaction, and interactive media. The first area is in activity recognition. Attachments of strain sensors on our shirts or knee or pressure sensors in our shoes for example, could classify body postures which benefits rehabilitation purposes and sport trainings [50]. Large textile pressure sensor arrays are also useful for location detection, activity recognition, and medical monitoring when attached to chairs, floors, or beds [30,39]. For personal health, textile electrodes can be embroidered in our shirts to measure physiological signals such as respiration and heartbeat [44]. Embedding textile sensors and actuators on garments could also be beneficial for thermal regulation, sweat analysis, and near-infrared spectroscopy [23].

In the area of physical interactions, besides musical controllers that will be further discussed in this thesis, having gesture and pressure sensitive textiles as a control surface could be useful in smart-home, automotive, and apparel applications [1,23,27,43]. The attachment of textile actuators and display in fabrics also allows us to express ourselves and communicate in a novel way [50,51]. Current applications have showed a great prospect in future textiles as new materials and integration strategies are introduced.

2.3 Multi-modal Electronic Skin and Sensate Surface

Biological skin is the most profound example of a flexible, multi-modal, fine-grained, dense sensor network. Having electronic skin with such capability could therefore catalyse new developments in areas such as human augmentation, robotics, prosthetics, and medicine. Inspired by the capability of our somatosensory system, many researchers have started to develop and deploy electronic skins as distributed sensor networks. Figure 2.15a shows Tribble, a polyhedron decentralized sensor networks composed of patches of multi-modal sensors (FSR, whisker, light, temperature, microphone) and actuators [53]. As materials, fabrication technologies, and system integrations become more advanced, it is now possible to develop electronics on novel substrates; these advances therefore triggered new research areas such as Electroactive Fabrics and Epidermal Electronics [33,54]. Son *et al.* fabricated a skin patch with sensing (temperature and strain), actuation (drug-release), and storage (non-volatile RRAM) capability [55]. Even though these miniaturised electronic systems are not currently scalable and low-cost and there are still many challenges remaining, such as in miniaturizing the processing, power supply, and transmission modules, these findings show a promising future towards the invisible and ubiquitous electronics.

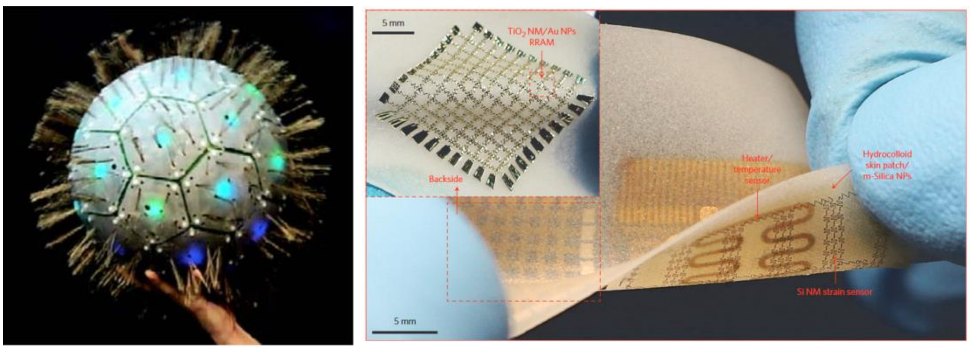

(a) (b)

Figure 2.15a) Tribble: a tactile reactive interface b) A multifunctional skin patch by Son *et al.* (reprinted [53,55])

On the other hand, there are also efforts in realizing sensate surfaces on a large scale. ZTiles for example, consists of pixelated tiles forming a mesh sensor network with each tile containing 20 FSR pressure sensors [53]. Gong *et al.* explored novel conductive inkjet printing on a flexible substrate to develop a one layer, multi-modal (proximity, touch, pressure) sensing surface [56]. Since it involves roll-to-roll manufacturing, it can also be fabricated at a large scale, enabling floor or wall sensing applications, for example, to detect location, foot-strikes, or NFC/GSM signals.

2.4 Project Goals and Contribution

As previously discussed, smart textiles have been experiencing a great development resulting in several new advances in flexible and deformable musical interfaces. Even though they are expressive, almost all of them are played only to shape or control sound, instead of also generating it. This makes them hard to perform and compose music with, as they are lack of discrete controls. Giovanni *et al.* performed a user study on how musicians interact with deformable interfaces. The results showed that musicians only interact with these interfaces (squeezing, pressing, pulling, stretching) as a way to manipulate and filter sound rather than generating it [78]. These controllers therefore are better suited as expressions or keyboard complements instead of stand-alone pitch generation, especially for a performance that requires precision.

Verplank in his' Interaction Design Sketchbook', argued that buttons are a discrete, sequence of presses, while handles are analogue, relating to gestures; he used buttons for precisions and handles for expressions [57]. This is what essentially makes keyboards and other musical controllers adapted from acoustic instruments deterministic, hence there have been a large amount of efforts in making keyboard controllers more functional and expressive by adding continuous controls [58]. Since learning a new interface requires a significant effort, people tend to choose interfaces with which they are most familiar with [10]. Therefore, some of the extremely novel, lack-of-discrete controls electronic musical controllers did not survive and mostly there only for personal use and amusement. The ROLI Seaboard is one successful example of new expressive keyboard interfaces combining discrete and continuous controls on novel silicone surface; it has gained a tremendous amount of public attentions since its commercialization.

The overall goal of this research project is therefore to build a multi-sensory, fabric-based, expressive keyboard controller. Even though portable keyboards made out of flexible PCB already exist, and the DIY community has developed many textile pianos, most of them are only discrete, touch sensitive, or a simple textile switch [1,35]. We are interested in making an expressive instrument based on current advances in smart-textile combining discrete and continuous controls. A fabric-based musical controller, besides giving a soft, new tactile experience, can also be stretched, squeezed, pressed, pulled, twisted, and even worn enabling new novel interactions in musical performances. Figure 2.16 illustrates our first conceptual sketch of the *'StretchyKeyboard'*: A fully-fabric based, musical controller.

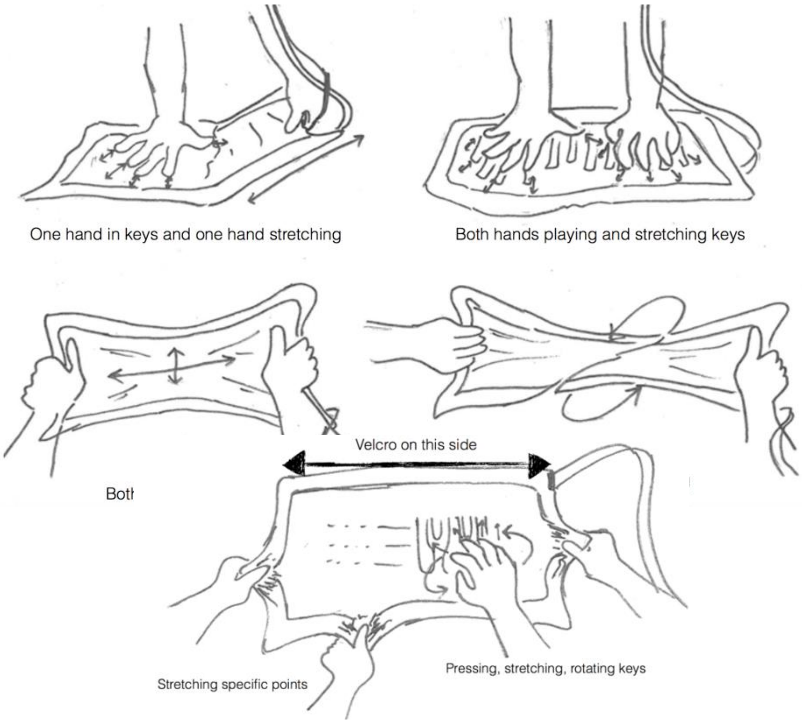

Figure 2.16: '*StretchyKeyboard*' concept in early sketches

The background research of this work has covered two main areas: electronic musical controllers and electronic textiles and ultimately converges to new keyboard interface and multi-modal sensate surface. Based on the dual relationship between electronic musical controllers and sensor systems [59], this research will give two main contributions:

- A fabric-based, electronic musical controller combining discrete and continuous controls. A multi-sensory fabric keyboard as a deformable musical interface.

- The design and implementation strategies of a novel electronic sensing system in textile-substrate. A multi-modal (proximity, touch, electric field, pressure, stretch) fabric sensate surface as well as other fabric interfaces (continuous position sensing) for physical interaction media.

Chapter 3:
Multi-sensory Fabric Keyboard

3.1 Structure and Construction

The stretchable keyboard is a textile-based electronic skin that comprises one octave of keys with multi-modal sensing capability, as illustrated in Figure 3.1 below. Multi-layer fabric sensors that could detect discrete and continuous signals of touch, proximity, induced hum, pressure, and stretch simultaneously were embedded and machine-sewn on each key. Table 3.1 describes each sensing modality in details.

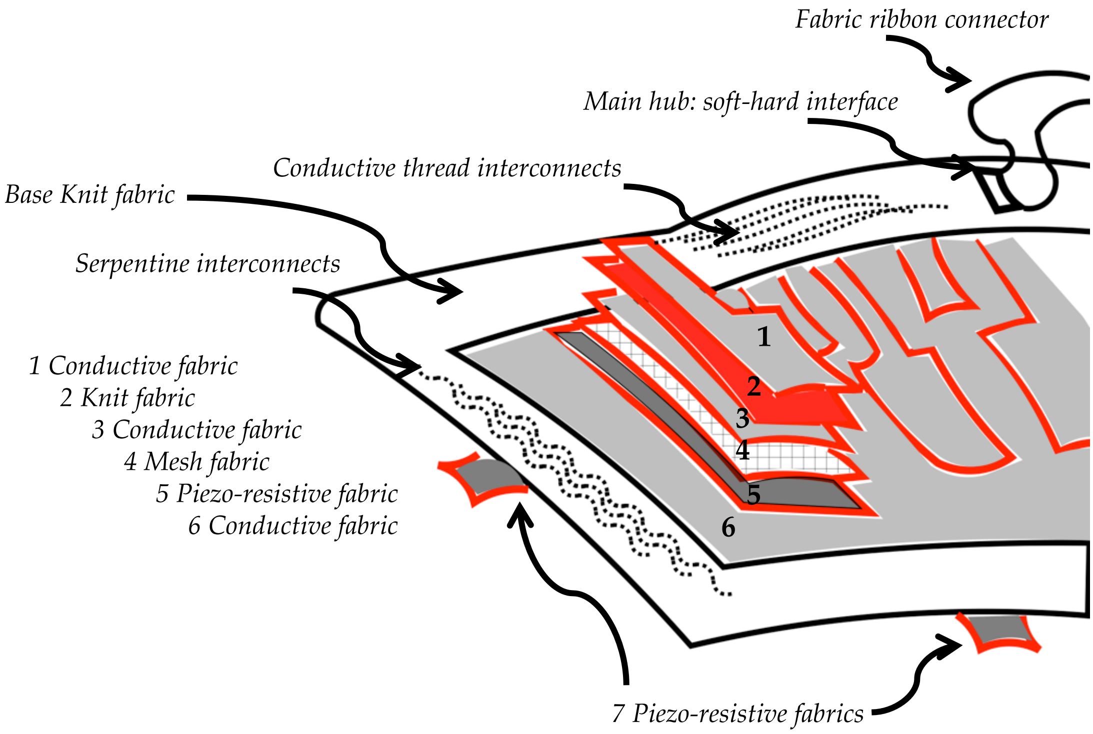

Figure 3.1: Textiles structure of the multi-modal fabric keyboard

Sensing Modality	Number	Layer	Location and Structure	Modes	
Proximity **Hum** **Touch**	12	1st	Each key, floating	Continuous/Discrete Continuous/Discrete Discrete	
Pressure	12	3rd - 6th	Each key, sandwich structure	Continuous	
Stretch (Keys)	1	6th - 7th	In-between keys, adjacent zebra-pattern	Continuous	
Stretch (Fabric)	4	6th - 7th	One at each left and right side, two at the bottom side, adjacent structure	Continuous	
Ribbon controller (x-slide)	1	Additional	Modular (snapping)	Continuous	Optional touch, proximity, and pressure
Trackpad (xy-slide)	1	Additional	Modular (snapping)	2D Continuous	Optional touch, proximity, and pressure

Table 3.1: Detailed information of each sensing modality with additional fabric interfaces (ribbon and trackpad controller)

At the outermost layer of each key, a floating conductive fabric was fused onto a substrate fabric (as a separation layer) with heat-activated, iron-on fabric adhesive. The floating fabric electrode functions as a touch sensor as well as either a proximity or passive electric field sensor. Below a separation layer, another conductive fabric was fused as a part of the pressure sensing elements. The separation layer with conductive layers at both sides was then transferred and sewn to the main fabric. This transfer process reduces the chances of different layers accidentally connecting and shorting to each other while sewing considering the space constraints. The embedded fabric pressure sensor consists of the previously transferred top electrode (bottom of separation layer) sewn on top of a mesh fabric with piezo-resistive fabric and common-ground fabric behind it. This results in a sandwich configuration with mesh and piezo-resistive fabric in between two conductive layers. The necessity to include mesh fabric as a part of the pressure sensing elements will be explained later in Chapter 4. This multi-layer structure lies on top of the stretchable base fabric.

Behind the fabric substrate, stretch sensors were attached at the edges of the fabric and in-between keys. Zebra pattern of conductive/piezo-resistive fabric was sewn so that each pressure and stretch sensor element does not give parasitic influence to each other. One side of each stretch sensor was connected to the interconnect lines while the other to the common ground fabric. Sewing two electro-active fabrics to one another using common threads connects them to each other resembling a contact via in IC. The common ground fabric considerably reduces the complexity of the interconnects, as it cuts the number of sensor's interconnects by approximately half. Instead of having two interconnects for every pressure and stretch sensor on the fabric, which results in 34 interconnects, using a common ground fabric reduces the interconnects to 18, or by 47%.

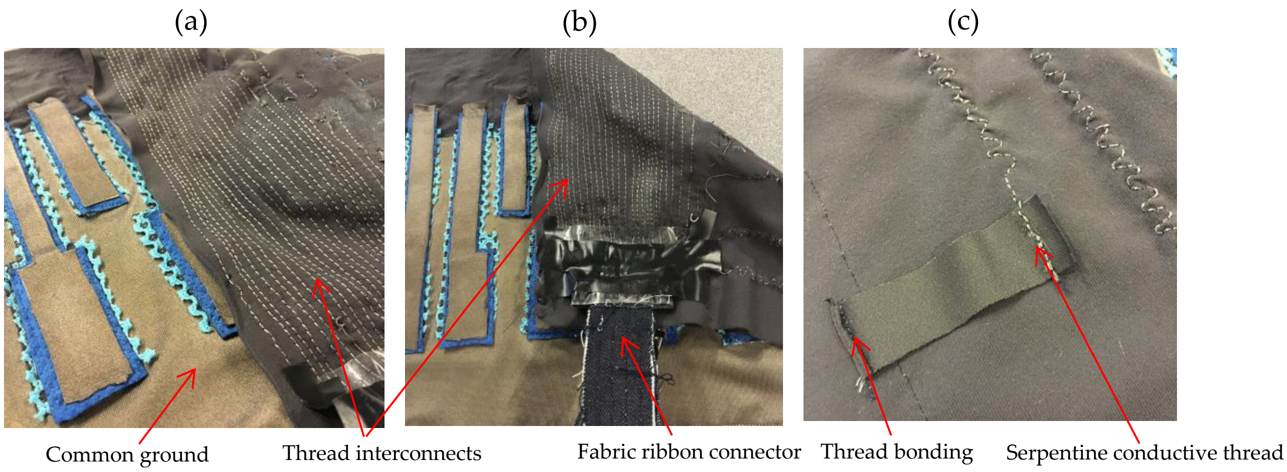

Figure 3.2: Main thread interconnects with the keyboard b) The bridge between the fabric ribbon connector and the main interconnects c) Stretch sensor sewn with conductive thread in serpentine structure and to ground with thread bonding (the common ground fabric is on the other side)

As illustrated in Figure 3.1, all of the fabric sensors have access to the base fabric for sewing their interconnects. The stretch sensors at the edges were connected to the main interconnects using serpentine patterns (Figure 3.2c); this was to ensure that upon stretching the fabric, these interconnects will be able to adapt to the elasticity preventing them from breaking. A total of 30 conductive thread interconnects were sewn to connect each fabric sensor to its read-out (Figure 3.2a). The dense conductive thread interconnects lead to the right corner of the fabric, where there is a soft-hard terminal for plugging the circuit board in the form of a PCB through a customized fabric ribbon connector (Figure 3.2b).

The design decision to incorporate pluggable connectors besides its function to bridge all of the sensory inputs to the "brain" for further processing originated from several motives including:

- Full separation between the soft elements, the fabric keyboard, and the hard element, the circuit board, making it possible for the performer to interact freely with the keyboard. Gestures such as lifting the fabric, stretching, twisting, and grasping are then possible and interactions will become more fluid.

- Customizable and modular circuit module. The fabric keyboard, which has a great array of sensors and modalities, facilitates multiple sensing methods. In this work, we demonstrated two PCBs capable of sensing proximity and passive electric field respectively. The modular circuit module also allows user to set their own communication interface, such as wired for Direct Serial or MIDI through USB, wireless for OSC through BLE/Wi-Fi connectivity, or direct connection to an onboard analog synthesizer with build in speaker. This design decision gives full flexibility towards further development of this fabric sensate surface as a musical controller.

- Customizable and modular sensate surface. The connector also enables the concept of extendable fabric keyboard. By master and slave configuration, each sensate surface can own a local processor that is responsible for getting all the sensor data of its vicinity and as a slave, periodically sending it to the master.

- Finally, having a separation between the soft and hard circuits extends the usability of this fabric keyboard. For example, when the user only wants to wear the fabric as a scarf or a decoration instead of as a controller or when the user wants to wash this fabric, the rigid module can be unplugged.

3.2 E-threads and Stretchable Interconnects

There are several methods in developing conductive threads as previously described. In this project, different types of conductive thread as shown in Figure 3.3 were tested to show whether they are machine-sewable and suitable for low-resistance interconnects. Most of the commercial threads are meant for hand-stitching in the DIY smart-textile community and are not necessarily machine-sewable. Since this project focuses on using automated processes in such a way that multi-layer smart fabrics can be produced in a short term and at scale, SINGER XL-150 was used as the sewing machine. The choice of threads and the tension settings of a sewing machine are crucial in order to sew with consistent results.

Orth covers different conductive threads mechanical and electrical properties that are suitable for commercial sewing and embroidery processes in more depth [60]. Silver-coated nylon thread, even though is perfect for sewing and embroidery as either or both top and bottom threads, is usually highly-resistive (100 Ω/cm) and poor in quality especially after multiple washing. It is more applicable for making resistive paths or sensors rather than interconnects. There is also multi-stranded silver-coated fibres thread available. In this case, the thread is very conductive (0.15 Ω/cm) but due to its hairiness and inflexibility, is difficult to sew with. Even though purely stainless-steel fibre thread is slightly thicker, making it incompatible as top thread, it was chosen for our main interconnects based on its compatibility as a bobbin thread, moderate conductivity (0.6 - 0.8 Ω/cm depending on 2/3-ply) and durability.

Figure 3.3: From left to right, Plug and Wear conductive yarn, LessEMF silver-coated threads, Liberator 40 silver fibres, (in rolls) Sparkfun stainless-steel thread 3-ply rough and smooth, Adafruit stainless-steel thread 2-ply (in bobbins).

The deformable nature of the sensor surface requires the development of stretchable interconnects. This is to ensure that when the fabric is stretched to its maximum allowable strain, there will not be any tension applied on the thread interconnects that could result into fractures. Stretchable materials and structures have attracted a great amount of research interests in the last decade, especially in the emerging area of conformal systems such as epidermal electronics, biocompatible sensing, stretchable displays, and other smart elastomeric surfaces [54,55]. Most of the current research on soft and stretchable electronics use silicone such as PDMS or Ecoflex as the substrate. The interconnects, such as Au or Cu, are deposited using micro-fabrication techniques. Other methods, such as embedded printing and screen printing of metal-polymer composite such as AgPDMS and cPDMS have also been introduced. However, these techniques are not cheap, fast, and scalable; therefore, are unsuitable for large sensing surface development.

Textile, on the other hand, is an attractive substrate for large sensing surface. Besides being omnipresent in our environments, textile production processes have existed for a long time and capable of large-scale manufacturing; for example, long arm sewing machine and jacquard weaving. Even though textile electronics have been well explored recently, the focus has been mainly on weaving smart fibres, large pressure sensing arrays, and embedding textile sensors on shirts. Knitted fabrics made out of lycra or spandex, based on their unique structure and exceptional fibre elasticity, has a relatively high stretchability, thus is a good candidate for a stretchable sensing surface. Since there are not any resources that perform in-depth analysis of stretchable interconnects on textile platforms, this part will cover different approaches in realizing stretchable interconnects for system-on-textile using current textile materials.

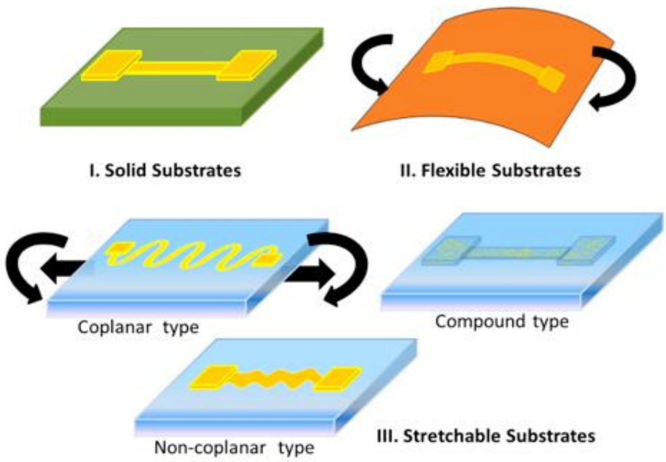

Figure 3.4: Electrical routings on solid, flexible, and stretchable substrates (reprinted [61])

Hocheng and Chen reviews current approaches on stretchable interconnects on elastomers as shown above in Figure 3.4 [61]. There are three types of routing: coplanar, non-coplanar, and compound. Coplanar routing relies on the serpentine structure of rigid interconnects that allows stretchability. In textiles, this can be done simply by using a special type of stitching pattern such as a zig-zag pattern on conductive threads. Other complex structures with more stretchability, such as horseshoe or self-similar patterns, can be done by using sewing-machine with CAD capability. The zig-zag pattern, when it is sewn, appeared to have smoother edges that look closer to serpentine due to the tension on the conductive thread as a bobbin. This is shown in Figure 3.5.

The theoretical effective stitch length of a zig-zag interconnect is given by,

$$initial\ length = NL\ \ or\ 2W\tan\left(\frac{\theta}{2}\right) \qquad (3.1)$$

$$effective\ length = N\ \frac{\sqrt{W^2 + L^2}}{2}\ \ or\ \frac{2W}{\cos(\frac{\theta}{2})} \qquad (3.2)$$

From these equations, the maximum strain can be calculated as,

$$max\ strain = \frac{\Delta l}{l} = \frac{1}{2}\sqrt{\frac{W^2}{L^2} + 1} - 1\ or\ \frac{1 - \sin\left(\frac{\theta}{2}\right)}{\sin\left(\frac{\theta}{2}\right)} \qquad (3.3)$$

by changing the width and loop length or the angle of a serpentine structure, one can estimate the stretching limit of a serpentine routing.

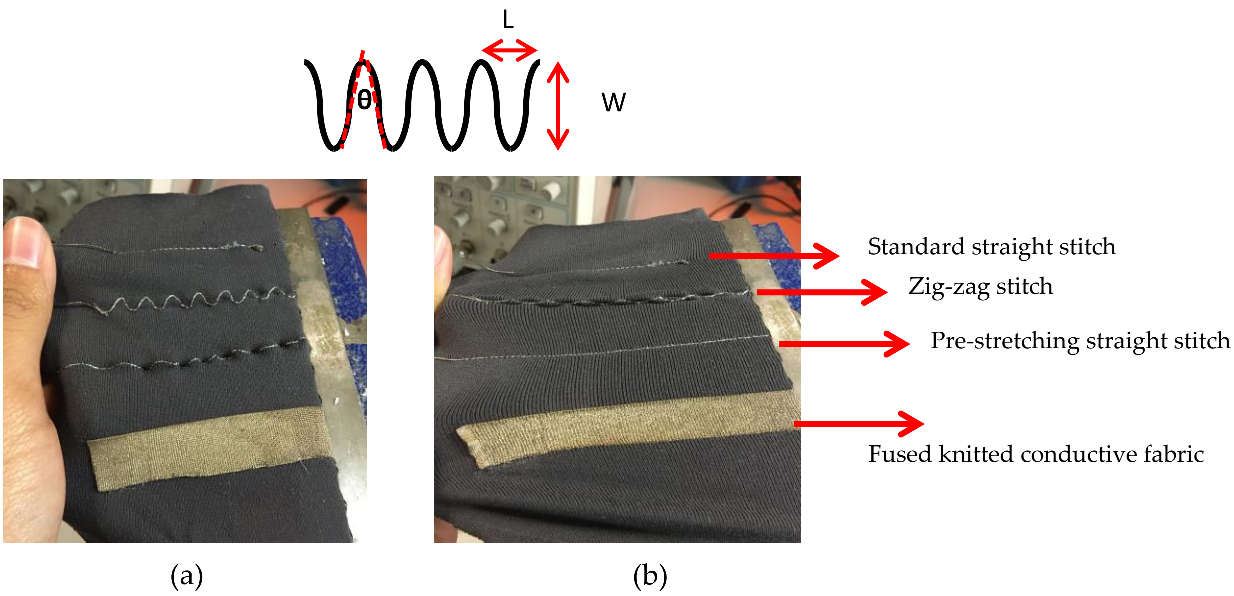

Figure 3.5: Three different types of stretchable routings on fabric; a) unstretched and b) stretched

It is important, however, to note that the maximum allowable strain on stretchable routings is given by the stretchability of the structure, and the maximum allowable strain of the interconnects itself. Even though conductive threads have a relatively high tensile strength, it could usually stand strain only up to 1% [62]. The tensile strength of a conductive thread is largely influenced by the tex or density of the fibres.

The second routing, which is the non-coplanar type, can be done by pre-stretching the substrate before sewing. The stretchability is given by the buckling mechanism and can be defined by how long the substrate is pre-stretched. This method, however, is more complicated than the previous method for large sensing surface, since it requires a setup that uniformly pre-stretches the entire fabric substrate. The third method involves an intrinsically stretchable material. One approach is to cut knitted conductive fabric in ribbons as shown in Figure 3.5. The conductive fabric from LessEMF could be stretched up to 100%. Double-sided iron-on fabric was used to fuse the stretchable ribbon fabric to the substrate by heating the layers. This method nevertheless is not suitable for dense and low-resistance networks since a wide ribbon is needed for a low interconnect resistance and a thin ribbon acts more as a stretch sensor than a routing.

Observation of these results concludes that the coplanar method, which involves sewing in a serpentine pattern, is the most suitable option for this purpose, as most of the commercial and industrial electronic sewing machines nowadays have this capability. The method is also the most straightforward, as it does not require any preparation or preconditioning. Another method that has not been mentioned is to print electronic materials, such as conductive ink using screen-printing or inkjet-printing as a compound type routing.

Several companies such, as DuPont have been developing conductive inks for stretchable interconnects especially for textiles using silver or carbon mixed with elastomers [63]. For large scale fabrication, this method could perform faster than sewing or weaving. However, there are several challenges in printing electronics on such a novel substrate. The first one is that it needs an interfacial layer to reliably print the interconnects as a substrate with certain surface properties as required for a good ink contact; this also means that woven textiles, where the fibres structures are more dense, are preferable than stretchy knitted fabrics which have a relatively considerable gap in their structures. In addition, there are some limitations in engineering the stretchability, unless methods previously discussed here are also applied.

Using conductive threads is particularly interesting in this project, because it covers the design and implementation strategies of fabric sensate surfaces using a sewing machine, anyone who knows how to sew and hand-stitch can also apply these strategies to make their own intelligent fabrics. The materials and equipments used in this project are easily available. Anything that can be machine-sewn can be fabricated at large scale, and in contrast, it can also be hand-stitched, allowing this project to contribute also to the DIY community.

3.3 Electroactive Fabrics

Realizing a stretchable sensate surface requires not only stretchable interconnects, but also stretchable fabric substrates and sensors. Figure 3.6 below shows some fabrics that were used in the project. Note that all the fabric used in the fabric keyboard, electroactive or not, are four-way stretch, while the additional controls such as the fabric trackpad and ribbon-controller, use a combination of woven and mesh fabrics.

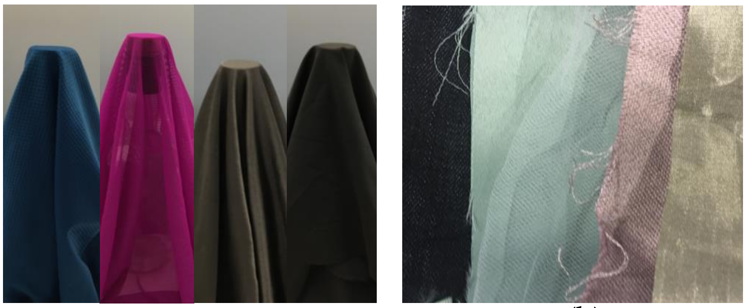

(a) (b)

Figure 3.6: a) Knitted (common, mesh, conductive, piezo-resistive) and b) Woven (jeans, satin, conductive taffeta, conductive woven) fabrics used in this project.

There are currently many types of conductive fabrics: woven, non-woven, and knitted and many techniques in producing them: coating and weaving or knitting conductive or mixed nylon-metal fibres. Several types of conductive fabric were obtained from LessEMF Inc as listed in Table 3.2 below. It can be seen that knitted conductive fabrics, even though are stretchable up to twice its length, have a slightly higher surface resistivity than woven conductive fabric due to the fact that they have less structural density.

Fabric	Type	Composition	Surface Resistivity	Stretch
Stretch Conductive Fabric	Knitted	76% Nylon 24% Elastic fibre Ag coating	<0.5 Ω/sq	100% length 65% width
Soft & Safe Fabric	Woven	70% Bamboo fibre 30% Silver fibre	<1 Ω/sq	-
CobalTex Fabric	Woven	100% Polyester Ni/Cu/Co fibre	<0.1 Ω/sq	-
Copper Taffeta Fabric	Woven	100% Polyester Cu fibre	0.05 Ω/sq	-

Table 3.2: Properties of different conductive fabrics

Table 3.3 below shows three different resistive fabrics customized for this project. Woven resistive fabric made out of carbon fibre woven in a polyester fabric is particularly useful for making fabric potentiometer. Piezo-resistive knit fabrics on the other hand, based on their electrical behaviour that changse upon force and strain, can be used for pressure and stretch sensing. The piezo-resistive fabrics in this project were obtained from Eeonyx Corporation.

Fabric	Type	Composition	Surface Resistivity	Stretch
Ex-static Resistive Fabric	Woven	13% BSAF Resistat 87% Polyester	10^5 Ω/ sq	-
LG-SLPA Piezo-resistive Fabric	Knitted	9% Elastane 91% Nylon PPy coating	10^4 - 10^5 Ω/ sq (on request)	140% width 90% length
LTT-SLPA Piezo-resistive Fabric	Knitted	28% Elastane 72% Nylon PPy coating	10^4 - 10^7 Ω/ sq (on request)	155% width 105% length

Table 3.3: Properties of different resistive/piezo-resistive fabrics

There are two main approaches in producing piezo-resistive fabrics: by immersion of fabrics into polypyrrole (PPy) or carbon-loaded rubber (CLR) solution [33]. A work by Li *et al.* describes the procedure of making a PPy-coated fabric with two methods which yse CVD and solution polymerization [64]. Both methods involve immersion of substrate fabric to sodium and ethanol solutions before deposition and annealing. Using CVD will deposit a fine thin layer of PPy on the fibres, which means a high strain sensitivity, while solution polymerization method will result in a thick non-uniform layer of PPy, making it less sensitive to strain; however, with good mechanical stability. Therefore, a compromise of these two methods is proposed in order to develop piezo-resistive fabrics with good electrical and mechanical properties. A similar technique could be done to develop a CLR-based fabric sensor by coating the fabric material with a composite of carbon and silicone before annealing.

3.4 Soft-hard connections

In this section, integration strategies are explored to connect the fabric sensate surface to its read-out circuit in the form of either flex or board circuits.

Unlike stainless steel threads, purely silver -fibre conductive threads are mostly solderable. However, since we used stainless threads as it is machine-sewable, and we would like to develop a plug instead of soldering a direct connection, female-type connectors were considered instead. The first trial used FFC connector generally used for ribbon flat cables. Since this type of connector has two holes on each pin and a snap, it worked reliably by looping the conductive thread several times before clamping it. However, a couple of short-circuits occurred mostly because of the short pitch between the pins and the dense interconnects. This can be solved by encapsulating each thread, even though it would take a relatively high effort. A customized soft-hard connector was built instead at the end by stripping the wires common female ribbon connector and making a loop, as shown in Figure 3.7 below. The thread was then tightened to this loop and a low-temperature silver paste was applied to ensure a firm connection before sealing it. This mechanism proved to work better, since it is less dense and provides a robust connection, especially when there are a lot of movements on the fabric.

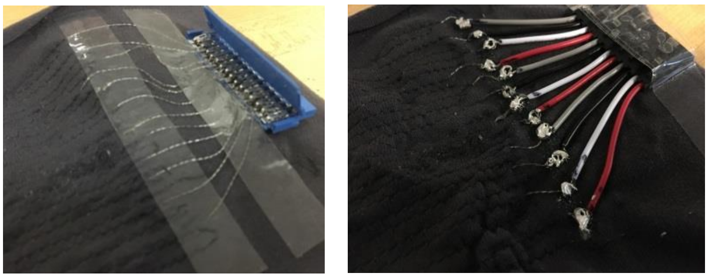

(a) (b)

Figure 3.7: Connectorization with a) FFC and b) customized female ribbon connector

Another soft-to-hard connection for the additional controls of the keyboard is shown Figure 3.8. Since the ribbon-controller and trackpad were designed to be plug-and-play and modular, common fabric snaps were used as their connections to the main keyboard, because they are already conductive.

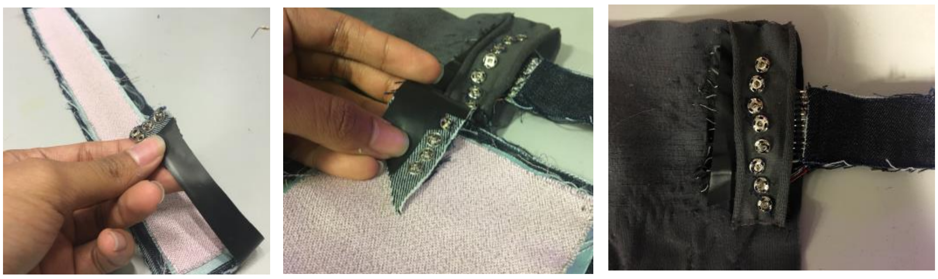

(a) (b) (c)

Figure 3.8: a) Ribbon-controller with snap connector (male) b) Trackpad with snap connector (male) c) Keyboard with a snap hub (female)

Chapter 4:
Sensor Design and Characterization

4.1 Sensing Elements

In this section, we will cover the design of each sensing modality, as well as its characteristic. Design of the additional controls: ribbon-controller and trackpad, will also be covered in Chapter 4.2. For further sensor analysis, refer to Chapters 5 and 7.

4.1.1 Touch and Proximity

The touch and proximity sensing in this multi-sensate surface are based on capacitive coupling between our hands a conductive plate. There are other possible techniques [83], such as using multiple elements, where finger approach disrupts electric field coupling between a pair of electrodes, allowing a new current path to ground; or using a conductive electrode attached on our hands where one of the electrode acts as a transmitter and the other, as a receiver resulting in a much more sensitive response to proximity using high frequency coupling. These techniques do not meet the design constraint, since we would like each key to respond to proximity. A single electrode mechanism with one layer of conductive fabric was then constructed as shown in Figure 4.1 below where there is an electric-field change between the finger (virtual ground) and a charged electrode. The total capacitance this floating electrode can be measured by using Equation 4.1 and 4.2 below, where A represents the area of overlap, ε_r is the relative permittivity, $\varepsilon_o$is the electric constant, and d is the separation distance between the two plates.

$$C = \frac{\varepsilon_r \varepsilon_o A}{d} \quad (4.1)$$

$$C_{total} = C_{fing} + C_{gnd} + C_{env} \quad (4.2)$$

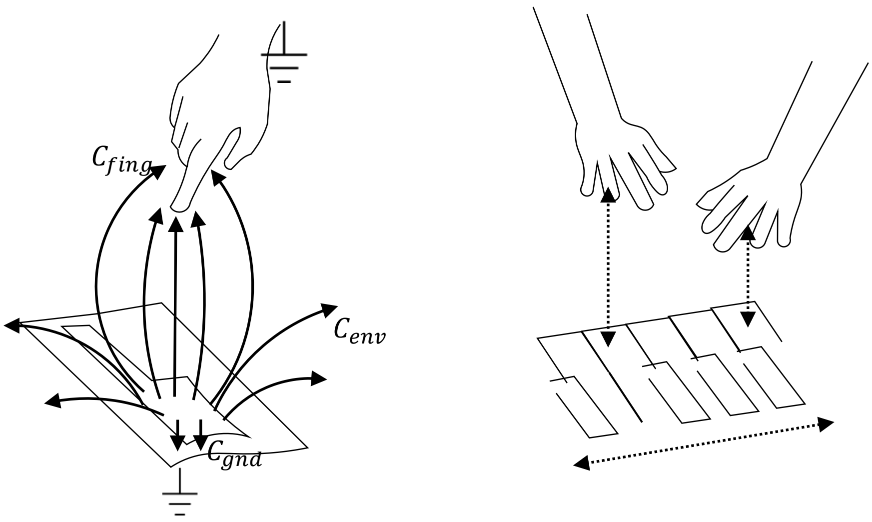

Figure 4.1: a) Electric field lines between a conductive fabric top layer and an approaching finger b) two hands hovering around the poly-proximity keyboard

Figure 4.1b shows an example application of our poly-proximity keyboard, where the hands can hover in the air to trigger discrete notes and then towards and against the keys to control sound parameters similar to a laser harp. Proximity sensing ultimately uses the same approach as touch sensing, but with much more sensing resolution and sensitivity on the read-out to detect this very small change of capacitance. In this project, the MPR121 Proximity Touch Controller was used. The fact that this capacitive sensing chip has 12 floating inputs, great sensitivity, and features proximity/touch threshold detection makes it suitable for the purpose of building one octave keyboard.

Several tests were conducted on this controller to see the influence of sensor's property to the sensitivity and dynamic range of reading. The results of these tests can be observed in Figure 4.2 below. It shows that the conductivity and area of each sensor contribute towards its sensitivity and dynamic range. In general, the capacitance drops exponentially as a finger approaches closer to the surface and then sharply triggering a touch event from the controller chip. Therefore, the touch state can also be defined as the condition when the proximity is close to the "zero" level.

Conductive woven fabric is shown in here to perform better than knitted fabric, since it has a greater conductivity, as listed in Table 3.2. With a pad size of 12x12 cm, proximity of up to 20 cm can be detected, while 18 cm is the maximum distance detectable by the knitted sensor pad. Cutting the sensor pad to a smaller size (in this case, representing a piano key), also reduces its response further to 12 cm. These observations agree well with Equation 4.1 and 4.2 above.

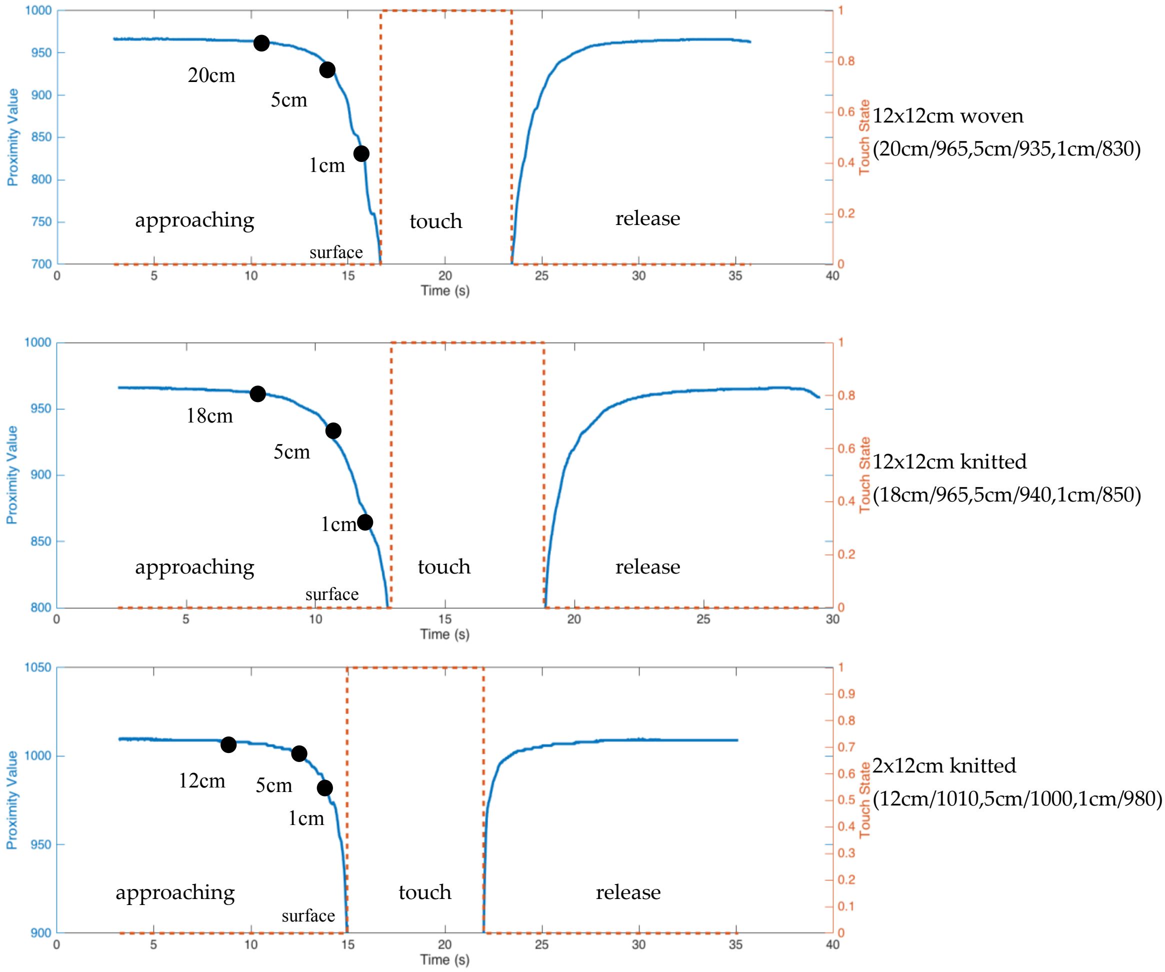

Figure 4.2: Capacitance change from finger approach, touch, and release on three different scenarios showing both proximity capacitance value and touch state

We observe a considerable increase in sensitivity and linear response of up to 25cm as shown in Figure 4.3 when using the multiplexed sensing feature or '13th' electrode of MPR121. This is because multiplexing all electrodes gives an effective large sensing surface area of 22x12cm; note that multiplexing here means the grouping of all electrodes into one, as described by MPR121 [71]. This feature has not been much exploited, even though it could have many interesting applications especially in low power electronics. For example, by letting the system to sleep while the sensors periodically detect an approach. In musical controller perspective, a performer could have the option to change from poly-proximity to multiplexed-proximity by triggering a switch or perhaps, the controller could automatically transition as their hands wave from higher distance towards near proximity.

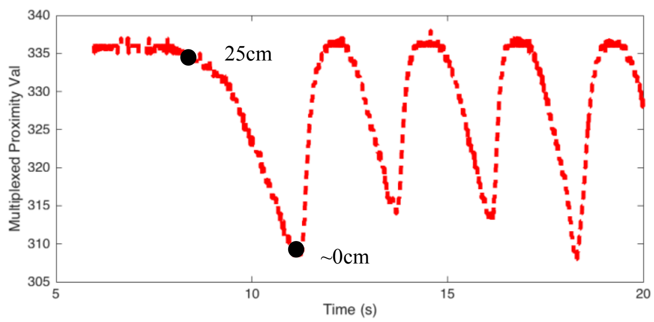

Figure 4.3: Multiplexed sensing capacitance change in response to approach

4.1.2 Electric Field

Another modality that has been explored in this project is the ability to sense electromagnetic field, specifically electric hum. Zimmerman *et al.* describes several approaches in using electric-field as physical interaction interfaces [65]. As shown in Figure 4.4, our body can act as either a shunt disrupting electric field between a transmitter and a ground, as a transmitter, by coupling our body to a transmitter itself, or as both by crossing over between these modes. The fact that electromagnetic waves are all around us makes us a “living transmitter” or “living antenna” and motivates the exploration of this approach.

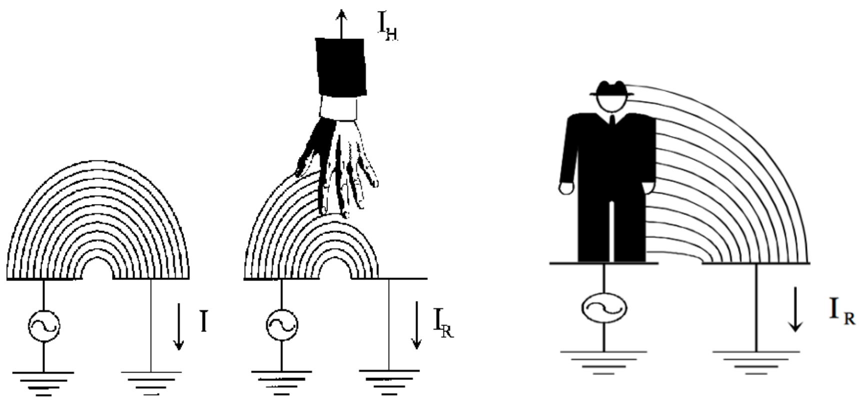

Figure 4.4: Human body as a shunt and as a transmitter (reprinted [65])

AC noise from the main power line that typical ranges from 50 to 60 Hz depending on the country, generates one of the strongest electromagnetic background around indoor environment that easily gets coupled to our body. By directing this to an IV converter, as covered in the next chapter, we can detect the strength of this AC coupling. Figure 4.5 shows the waveforms of this AC hum sensing on 2x12 sensing pad in two situations (closer and further away from the main source). It can be observed that we can measure the current coupled by the mains hum to our body to detect both touch and proximity.

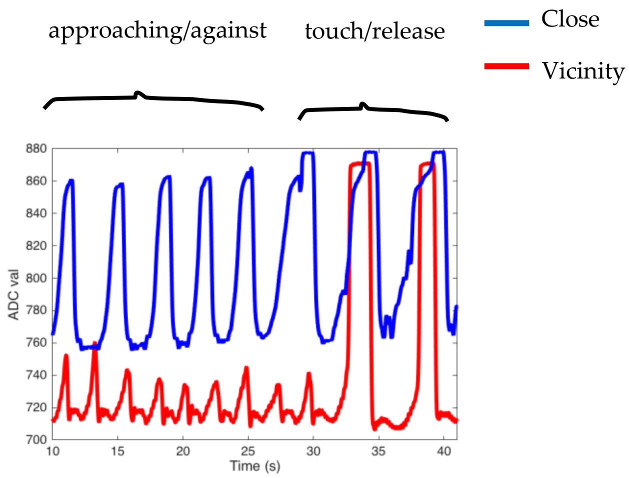

Figure 4.5: Passive AC hum detection with finger approach and touch in two cases: closer and further away from the EMI source.

When our body is further away from the main source (red), the proximity effect is visible up to 5 cm from the pad and jumps to a steady value as our finger strikes to the pad. Controlling the trans-impedance gain and band-pass gain of the circuit could improve the dynamic range. On the other hand, the signal strength is largely amplified when our body is closer to a main source (blue) resulting in a more sensitive reading to proximity of up to 10 cm. The size of the pad does not influence the sensor response that much, as the approach deals more with the current magnitude than field coupling. Threshold calibrations are crucial in this method to detect both touch and proximity as the response is largely influenced by our body's characteristics as an antenna and the electromagnetic noise strength around our environment.

Nevertheless, the most attractive and novel scenario of using electromagnetic coupling is when our body acts as a receiver antenna as, illustrated in Figure 4.6. After a finger strikes to a conductive fabric key, the key then becomes a receiver and the electromagnetic noise strength picked up by the keys can then be controlled by moving the other hand towards an electromagnetic source which in this case, is a minimally shielded device connected to the power line. The sensitivity depends on the field strength of the source, but in our case, it ranges from 60cm to 1m. The waveforms reveal the relative distance and different gestures as our hand approaches a transmitter resulting in an instrument that works similarly as a theremin. This enables us to continuously control certain sound parameters by performing non-contact gestures while as well in contact physically with the keyboard

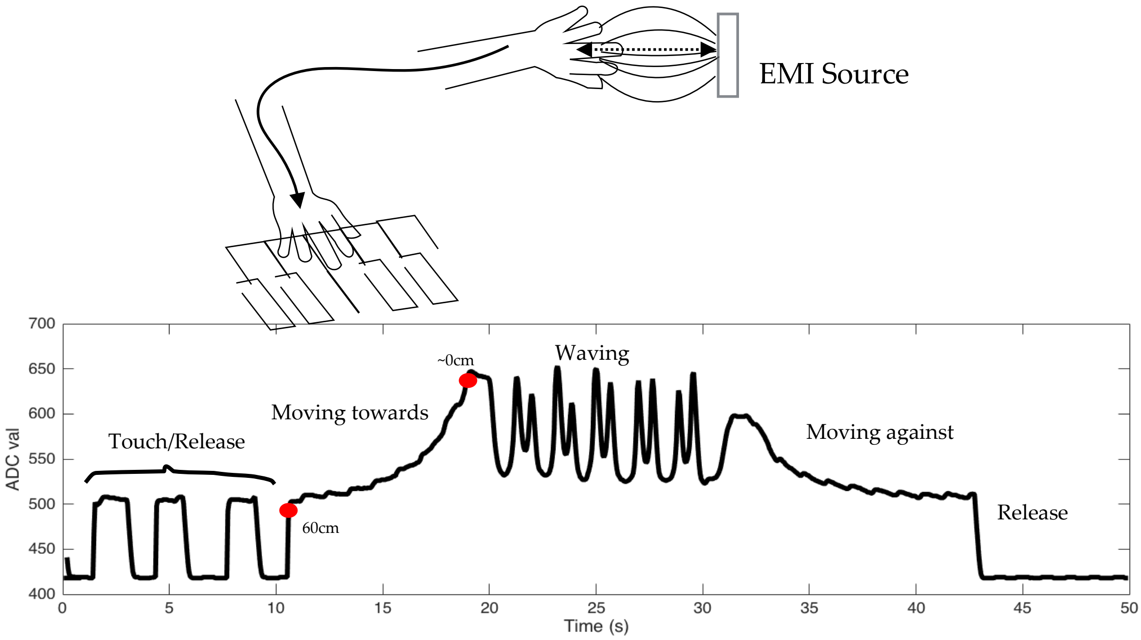

Figure 4.6: a) Current transfer between a source and poly-receiver b) Waveform of electric field sensing as a finger touches and the other hand waves towards and against the source (red dots show the distance of our left hand relative to the source)

4.1.3 Pressure

There are many fabric pressure sensors existing, mostly capacitive or resistive-based. Capacitive fabric pressure sensors are challenging to implement, since common textiles perform as a bad dielectric and it is very challenging to make a reliable interface between each layer. Their permittivity as an insulator could change over a number of uses, time, and condition. The systems to implement them are also rather complex, and mostly require oscillation-based circuits due to the small change in their capacitance [30]. Therefore, based on these observations and because of the nature of this project, resistive fabric pressure sensing was implemented instead. Even though there are several piezo-resistive sheets around, they are mostly woven or non-woven, such as Velostat. Using knitted fabric for every part of the sensate surface is particularly interesting in this project, since they are soft, conformable, and deformable, supporting the basis of this work.

The pressure sensing element, as illustrated in Figure 4.7, is a multi-layer structure made out of piezo-resistive fabric and mesh fabric sewn in between two conductive fabrics. The piezo-resistive fabric is a knit fabric coated with PPy conductive polymers in certain concentration that can be requested. In this case, we used Eeonyx LTT-SLPA-20k, its characteristics can be seen in Table 3.3. Since it is piezo-resistive, the resistivity of this fabric changes with force. Similar to how an FSR works, a higher pressure compresses the conducting molecules coated onto the fabric. These molecules then form a network with each other, allowing more current to flow and reducing the resistance around the area in contact. Therefore, the larger the force area is, since these networks can be assumed in parallel (Figure 4.7b), the lower its total resistance becomes.

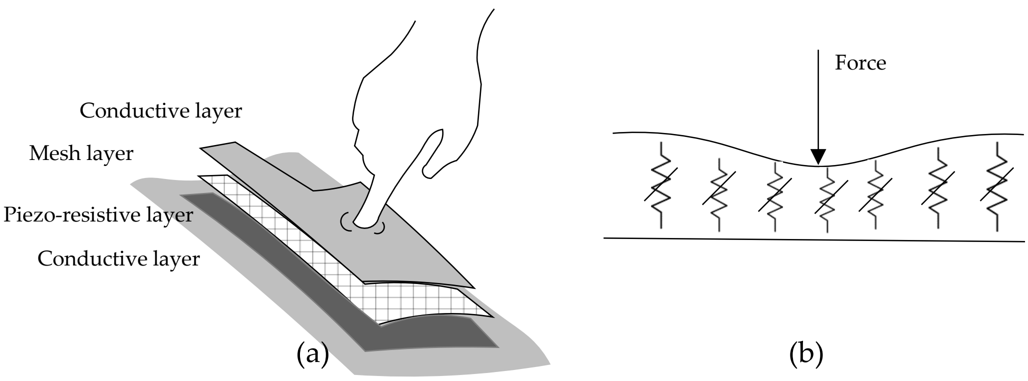

Figure 4.7: a) Multi-layer structure of fabric pressure sensor b) Resistance network in a piezo-resistive layer

The decision to include mesh fabric in the structure manifested from the non-uniformity of resistance baseline values after the first development of this pressure sensing fabric. It was experienced that, as the sewing line gets closer to and further from the border of the piezo-resistive fabric, the tension applied by this straight stitch around the sandwich structure of the fabric changes considerably, resulting in a non-uniform resistance baseline even when the fabric is on its uncompressed state. The introduction of a mesh layer solves this problem, as it will separate the conductive fabric with the piezo-resistive fabric and avoid tensions and accidental contacts between them.

Nonetheless, adding a mesh layer as a part of the pressure sensing element could possibly reduce the sensitivity of the pressure sensor. We then experimented and characterized different types of mesh fabric to test the relationship between the gap size and thickness with each sensor's sensitivity. As shown in Figure 4.8a, three types of mesh fabric were tested: a purple thick nylon-spandex mesh (diameter:0.5mm), a white thin net mesh (d:1mm), and a teal polyester knit mesh (d:3mm).

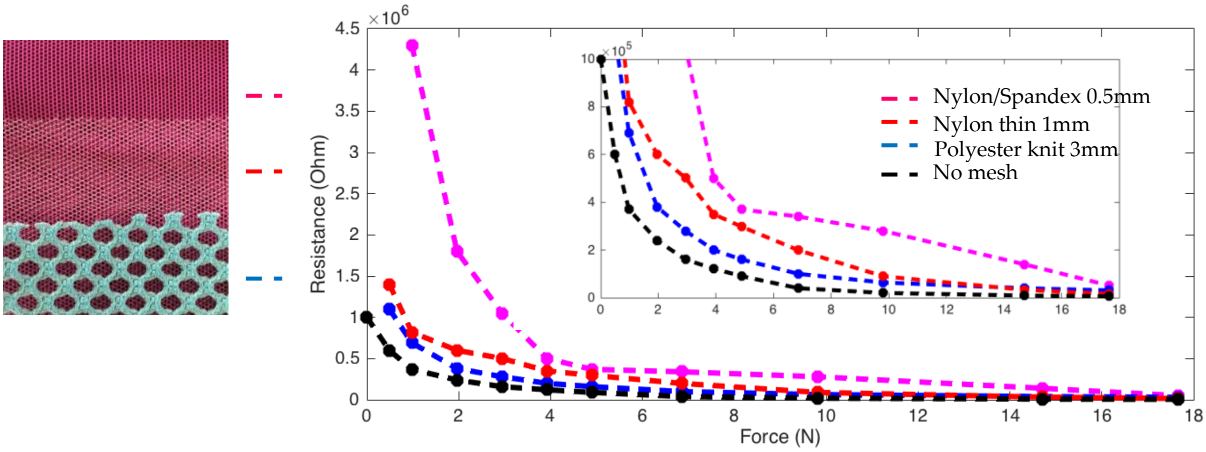

(a) (b)

Figure 4.8: a) Mesh fabrics under-test b) Pressure sensor's response to force with different mesh fabrics

Figure 4.8b shows the characterization results of fabric pressure sensors with and without mesh fabrics inside. Several values of mass were applied on top of a supporting base with a diameter of 1.7cm representing a finger surface. The force applied (0-18N) is sufficient enough to get an idea of typical piano keystrokes [66]. The results explain that even though the pressure sensor without a mesh fabric is very sensitive towards very low force, due to the pre-tension as previously explained, the resistance begins with a finite value instead of infinite (open-circuit) reducing its sensitivity at a higher force. Using a smaller hole and thicker mesh, in the case of nylon-spandex mesh, is not suggested as it will not be able to read soft presses.

The options were then narrowed to thin mesh, or knit mesh with a larger gap. Since thin mesh practically could short the pressure sensors interface if the sewing tension is too high (since it is very thin), knit mesh was finally the one used. It has a larger gap, which means that it also responds well to soft presses. This fabric is rather thick and squishy, enhancing the tactile feel of this pressure sensor. Figure 4.9 shows the measurements taken on the fabric pressure sensor with a knit mesh. The pressure sensor was connected in a voltage divider configuration with a 100kΩ reference resistor and then directed to a high-impedance buffer before going to a microcontroller for ADC reading. It can be observed that this pressure sensor works reliably and is able to detect soft taps, harder presses, as well as expressions.

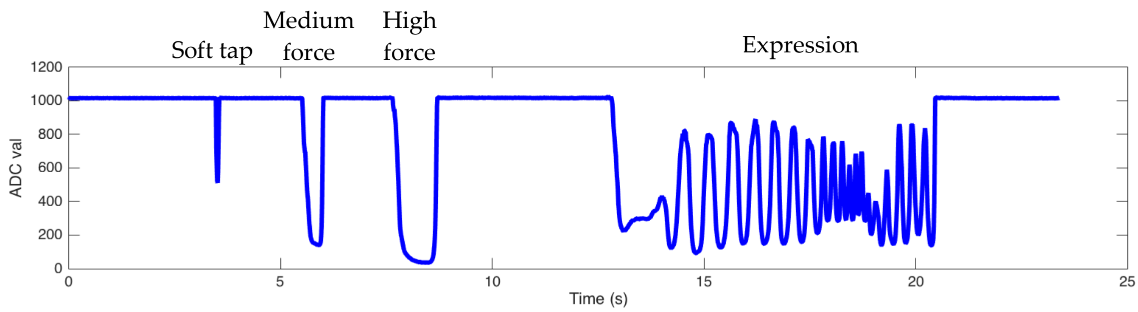

Figure 4.9: Fabric pressure sensor readings to soft tap, presses, and expression

4.1.4 Stretch

Piezo-resistive fabric was also used in this project for developing stretch sensors. Knitted fabric, due to its characteristics which are stretchable, sewable, and customizable, is a good textile substrate for coated stretch sensors. The coated fabric can be cut in different sizes in order to engineer its base resistance and durability. Not only seamless, coating the fabric itself with strain-sensitive material also eliminates the necessity of an interfacial layer or transfer process in the case of a printed or cured carbon-elastomer composite strain sensor. Their ability to be sewn also makes it possible to integrate them to any fabric.

However, even though knitted fabric strain sensors have been widely used recently by the DIY community, there has not been any rigorous analysis performed on their electrical response to stretch. It would therefore be interesting to see how the complex interlocked structures of knitted fabrics influence their electrical response to strain. By observing these characteristics, it is possible to study the stretch sensors working range, so that we can customize these sensors to conform to any particular range and avoid over-stretching them. The Instron 4411 Universal Testing System machine was used in this characterization to study the mechanical and electrical response of several fabric stretch sensors with various strain elongations.

Figure 4.10 shows a piezo-resistive fabric undergoing a strain test. In order to measure the resistance change, both of the clamps were insulated with electrical tape because it was found that there is an electrical path between these clamps. A copper tape was then applied on each insulated clamp before tightening it along with the fabric sensor under-test. These copper tapes provide connection from each side of the fabric sensor to the read-out circuit that comprised a potential divider, buffer, and micro-controller. The data from both the

Instron and micro-controller were then recorded through serial communications to a computer.

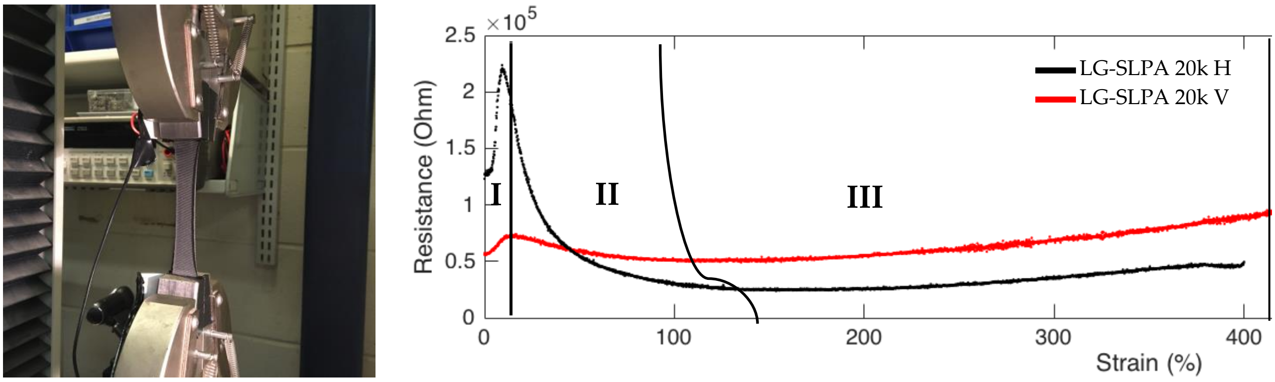

(a) (b)

Figure 4.10: a) A fabric stretch sensor undergoing a strain test b) Characterization results of two fabric stretch sensors showing three main regions of behaviour

As shown in Figure 4.10b, we can observe the resistance behaviour of stretching two piezo-resistive fabric cuts (2 x 6 cm) in course (vertical/V) and wale (horizontal/H) directions to up to four times than their original lengths. There are several interesting features in this behaviour. We can separate these into three regions and compare them with the typical behaviour of yarns in knitted fabrics under deformation, as illustrated in Figure 4.11.

- The initial region (I), which shows an increasing trend, is due to the slippage of yarns from its relaxed state. As this reduces the contact area between the interlocked points throughout the fabric, the total resistance increases until it reaches a peak.

- The second region (II) is the most important, since this is the main change that determines most of the degree of stretch on the fabric sensor. It tends to decrease in pattern due to the orthogonal compressive stress when the fabric further stretches, as the loops now strengthen and form a firm contact with each other horizontally, reducing the total resistance of the fabric sensor.

- The last region (III), occurs when further tension triggers micro-cracks on the piezo-resistive coating; therefore, reducing the conductive pathways and its total resistance. This region should then be avoided since it could damage the ability of the stretch sensor to return to its baseline value, influencing the sensor's repeatability.

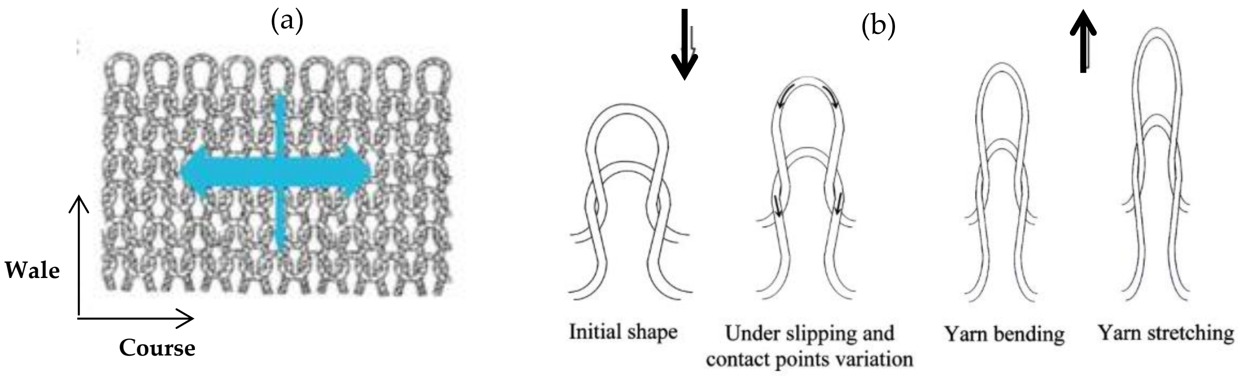

Figure 4.11: a) Current density in a knitted fabric b) Deformation of interlocked structure along wale direction (reprinted from [67,68])

From the previous results in Figure 4.10, it can be estimated that the maximum strain the stretch sensor could handle is around 100-150%, which is around the maximum recommended strain of the knitted fabric itself. We then characterized both electrically and mechanically two types of knitted fabric sensor: LG-SLPA (9% Elastane, 91% Nylon) and LTT-SLPA (28% Elastane, 72% Nylon) with two surface resistivities (20k and 60kΩ) and different cuts direction (course and wale) in terms of strain applied. All results are shown in Figure 4.12.

In comparison, it is apparent that having a lower surface resistivity will reduce the resistance range given by the stretch sensor as more conductive coating is introduced. More concentration of conductive coating also results in a higher tensile strength. In terms of the types of fabric, it can be observed that LG-SLPA, with less amount of elastane and lower stretchability, has a lower resistance sensitivity towards strain, especially in the wale direction, whereas LTT-SLPA, with more elastane knitted in the fabric, provides a higher sensitivity in both cases. Based on the mechanical property, the fabric sensors cut in course direction proved to have lower tensile strength and resistance compared to the stretch sensors cut in the wale direction.

Knitted fabric structure in Figure 4.11a explains this relationship. Yarn structure in the wale direction provides slippage and contact points which correspond to its higher tensile strength, while the yarns in course direction have less slippage and contact tensions with their neighbours, making the more stretchable upon tension. Therefore, stretch sensors in course direction tend to be less sensitive in resistance, as its structural change is not as dynamic as stretch sensors in wale direction; however, this could change as the fabric becomes more elastic (see Figure 4.12c and d in the case of LTT-SLPA).

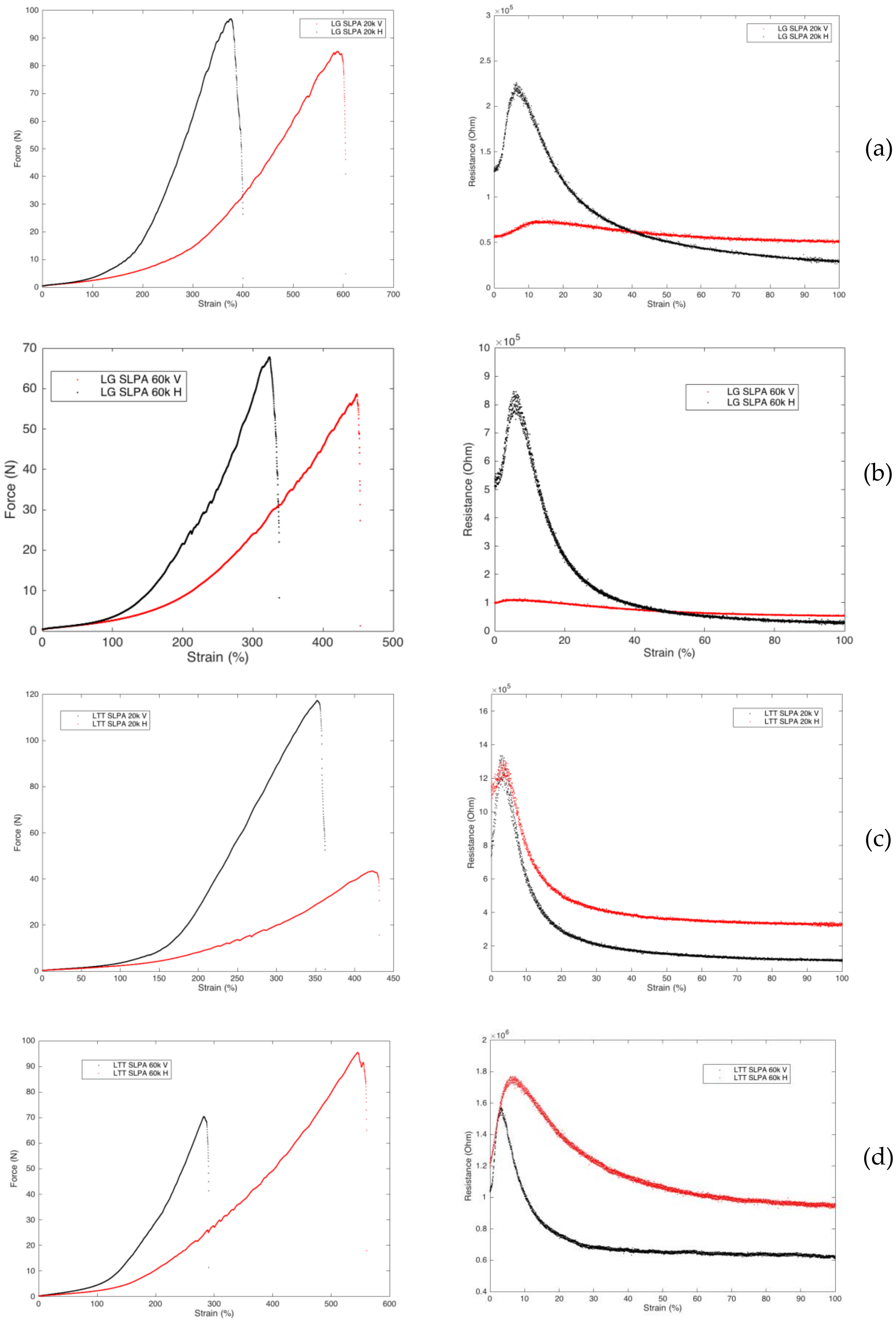

Figure 4.12: Tensile strength and resistance measurement of fabric stretch sensors with two different cuts (course/V and wale/H), elasticities, and surface resistivities

Finally after observing each of the fabric sensor's properties, we decided to use The LTT-SLPA-20k fabric, cut in wale direction because of its both good mechanical and electrical properties. Several observations worth mentioning are:

- Transferring these fabric sensors onto another fabric substrate improves their reliability, as the substrate provides additional support to recover them back to their original length.
- This support substrate also increases the ultimate tensile strength of the sensor, which then correlates proportionally to the tolerable stretching distance.
- Having larger fabric sensor width, although reduces the baseline resistance, improves the structural integrity of the sensor thus, increases its durability.

Figure 4.13a shows a sample of a fabric stretch sensor sewn onto a stretch knit fabric for further testing. The sample was prepared by cutting a ribbon of piezo-resistive fabric sensor in the wale direction and then sewing conductive thread at both ends of the fabric sensor onto a stretch fabric substrate.

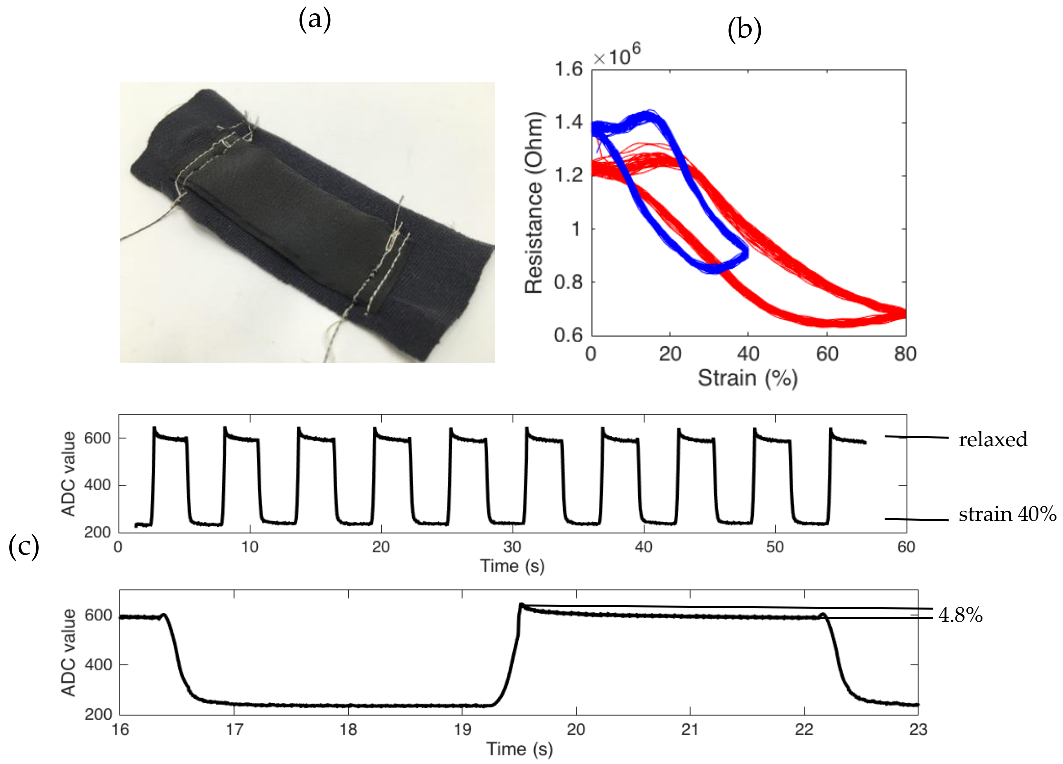

Figure 4.13: a) stretch sensor sample b) hysteresis and repeatability test c) square-wave testing showing relaxation behaviour (strain 40%)

The result of the first testing, which was to examine the hysteresis and repeatability of the stretch sensors, is shown in Figure 4.13b. Two fabric stretch sensors, both with similar size, were stretched back and forth 100 times at 40% and 80% strain. The results confirm the hysteresis behaviour of the fabric sensors, which is mainly caused by the structural change of yarns upon tension and relaxation. Both sensors also show a good degree of repeatability; some noise exists, but this is mainly caused by the initial adaptation of the sensor-thread interface. A stronger tension when sewing the conductive threads into the fabric will most likely reduce this noise. Another critical behaviour is the sensor relaxation time, which is revealed in Figure 4.13c with square wave testing. The sensor undergoes relaxation period of around 2s, when it is stretched back and adapts its resistance by around 30 ADC points from the initial value (4.8%). Finally, Figure 4.14 below illustrates some of the applications of stretch sensors embedded in a stretchable fabric.

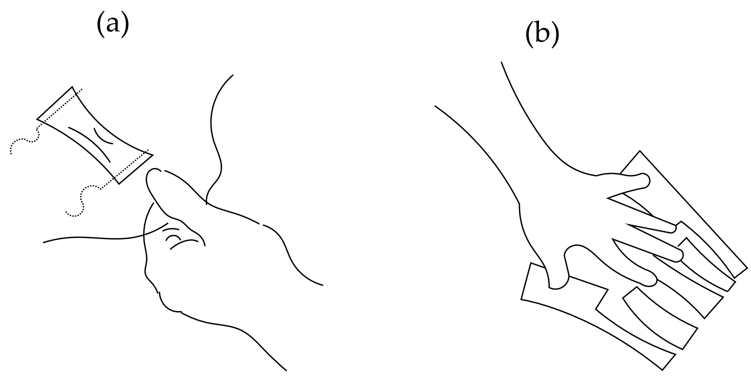

Figure 4.14: Several applications of stretch sensors for physical interaction intended in this project: a) pulling and b) expanding fingers

4.2 Additional Fabric Interfaces

4.2.1 Fabric Ribbon Controller

The ribbon controller is a long sensate surface that measures position along one axis, allowing continuous expression by sliding our finger sideways. It is designed to be "plug and play"; therefore, is modular and can be attached by snapping the metal connectors to their pairs on the main keyboard. Since there has not been any prior effort in making a fabric-based ribbon controller, different smart textile materials and configurations were explored in this project. Figure 4.15 shows the structure of various fabrics embedded inside the ribbon controller. It consists of a multi-layer combination of common, mesh, conductive, and resistive fabrics. The main substrate allows the integration of these different layers and provides a base for the conductive thread interconnects to the terminal. Additional stacks for detection of touch and proximity as well as pressure can be integrated as necessary with a separation fabric.

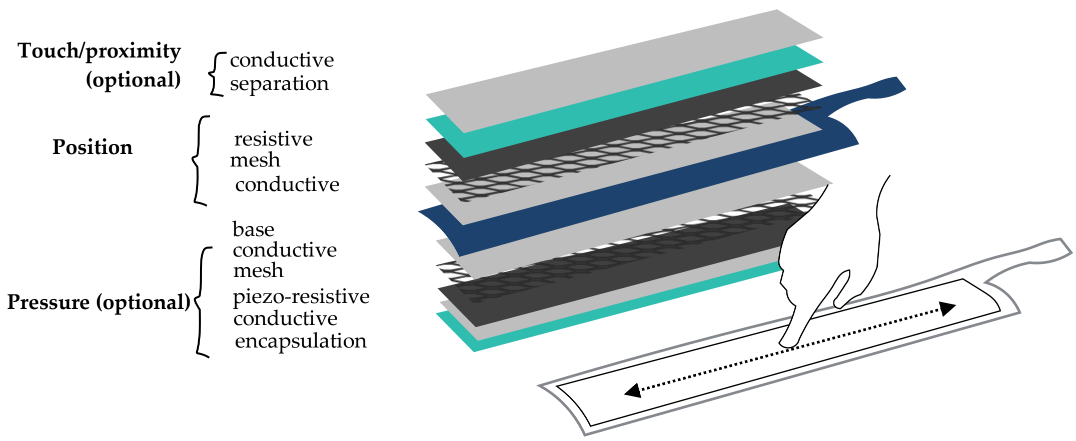

Figure 4.15: The structure of a fabric ribbon-controller

Figure 4.16 provides two methods of location sensing in a fabric-based ribbon controller. The first method is based on a voltage gradient between two lines at both ends of a piezo-resistive/resistive fabric. When a finger strikes the pad, connection is made between the resistive fabric and bottom fabric through a mesh fabric. The bottom fabric is conductive and is connected to an ADC to read the voltage in a potential divider configuration. This voltage value directly correlates to the position of the finger in respect to ground; the ADC input is high impedance (see Chapter 5.4). The second method is based on calculating the resistance of a resistive fabric from one edge to the contact point. It requires external reference resistor to form a potential divider. This configuration could only work with a resistive fabric as piezo-resistive fabric also has a z, pressure change.

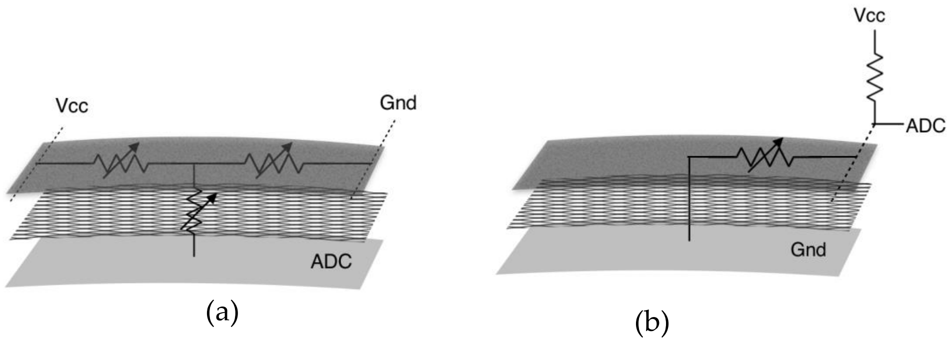

Figure 4.16: Two methods of position sensing a) voltage gradient b) resistance

The second method was the one finally used since it only requires two instead of three thread connections; therefore, reducing the implementation effort. Woven resistive fabric made out of 87% polyester and 13% carbon resistive yarn, in 30cm length was sewn altogether with mesh and conductive fabric on top of a main fabric substrate with. Figure 4.17a shows the ADC readings of the ribbon-controller in action and its linearization to resistance (Figure 4.17b). Another thing to note that this method also enables touch-detection with thresholding since there is a considerable jump observed from the steady state value as the ribbon detects a touch event. We also discovered a circuit configuration that could give both pressure and position values of the ribbon connector simultaneously using configuration in Figure 4.16a. The circuit is illustrated below in Figure 4.18.

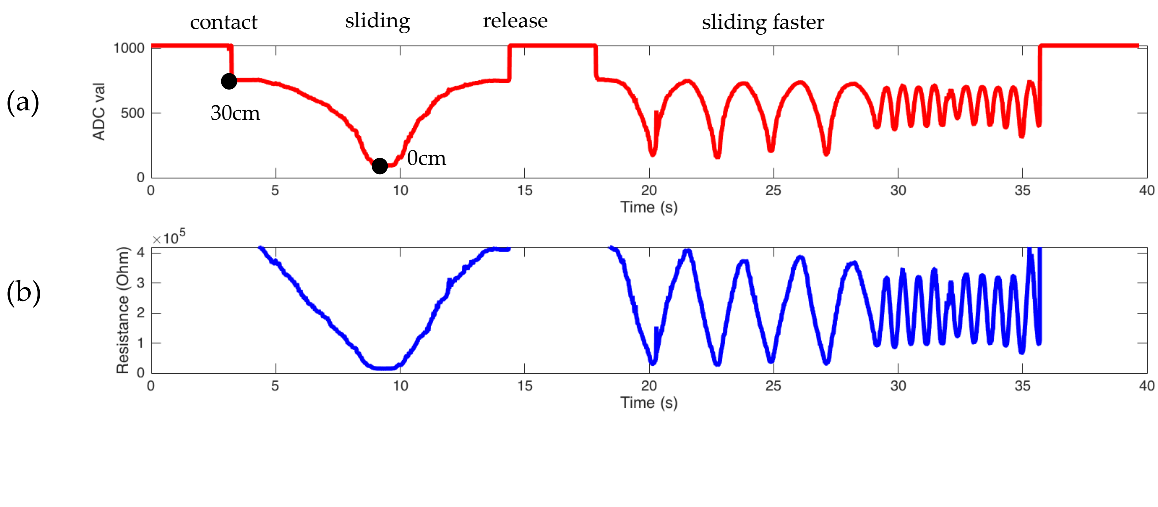

Figure 4.17: a) ADC readings of ribbon-controller testing b) conversion to resistance

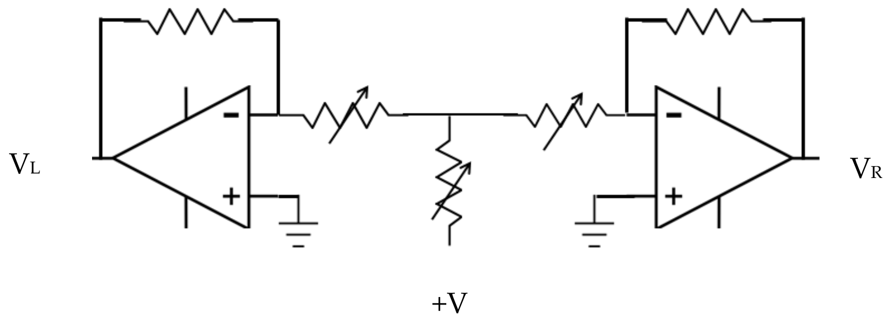

$$P = V_R + V_L \qquad x = \frac{V_R - V_L}{V_R + V_L}$$

Figure 4.18: Analog circuit for simultaneous sensing of location and pressure in Figure 4.16a

4.2.2 Fabric Touchpad

The development of fabric touch interfaces, especially for gesture controllers, has received a great amount of interest from the smart-textile community. In this project, we designed and implemented a fabric trackpad as an extension of a musical controller. Similar to the ribbon-controller, the trackpad was designed to be modular and can be snapped to the keyboard to extend performer's expressions.

There are several techniques for developing a touchpad, mostly adapted from the current touchscreen technology: resistive, capacitive, infrared, and surface acoustic wave [69]. The last two methods involve light transmission and ultrasonic waves and are not feasible for deformable fabric interfaces with the current smart textile technologies. Since our trackpad will be used as an extension of the keyboard, single-touch capability with a relatively high resolution for continuous control is sufficient. Resistive technology is therefore suitable in this case, and how this technology is adapted to the fabric-based musical interface will be explored in this section.

Even though there has been a considerable amount of effort on developing resistive-based fabric touch interfaces, most of them require conductive traces on the finger as a ground

[35]. Measuring the Cartesian coordinate of the finger therefore requires building and calibrating a model. This approach is therefore not robust and independent. Inspired by the maturity of current resistive touchscreen technology illustrated in Figure 4.19, we tested two approaches: 5-wire and 4-wire configurations in our fabric trackpad design.

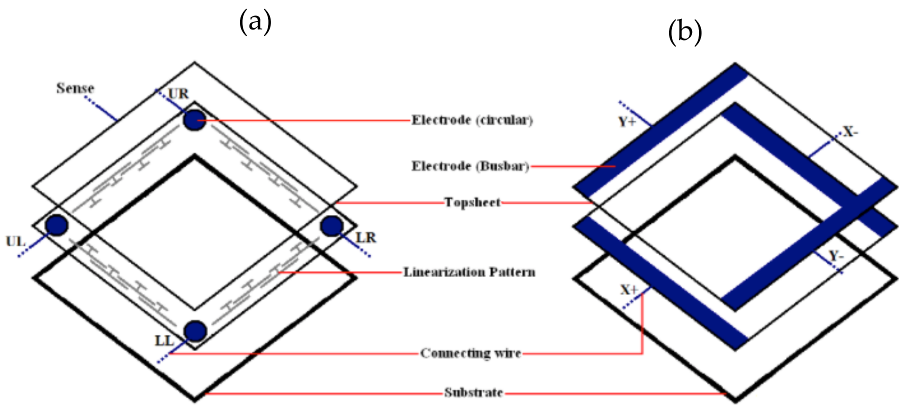

Figure 4.19: Electrodes configuration in a) 4-wire b) 5-wire resistive touch screen (reprinted [70])

The first approach, the 5-wire configuration, was realized by sewing a conductive fabric on top of a fabric substrate followed by mesh and resistive fabric. Four conductive connections were then embroidered on each corner of the resistive layer. This structure is presented in Figure 4.20 below. To measure the coordinate of the finger, the corner points are periodically set to either represent a low, high, or high-impedance, as shown in Table 4.1. If two neighbouring points represent the same value, a high for example, the voltage across these two points should be the same assuming an equipotential voltage distribution on the resistive layer. Setting the other two points to ground will result in a unidirectional voltage. This voltage gradient can then be read by the global conductive layer to measure the position of touch point in an axis. Alternating the voltage gradient to another direction will give position of the complementary axis.

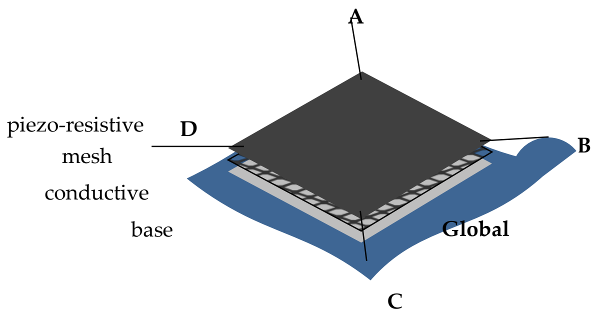

	A	B	C	D	Global
Initial/Standby	Gnd	Hi-Z	Hi-Z	Hi-Z	Pull up
X-Position	Gnd	Vcc	Gnd	Vcc	ADC/Hi-Z
Y-Position	Gnd	Gnd	Vcc	Vcc	ADC/Hi-Z

Figure 4.20: 5-wire configuration of fabric touchpad; Table 4.1: 5-wire settings for position sensing

To test the touchpad in 5-wire configuration, we drew two square patterns, one close to the edge and one close to the centre point, as well as a star pattern. Figure 4.21 below shows the results of these tests. It can be observed that there is a non-linear behaviour on both patterns closer to the edges. The non-equipotential voltage distribution across the edge is the reason behind this. As the touch point is further apart from the voltage source, due to the unequal resistance distribution across the layer, the voltage starts to drop. To solve this issue, a linearization pattern as illustrated previously in Figure 4.19 can be applied by sewing conductive thread in certain patterns across all sides. However, it is rather challenging in practice since it requires a highly precise, symmetrical pattern across all sides.

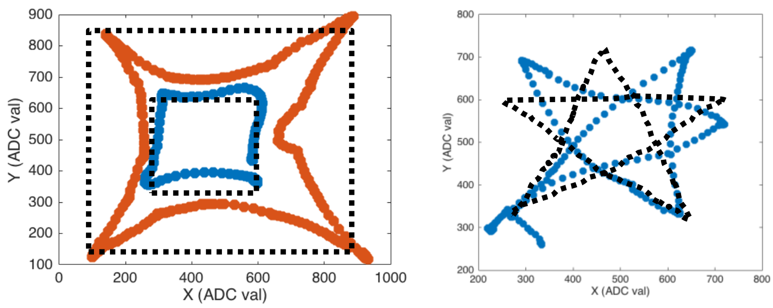

Figure 4.21: 5-wire configuration drawing tests

The second approach is shown and explained in Figure 4.22 and Table 4.2. The 4-wire configuration comprises of two resistive fabrics in between a mesh layer. Conductive threads were sewn at two opposing sides of each resistive fabric orthogonally to each other. In this approach, one of the conductive lines on each resistive fabric becomes ADC line while the other one is set to high-impedance. The other resistive fabric gives a voltage gradient by setting each conductive line either low or high. This mechanism happens alternately, as the voltage read by the other fabric pair as an ADC contact represents either the x or y-position value.

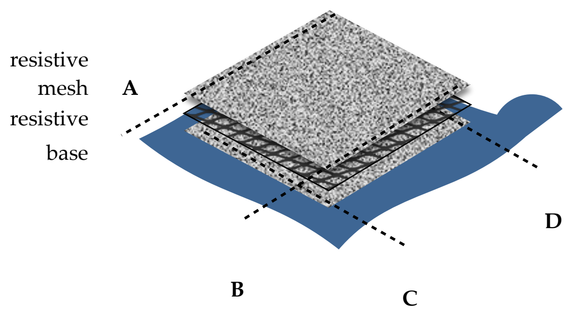

	A	B	C	D
Initial/Standby	Hi-Z	Hi-Z	Hi-Z	Hi-Z
X-Position	Vcc	Gnd	Hi-Z	ADC/Hi-Z
Y-Position	ADC/Hi-Z	Hi-Z	Vcc	Gnd

Figure 4.22: 4-wire configuration of fabric touchpad; Table 4.2: 4-wire settings for position sensing

Similar drawing tests were conducted on this resistive fabric trackpad with the 4-wire configuration. As shown in Figure 4.23 below, it performed better compared to the previous configuration. There is no problem in voltage distribution anymore since in this 4-wire technique, two resistive layers are required, and the voltage gradient in both cases now becomes unidirectional. Some noise can be observed in these raw data; this is mostly influenced by the blunt contact area from our finger. Nonetheless, the results still show that this fabric trackpad could read several simple to complex stroke patterns satisfactorily. The quality can be improved by adding a smoothing capacitor on the hardware or averaging on the software side. Finally, Figure 4.24 demonstrates a complete design of the fabric trackpad in the 4-wire configuration integrated with pressure, touch, and proximity sensing.

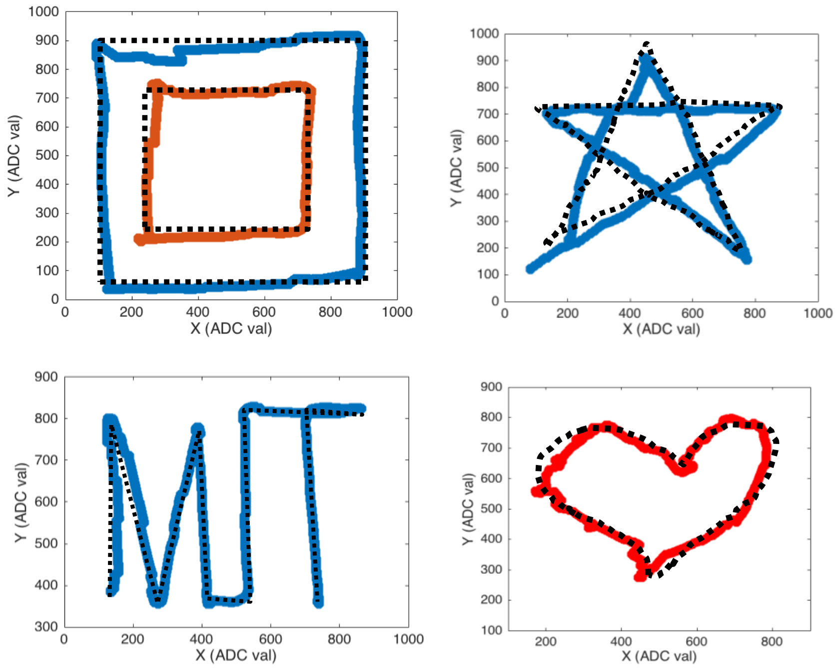

Figure 4.23: 4-wire configuration drawing tests

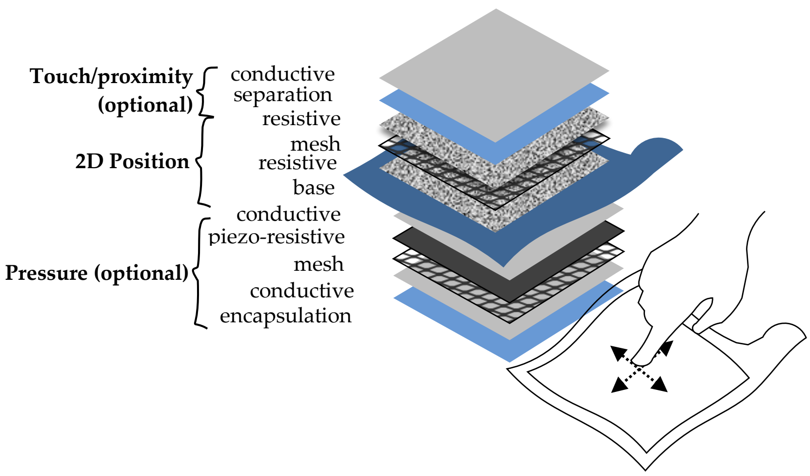

Figure 4.24: Final structure of the resistive fabric trackpad

Chapter 5:

Hardware Design and Implementation

5.1 Electric Field Sensing

Our body is a "living antenna" that could couple electric fields transmitted from the environment. We designed a circuit to specifically sense the electromagnetic noise shunt to our body from the power line (50-60 Hz) as used in [56]. The circuit is illustrated in Figure 5.1 below. It consists of three stages: trans-impedance amplifier, band-pass filter, and envelope detector.

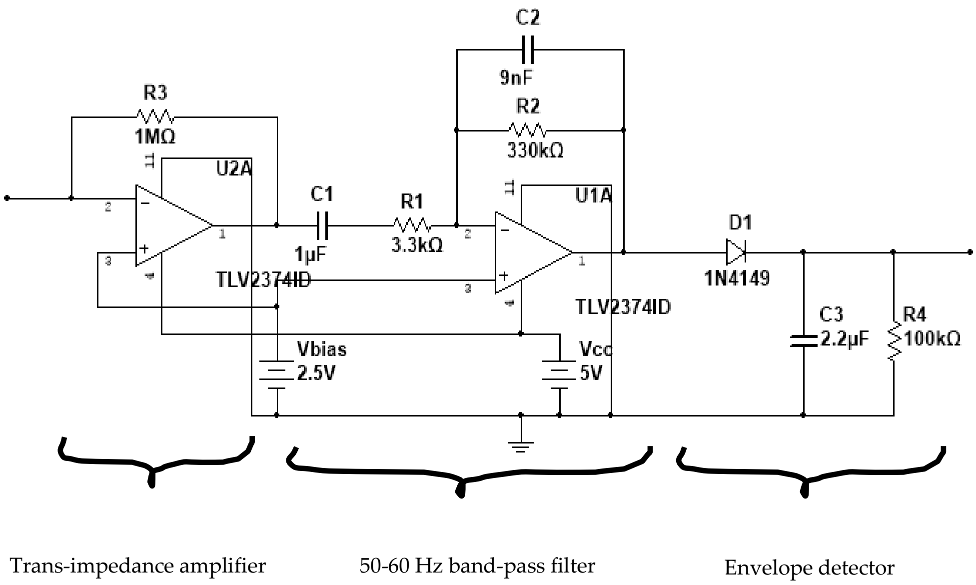

Figure 5.1: 50-60Hz passive electric field sensing circuit

The trans-impedance amplifier converts the current coupled from our body into voltage as our finger approaches a conductor. The feedback resistor amplifies the current by a factor of R_f, as written in Equation 5.1 below.

$$V_{tr} = -I_p x\, R_3 \quad (5.1)$$

This signal then goes through an inverting band-pass filter that attenuates unrelated frequencies and magnifies the signal of interest at a frequency around 50-60 Hz which is the standard for AC mains hum. The gain and cut-off frequencies are given by,

$$Gain = -\frac{R_2}{R_1} \qquad (5.2)$$

$$fc_1 = \frac{1}{2\pi R_1 C_1}, fc_2 = \frac{1}{2\pi R_2 C_2} \qquad (5.3)$$

After figuring out all of the components with the standard values, the frequency response of the circuit was simulated with the result given in Figure 5.2 below.

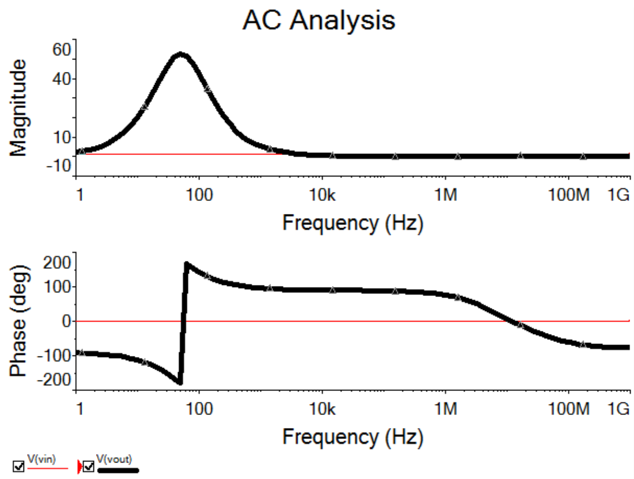

Figure 5.2: AC analysis of 50-60Hz BPF

The band-pass filter gives an expected response with the highest magnitude around 50Hz and Q-factor of 1.6. We used the TLV2374 due to its rail-to-rail input and output capability and we biased the non-inverting input of the TLV2374 to avoid working in negative voltage swing. To accommodate this bias voltage, a voltage follower biasing as shown in Figure A.4, Appendix A was integrated into the circuit design.

Because there are twelve electrodes in our keyboard, a multiplexer is required to sense electric hum from each electrode. Our first attempt was to multiplex the signals from each trans-impedance amplifier before the band-pass filter stage (Figure 5.4a). However, there were some challenges faced around the envelope detector. Due to the slow charging-discharging, low-frequency of the signal of interest (period of 1.7-2ms), the capacitor in the envelope detector could not cope with the multiplexer speed, resulting in parasitic voltage from one reading to another (Figure 5.3a). Changing to a lower capacitor and higher resistor value (0.22uF,1M) solved this problem (Figure 5.3b). However, care must be taken so that the time-constant of the envelope detector is in an acceptable range (as given in Equation 5.4;

f_m and f_c are modulation, frequency associated with human notion and carrier frequency, the 60 Hz power line frequency respectively); this is in order to minimise peak clippings and ripple distortions on the output.

$$\frac{1}{f_m} > \tau = \frac{1}{RC} > \frac{1}{f_c} \quad (5.4)$$

Since there was a lot of compromise with this circuit, we altered the circuit design to Figure 5.4b. Even though this means that the circuit is now larger, the result will give a more independent signal from each electrode as the multiplexer can now switch at a much faster rate.

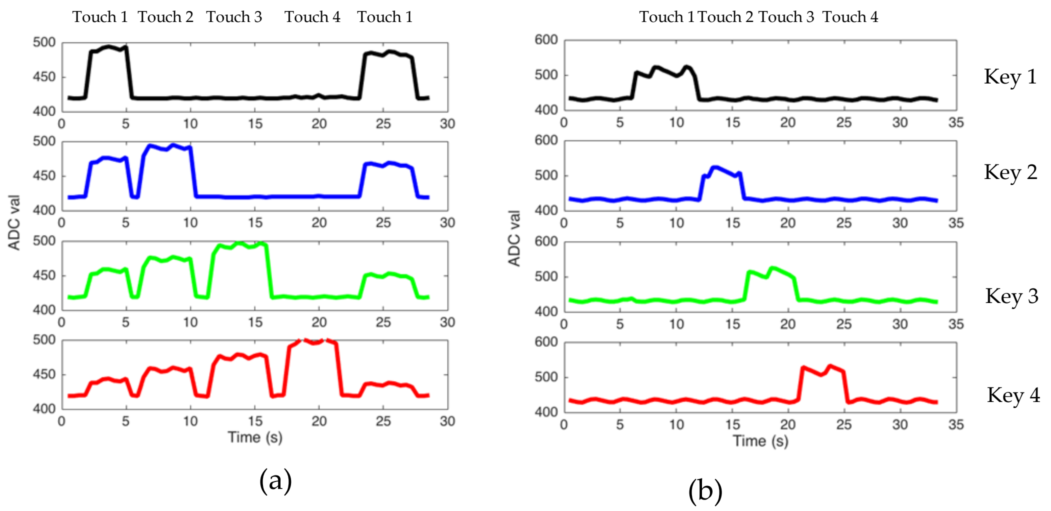

Figure 5.3: a) Observed parasitic effect in the multiplexing caused by the envelope detector's response b) after changing RC values

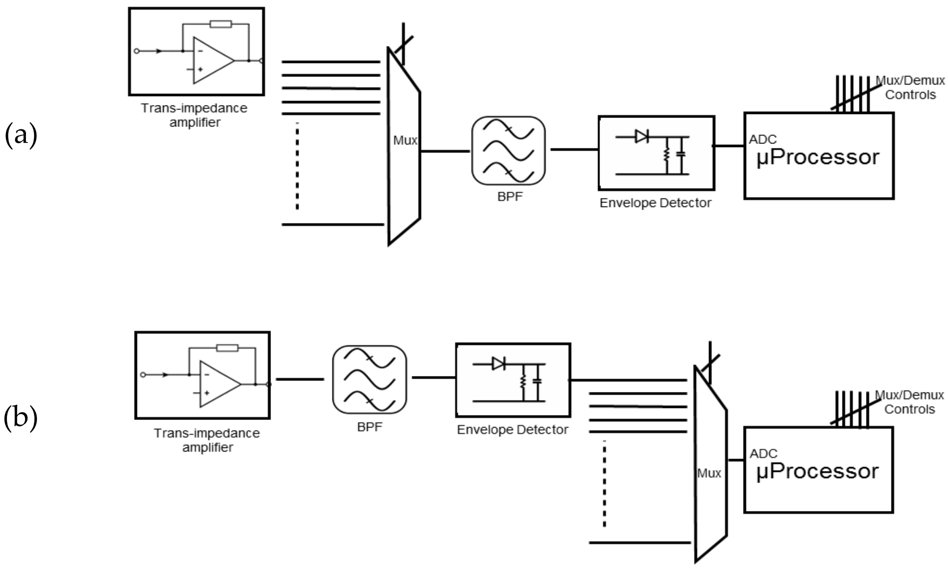

Figure 5.4: a) Previous approach of multiplexed hum sensing b) after revision

5.2 Capacitive Sensing

As previously covered in Chapter 4, the touch and proximity sensing rely on the capacitance change between our body as a virtual ground and a floating electrode. MPR121 12-pad touch sensor controller was used to measure capacitance from each electrode in this project. Not only does it have 12 channels that are perfect for one octave keyboard design, but it also has a good sensitivity and high dynamic range (1pF to 2nF) enabling proximity detection. Its I2C protocol allows four different addresses; therefore; therefore, the sensor input is extendable to up to 48 channels and can be extended more with I2C multiplexer. The sampling interval, which could be as fast as 1ms is sufficient for DMI design.

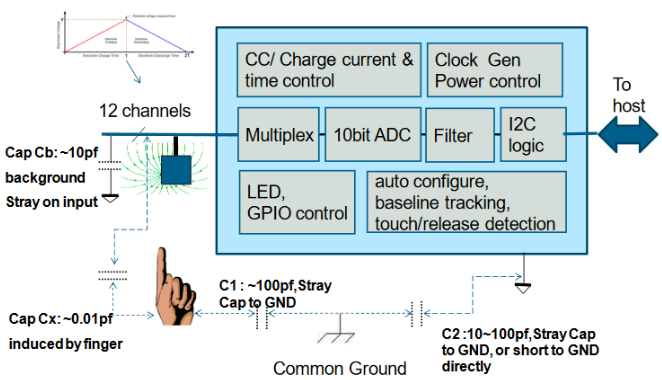

Figure 5.5: MPR121 capacitance measurement (reprinted from [72])

There are different ways of measuring capacitance; most of the methods use frequency-based oscillator circuit, time response of charging/discharging cycle, or charge measurement. The MPR121 works by measuring the voltage given by charging each electrode for a specified time and current. These current and time variables should be carefully set depending on the electrode design and stray capacitance; given a 10-bit ADC (1024 discrete values), the sensor therefore could detect a capacitance change as low as 0.01pF from a 10pF steady state. Trial and error tests were conducted to find the most suitable setting of these variables by observing the ADC steady value until it reaches its maximum, which is 1024. As a finger approaches, some of the charged current gets coupled to our body, reducing the voltage output from its steady value.

The touch/release detection works by real-time comparison of electrode data and an adaptive baseline value. There are three levels of filtering involved in the process; the last filter deals with a very low frequency that represents a slow capacitance change. This slow change is mainly caused by long-term use and environmental change and defines the baseline value. Setting touch/release thresholds to high values avoids capacitive noise from the environments, but could delay the touch/release detection and vice versa for low thresholds value.

This controller could also detect proximity if set carefully, setting a low threshold value also enables proximity/release detection. Moreover, the MPR121 features a multiplexed sensing configuration or the '13th' electrode that combines all the pads from each channel to represent a large sensing surface. As previously tested in Chapter 4.1.2, using this configuration considerably boosts the sensitivity of the sensing electrodes to proximity with a compromise of multiplexing all pixelated electrodes into one, hence not knowing the hand's position across the keyboard as a poly-proximity instrument.

5.3 Resistive Sensing

Most of the fabric sensors in this project, including the pressure, stretch, ribbon-controller, and touchpad, require resistive-based sensing to convert physical movements to digital values through the ADC. Figure 5.6 provides the most common circuits for resistive-sensing with their corresponding equation. Sensitivity, gain, linearity, power consumption, and voltage biasing are some of the factors involved in the design of resistive sensing circuits.

Non-inverting amplifier and current-voltage converter configurations have settable gain and linear response to resistance change; however, they need voltage biasing, which adds more complexity to the circuit design and because of this, could not utilise the whole available range of voltage swing. Wheatstone bridges on the other hand, are mostly used to detect a small change in resistance with high precision; for example, from a strain gauge or thermometer. Since based on the characterisations, most of our sensors give a considerable change and dynamic range, it is not necessary to use this approach, as it will require at least three resistors with a signal conditioning and amplification stage afterwards.

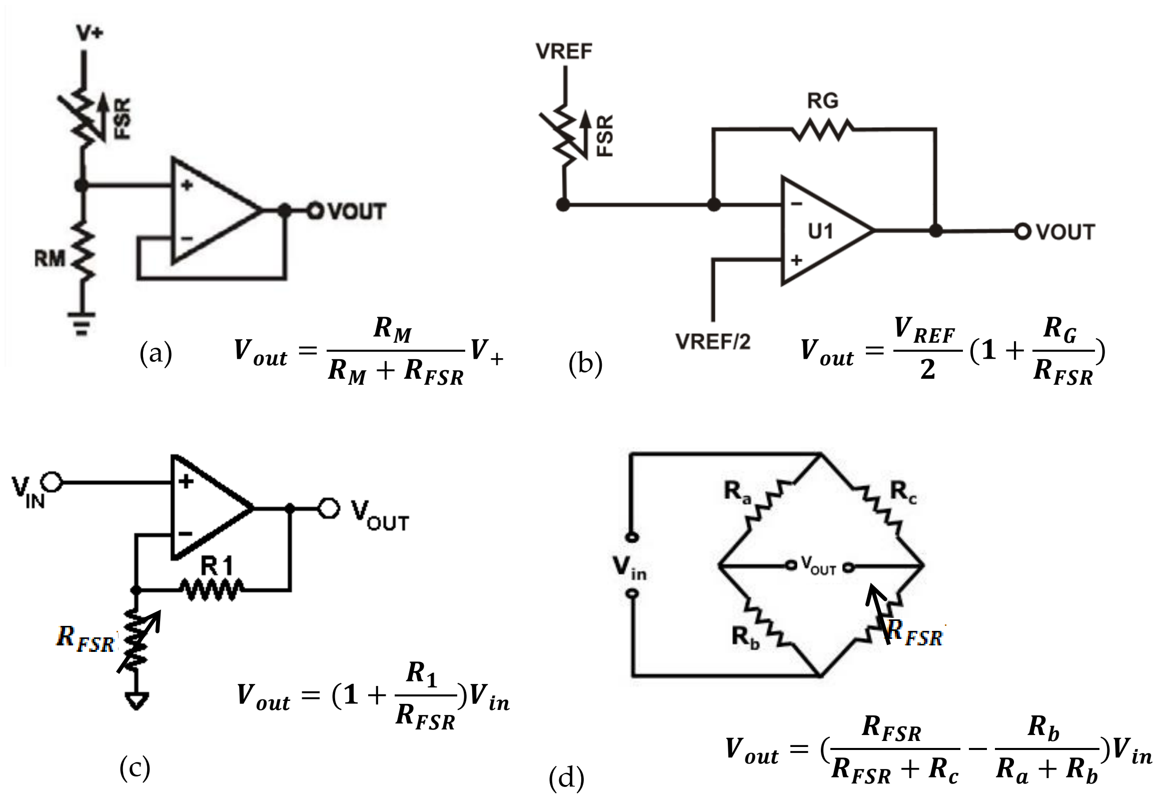

(a) $$V_{out} = \frac{R_M}{R_M + R_{FSR}} V_+$$

(b) $$V_{out} = \frac{V_{REF}}{2}\left(1 + \frac{R_G}{R_{FSR}}\right)$$

(c) $$V_{out} = \left(1 + \frac{R_1}{R_{FSR}}\right) V_{in}$$

(d) $$V_{out} = \left(\frac{R_{FSR}}{R_{FSR} + R_c} - \frac{R_b}{R_a + R_b}\right) V_{in}$$

Figure 5.6: Resistive sensing circuits a) potential divider b) trans-impedance amplifier c) non-inverting amplifier d) wheat-stone bridge

We used voltage divider with buffer circuit in this project as sensor linearization and amplification can easily be done through software. Power consumption is one of the biggest concerns in using this configuration. However, this only applies to low-resistance sensors as our fabric sensors perform on a high kΩ range (Chapter 4). The focus was then to find the value of reference resistor that could give the best output sensitivity to maximise the resolution of the sensor reading irrespective of the number of ADC bits and voltage supply. Assuming that a sensor has resistance range from 10k to 100k Ω, we can examine Figure 5.7 to find the differential voltage between voltage outputs of a resistive sensor value with 10k and 100k Ω as a reference resistor. We can observe a maximum point in this differential voltage output that corresponds to the optimal reference resistor value. By differentiating this function,

$$\frac{d}{dR}(V_{max} - V_{min}) = 0 \quad (5.5)$$

$$\frac{d}{dR}\left(\frac{R_{max}}{R_{max} + R} - \frac{R_{min}}{R_{min} + R}\right) = 0 \quad (5.6)$$

We can get this equation,

$$\frac{R_{min}}{(R_{min} + R)^2} - \frac{R_{max}}{(R_{max} + R)^2} = 0 \quad (5.7)$$

Rearranging and solving Equation 5.7 gives optimum value of the reference resistor, which is given by,

$$R = \sqrt{R_{max} \; x \; R_{min}} \quad (5.8)$$

Plugging 10k and 100k Ω to this equation gives reference resistor value of 31.62k Ω as extrapolated by the maximum point in Figure 5.7 to the x axis. Therefore, providing a prior knowledge of the working range of a sensor, this equation can be used to find out the optimal reference resistor in a potential divider circuit.

Finally, to accommodate the change of multiple resistive sensors, we integrate a multiplexer to subsequently connect each sensor to the read-out circuit, as illustrated in Figure 5.8.

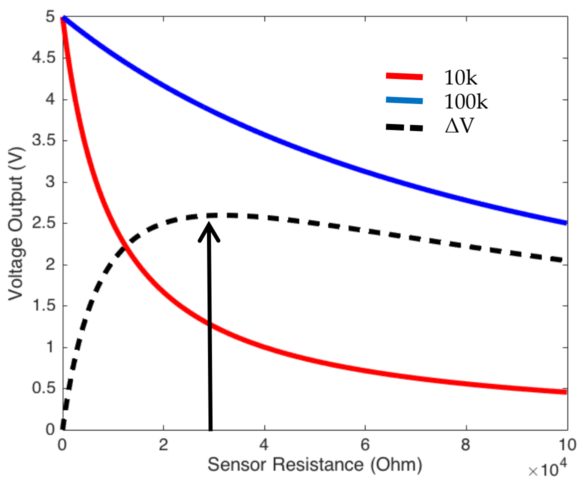

Figure 5.7: Voltage outputs of a resistive sensor value with 10k and 100k Ω reference resistors and the differential voltage output

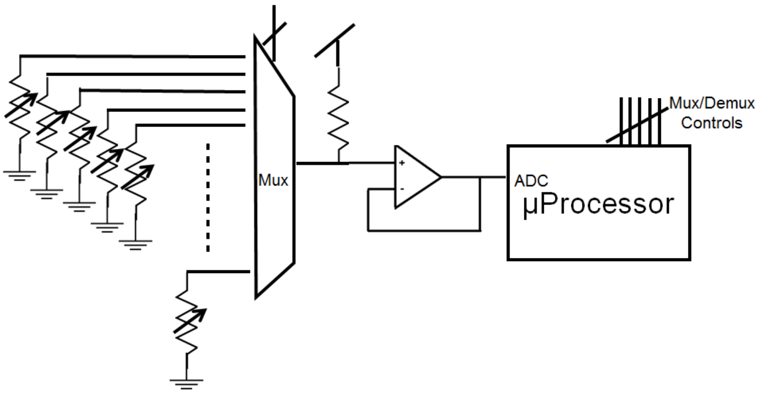

Figure 5.8: Multi-resistive sensing mechanism

5.4 ADC Interfacing

To get the most accurate analogue-digital conversion, the ADC limitation must be treated carefully. At the interface between voltage to be read and the ADC input, we need to ensure that the source impedance of the circuit is within the acceptable range. Figure 5.9 shows the equivalent sample and hold circuit of the ADC in series with source impedance.

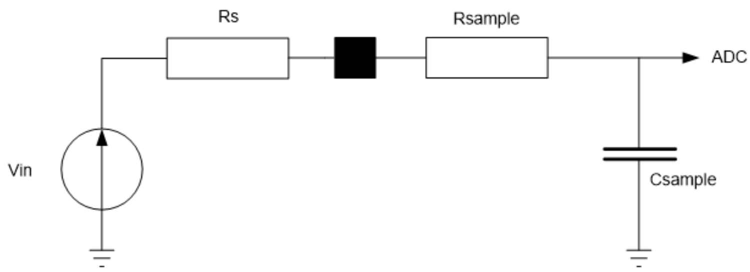

Figure 5.9: ADC sample and hold circuit diagram (reprinted [72])

From the SAMD21 datasheet, the ADC frequency (minimum sample-hold time), number of bits, sampling capacitance, and input channel source resistance define the acceptable source impedance as in Equation 5.9 below,

$$R_s + R_{sample} < \frac{T_s}{C_{sample} * \ln(2^n)} \quad (5.9)$$

Assuming a 10-bit ADC with frequency of 2MHz, and by plugging in the other variables C_{sample} *and* R_{sample} based on value specified on the datasheet, we find a maximum source impedance of 17kΩ. A potential divider circuit's source impedance is given by $R_s \; || \; R_{ref}$.

Since most of our sensor range in hundreds of kΩs, they will mostly be outside this limit. Therefore, a buffer circuit is needed on every read-out, as it separates both circuits from loading effects and provides low source impedance to the ADC.

5.5 PCB Design

The hardware was designed using Eagle PCB with the circuit schematics, layouts, and 3D visualisations provided in Appendix A. Based on the design of our fabric keyboard, we fabricated two different boards with their own features as shown in Figure 5.10.

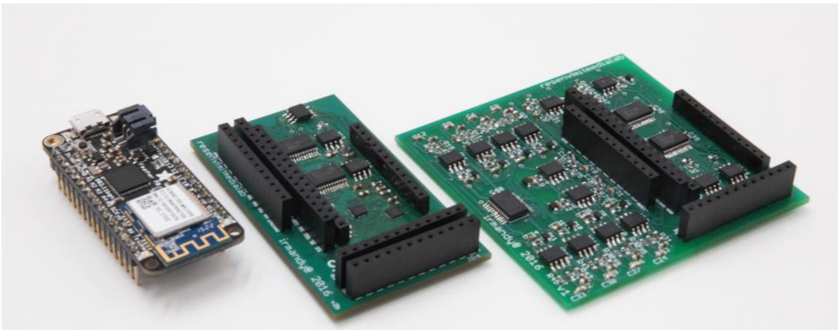

Figure 5.10: Adafruit Feather M0 Wi-Fi, *StretchyKeys*, and *ThereminKeys* (from left to right)

The first board (*StretchyKeys*) on the left consists of:

- 2 x 12 touch and proximity sensing channels
  (12 for the keys, the other 12 for miscellaneous use such as ribbon controller, trackpad, fur, or keyboard controls/settings)
- 12 pressure sensing channels
- 6 stretch sensing channels + 1 additional stretch sensing channel
- Trackpad channels
- Ribbon-controller channels
- Stroke sensing channels

The second board (*ThereminKeys*) on the right consists of:

- 12 electric field (hum) sensing channels
- 12 stretch sensing channels + 1 additional stretch sensing channel

- 12 pressure sensing channels

The second board is twice as large as the first because of the 50-60Hz field sensing circuit which took a considerable amount of space.

Both of these boards have configured pin-headers for stacking the main hub and connecting it to the fabric controller through a customized fabric ribbon connector. We used an Adafruit Feather M0 Wi-Fi, as the main hub as it is miniature (5.36 x 2.3 cm) and comprises 48MHz microprocessor, Li-Poly battery charger, USB connections, power management circuit, and a Wi-Fi module, giving us flexibility in using either wired (Serial or MIDI) or wireless (OSC) protocol. We chose Wi-Fi because of its direct approach to interfacing with OSC through UDP. These headers are also compatible with other Feather modules, such as BLE or RF, enabling us to change communication protocol as necessary.

Chapter 6:
Sensor-Computer Interfaces and Musical Mappings

6.1 Digital Musical Instrument Model

An electronic musical controller can have a direct interface of controlling a sound; for example, in analogue synthesizers where knobs and sensors directly manipulate and shape an audio signal that in the end drives a speaker. Another approach that has become common is to separate the controllers and the sound synthesis, by communicating through a general protocol such as MIDI or OSC. We use this digital approach instead since these protocols are widely used and allow performers to customize the musical parameters of each sensor and to map these parameters based on their preferences using any existing audio synthesis software.

Figure 6.1 below represents the principle of the instrument developed in this project. The gestural controllers include the main fabric keyboard with additional extension such as ribbon-controller, trackpad, and stroke. The controllers convert each sensor's response to meaningful signals that are then converted by the hardware to digital values.

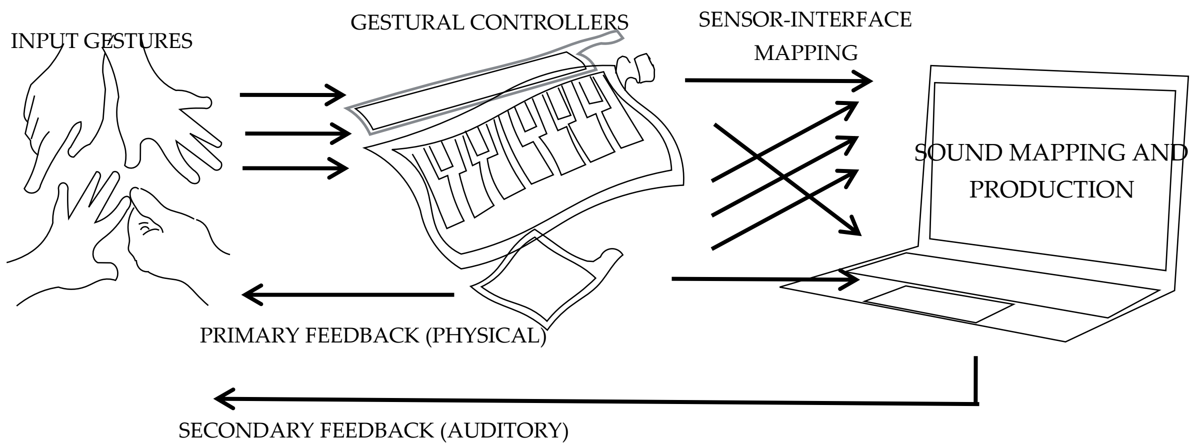

Figure 6.1: From gestures to sound and effects

The sensor data will firstly be converted to match the specification of a certain protocol (MIDI, for example). A message will be then populated using these data and an address containing a status, channel, and any other marker data depending on the protocol used. The message is then received by audio software in a computer. This software could be either an audio synthesis environment, such as PureData or Max/MSP, or audio sequencer framework such as Ableton Live or GarageBand. The software will then process this message and generate or control a particular sound based on its patches or mappings, providing a feedback to the performer. We will discuss and compare three approaches of sensor-computer interfacing with sound mapping in this section. Figure 6.2 shows the performance setup of the *StretchyKeyboard*. The fabric-based musical controller is plugged to a PCB, which reads all of the sensor data and populate them to data packets (in this case, MIDI messages) on board. These packets are then sent to the computer and recognized by an audio software (in this case, Ableton Live).

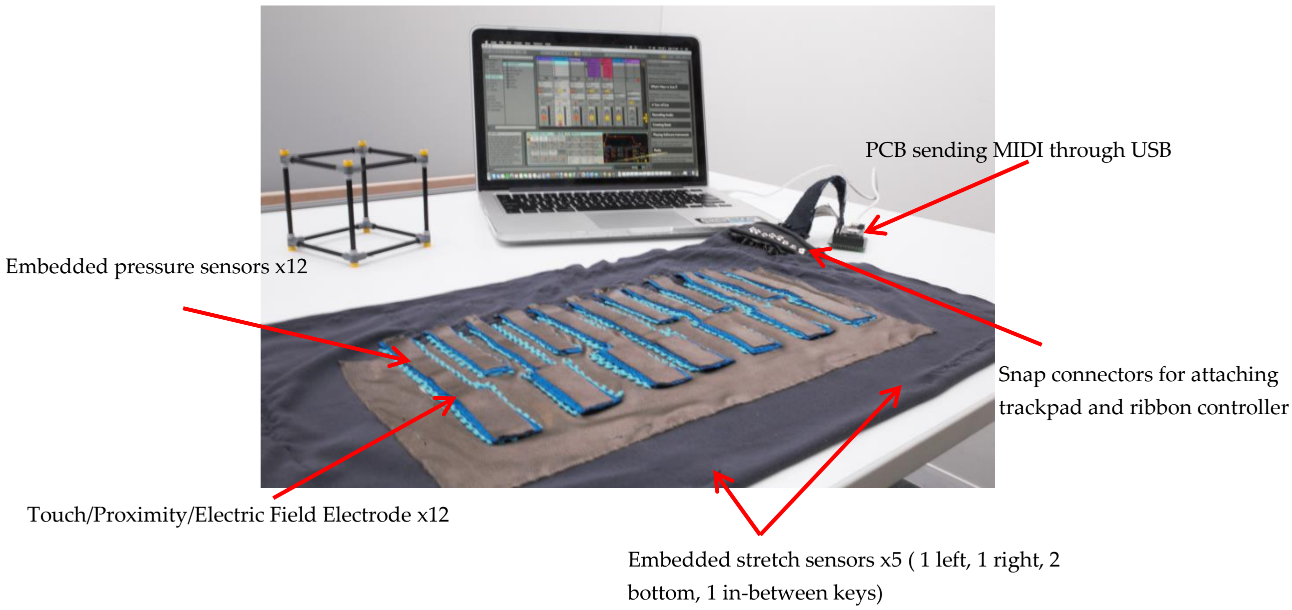

Figure 6.2: The fabric keyboard connected to Ableton Live through MIDI

6.2 Direct Serial Communication

In this approach, we use personalised data structure and transmit the data collected from the sensors by the microcontroller to the computer using serial communication (hardware UART). Max/MSP will then receive and parse these data into chunks before triggering or giving expressions to a synth patch.

6.2.1 Data Collection and Transmission

The data collection per key takes around 1.46ms while the whole lot of packet (consisting touch, proximity, pressure, and stretch sensor data for one octave keyboard) collection takes 17.5ms. This latency is mainly caused by ADC readings, multiplexer switching, and MPR121 charging time per key. We defined our Serial baud-rate as 115200 bps. Adding the transmission cycle (1.5ms) gives a total data transmission and collection cycle of 19ms resulting in '*StretchyKeys*' overall frequency of 53 Hz while '*ThereminKeys*' runs in 62 Hz.

6.2.2 Data Structure

(address) a 1 byte	(space) 1 byte	(bool) touch 1 byte	(space) 1 byte	(int) proximity 4 bytes	(space) 1 byte	(int) pressure 4 bytes	(space) 1 byte	(int) stretch 4 bytes	x12 keys

Figure 6.3: Sensor data packet on each key

Based on the figure above, one key takes 18 bytes; for a packet which contains 12 keys, the total bytes is 216. There are a few redundant bytes, since we only use 10 bits ADC. However, cutting or rearranging these bytes will not reduce the latency significantly, as most of it is wasted on the data collection. It will also overcomplicate the next step because this structure makes data parsing and mapping easier and manageable.

6.2.3 Max/MSP Implementation

Figure 6.4 shows a screen capture of the Max/MSP patch that receives inputs from the microcontroller through serial communication. The route function parses each key based on its address. The parsed packet will again be split into chunks with the "*unpack*" function. Each sensor element is then processed and passed through a synth patch. In this example, the detection of touch generates a wave of choice, which is a phasor with a particular frequency. The pressure data then provides gain to this wave, modulating its amplitude.

This approach is compelling in a way that it allows full flexibility of sound generation and shaping. In max, one can synthesize and control essentially any kind of sound with any technique. However, this requires a significant effort in programming and is restricted in interoperability compared to other methods.

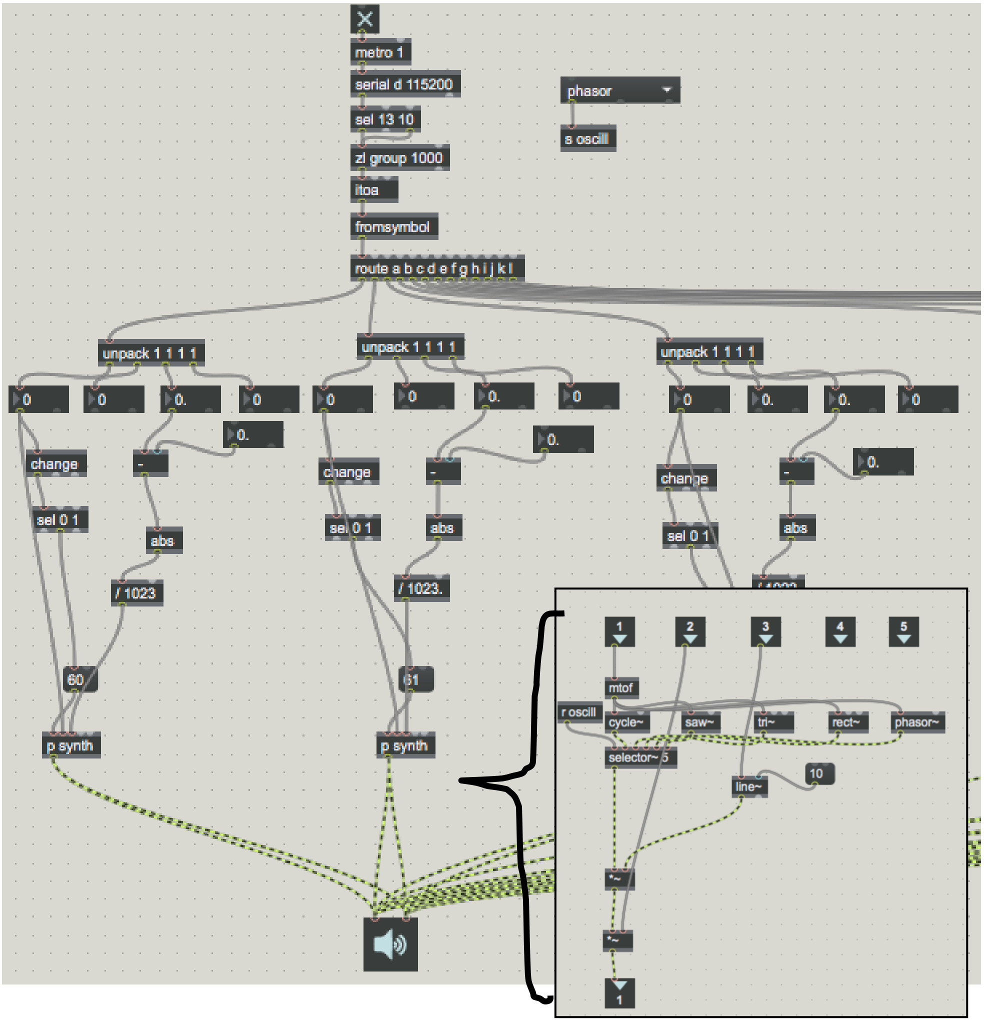

Figure 6.4: Max/MSP patch to parse data packets to each modality and feed the sensor data to a digital synthesizer

6.3 Musical Instrument Digital Interface

MIDI is a standard which enables electronic musical controllers, computers, synthesizers, and other devices to communicate with each other. Each protocol message, as shown in Table 6.1 below, has several bytes containing message type, channel number, and its data. From these specifications, we can recognise the limitation of aging MIDI standard; it only allows a maximum of 16 channels and 0 – 127 range of discrete values.

Message Type	MS Nybble	LS Nybble	Number of Data Bytes	Data Byte 1	Data Byte 2
Note Off	0x8	Channel	2	Note Number	Velocity
Note On	0x9	Channel	2	Note Number	Velocity
Polyphonic Pressure	0xA	Channel	2	Note Number	Pressure
Control Change	0xB	Channel	2	Controller Number	Value
Program Change	0xC	Channel	1	Program Number	-none-
Channel Pressure	0xD	Channel	1	Pressure	-none-
Pitch Bend	0xE	Channel	2	Bend LSB (7-bits)	Bend MSB (7-bits)
System	0xF	further specification	variable	Variable	Variable

Table 6.1: MIDI Status Messages (reprinted [73])

6.3.1 Data Collection and Transmission

In this approach, all of the sensor data (0-1023) are initially mapped to fit MIDI parameter values (0-127) before transmission. Since MIDI supports sending discrete control such as note on/off and continuous controls such as polyphonic pressure, channel pressure, and control change, we can effectively send MIDI messages based on their context. For example, note on and off messages can be triggered only if there is a change in a variable rather than constantly sending its values every period. Related events, such as polyphonic/channel pressure and pitch bend, can also be set only with touch events. This implementation reduces the transmission load of the system; therefore, improving its data-rate and latency.

The time it takes to cycle through the main data collection process is 17.5ms; this is the time period when no physical interaction occurs (no detection of touch and proximity). When all sensor modalities are triggered (including the stretch and pressure), which is the worst case scenario, the time period becomes 19.33ms, which includes both data collection and transmission cycle. Extending the keyboard with additional controls, such as trackpad and ribbon controller, increases the time wasted between cycles to 20.6ms. The overall frequency for the keyboard with its extension therefore ranges from 49 – 57Hz based on the activity performed.

6.3.2 Data Structure

Table 6.2 provides on-board mapping of each sensor's data to MIDI messages. It is evident that these are customizable and could change depending on the intended interactions.

In this particular example, the proximity could trigger discrete notes as our hands approach certain keys and modulate them as they get closer until they fade away. The note number is predefined in the code. Touching a key will also trigger a note number with velocity calculated by the pressure sensor after a certain delay (velocity delay). Since each key has its own pressure sensor, the keyboard also supports polyphonic after-touch/pressure that is activated after an expression delay which is currently set to 1s. The stretch sensors can be set to MIDI CC messages that will correspond to certain effects (filter resonance, frequency, glide, reverb, amp, distortion, *et cetera*) assigned in the audio software or pitch bend. The additional controls, such as ribbon-controller or trackpad, can be mapped as an independent instrument since it is integrated with touch and proximity sensing or as a keyboard complement with CC/pitch-bend messages.

Sensing Modality	Data	Number of Sensing Elements	Channel	Message Type	Converted Data
Touch	Bool	12	1	Note Off/On	Note Number
Pressure	Int Int	12	1 1	Note Off/On Polyphonic/Channel Pressure	Velocity (0-127) Pressure (0-127)
Proximity	Bool Int	12	2 2	Note Off/On CC	Note Number Value (0 – 127)
Stretch	Int	5	1	CC/Pitch Bend	Value (0 – 127)/ MSB (0-127)
Ribbon-controller Position Touch/Proximity	 Int Int	 1 1	 1 3	 Pitch Bend Note/CC	 MSB (0-127) Note Number / Value(0 – 127)
Trackpad Position Touch/Proximity	 Int Int	 2 1	 4 4	 CC Note/CC	 Value (0 – 127) Note Number / Value(0 – 127)

Table 6.2: MIDI mappings of '*StretchyKeys*'

6.3.3 Mapping with Ableton Live

After the MIDI messages are sent, it will be recognised by the audio sequencer framework to produce sound based on its mappings. We used Ableton Live 9 Suite which is a common tool for instrumenting, mixing, recording, and composing music for live performances. The GUIs to map MIDI messages in Ableton Live are shown in Figure 6.5 and 6.6 below; essentially, all "knobs" and controls can be easily mapped to a MIDI stream.

Figure 6.5: Ableton Live main GUI. In this example, three instruments (Column 1-3) are mapped to MIDI Channel 2 (Proximity) and 3 (Touch). Column 4 is used to record performances while Column 5 is used to map Audio Effects (Amp and Spectrum in this case). The bottom Soft Strings and Analog panels are intrinsic controls of each instrument which can be mapped to MIDI CC messages. We mapped 'Filter Freq', 'Filter Reso', and 'Motion' controls to our stretch sensors. On the top left corner, MIDI button can be used for parameter mapping (go to Figure 6.6)

Figure 6.6: In this MIDI parameter mapping panel, we can see all of the MIDI channels currently used and its corresponding Path/Controls. Parameter mapping can be done by pressing any available control (shown in purple) and correlating it to a MIDI message (by triggering the controller).

Although the MIDI standard has become widespread and its revolution has made it easy for us to map MIDI messages to audio software with a large library of sounds, instruments, and effects, the implementation is still somewhat confined, especially for continuous controls. It has predefined parameters and only allows a maximum of 16 channels and 0 – 127 discrete levels. This limitation brings us to the last section of this chapter, the Open Sound Control protocol.

6.4 Open Sound Control

The Open Sound Control (OSC) [79] is a one of the current protocols that resolves the shortcomings of the MIDI standard. This protocol is high-level and enables user-defined, dynamic, hierarchical message structures with high resolution data. This approach is also particularly interesting in this project as OSC messages can be sent through the internet using UDP/IP. Since there is an increasingly number of audio software supported by OSC implementations (such as Max/MSP), we are interested in using this protocol to send sensor data through Wi-Fi, allowing wireless communication between our keyboard and the computer.

6.4.1 Data Collection and Transmission

The OSC data management works quite similarly as before with MIDI implementation. A message is sent if there is an event and then periodically sent if it belongs to a continuous controller. The differences are now in the message structure and size, which do not have any constraint under the OSC.

To measure the latency of the transmission, as shown in Figure 6.7 below, we sent a data packet to a Max/MSP patch which then rebounded it. The time it takes from sending this packet to receiving it back again gives us the round-trip delay. Assuming that the transmission latency is half of the round-trip delay, the total latency of the system is,

$$t_{worst\ latency} = t_{collection} + \frac{t_{round-trip}}{2} \quad (6.1)$$

Since the mean of the histogram in Figure 6.7 is 8.5ms, and the worst latency of data collection is 19.33ms, the total latency of the system could then range from 4.25 to 23.6ms.

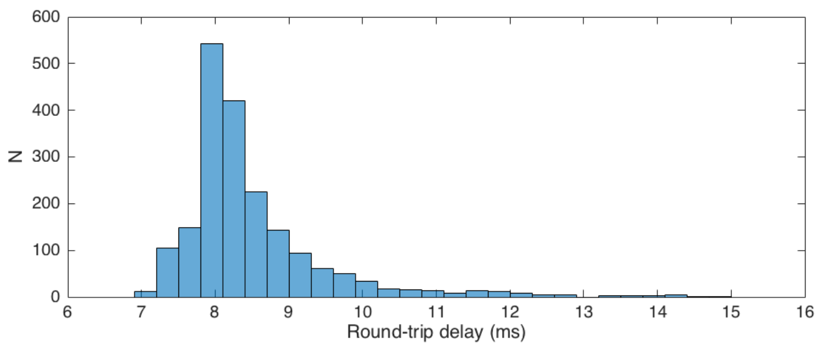

Figure 6.7: Round-trip delay histogram of Feather M0 Wi-Fi under-test

6.4.2 Data Structure and Sound Mapping

The data structures of OSC are open-ended with URI-styling. We set each address as a string of characters containing a main parameter with its sub-list as shown in Table 6.3 below. It is followed by the value, which could either be a floating number or signed integers.

Address 1	Address 2	Value type
touch/	0-11	Int
proximity/	0-11	Int
pressure/	0-11	Int
stretch/	0-4	Int
trackpad/pos/	x,y	Int
trackpad/	prox	Int
trackpad/	touch	Int
ribbon/pos/	x	Int
ribbon/	prox	Int
ribbon/	touch	Int

Table 6.3: A customized header and mappings for OSC packets

Since most of current audio software supports OSC, such as Max/MSP, we can receive these messages through a local wireless network by using "*udpreceive*" and parse it with "*route*" function with a similar process as explained in Figure 6.3. The total flexibility of OSC, unlike MIDI, however prevents it from being adopted universally. The fact that people could define their own data structures reduces this approach's interoperability. Therefore, a standardized dialect such as SYN has been proposed in order to fill this gap of inconsistencies [80].

Chapter 7:
Results and Evaluation

7.1 Multi-modal Fabric Sensate Surface

In this project, we explored the design and implementation of a multi-modal fabric sensate surface for physical interaction media and produced working prototypes. The concept is a soft surface that is not only flexible but also stretchable, extending its panoply of novel interactions. To realise this, all of the materials we used, either functional or not (except the conductive threads), are made out of stretchy, knitted fabrics. Conductive threads were machine-sewn to provide interconnects from all of the sensors to the main hub. Some of the threads were also sewn in serpentine structures around the region of stretch to avoid interconnects breaking. Twelve fabric keys were patterned with multi-layer textile sensors consisting of a floating conductive fabric followed by a fabric pressure sensor. Stretch sensors were also embedded around this fabric. The multi-layer configuration allows the keys to individually detect proximity, electric-field (hum), touch, pressure, and stretch.

(a) (b)

Figure 7.1: The multi-sensory fabric keyboard a) top b) bottom-view

To show the capability of this fabric sensate surface, several tests were executed on each modality in response to different stimuli. Figure 7.3 shows each key response to touch as a binary state. The touch sensing relies on the feature of MPR121 touch controller which involves adaptive baseline tracking with thresholding. As demonstrated in Figure 7.3, it is also capable of detecting multi-touch events.

The large area of each floating conductive fabric in this sensate surface enables near-proximity detection on each electrode by carefully setting the charging current and time of the MPR121. Since bigger electrodes result in a much higher sensitivity, as previously characterised in Chapter 4.1.2, each electrode could detect up to 20 cm of hands-approaching (with 12x12cm electrode); using typical key size (12x2cm) reduces the maximum distance to 12cm. However, in implementation, the sensitivity drops even lower to 5-8cm (Figure 7.4), mainly because of the use of bare conductive threads and the potential influence of the interconnect resistance that could relate to parasitic capacitance. Figure 7.2 shows the result of the total resistance characterized between each sensor and its sensing channel.

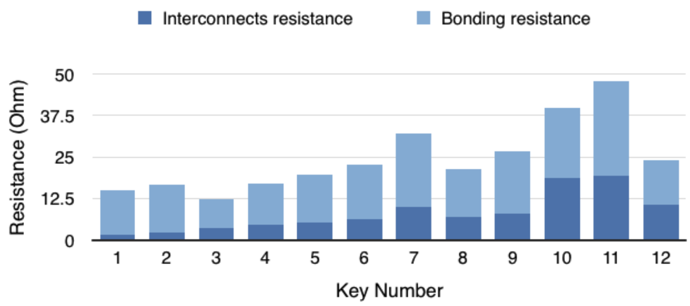

Figure 7.2: Total resistance on each routing

The total resistance includes both the interconnect's resistance and their contact or bonding resistance to the sensor and the main header. The most contribution is made by the contact resistance, which can be solved by sewing more loops with stronger tension or by using different types of thread which can be soldered easily. The routing resistance has a very low influence on the pressure and stretch sensors, since both of these sensors have a much higher resistance change.

Besides the multi-proximity sensing, another interesting feature of the MPR121 is the multiplexed sensing, that enables higher sensitivity to approach (up to 25cm) by combining all the pixelated electrodes into one single large sensing surface as explained in Chapter 4.1.2.

The fabric pressure sensors made out of piezo-resistive fabrics were designed so that they are uniform in baseline values (starting with an open-circuit state) without compromising much of their sensitivity to lower pressure from using a mesh fabric separation. The mesh fabric used in the end is a thick knit mesh which gives much more sensitivity to soft presses due to its large spacing. Figure 7.5 presents the response of fabric pressure sensor on each key to single press, multi- press, as well as expression.

We also studied the characteristic of different piezo-resistive fabrics in response to strain and discovered the best knit-structure for fabric stretch sensors (Chapter 4.1.5). These fabric stretch sensors were then sewn around the sides of the fabric and in between the keys as shown in Figure 4.1b. Instead of having stretch sensors on every gap between each key, to reduce the implementation effort, we customised and sewn a long stretch sensors with conductive fabrics embedded at the pressure sensing location (zebra-cross pattern) to avoid parasitic influence from the pressure applied to the stretch sensor. The response of each stretch sensor and the whole fabric to stretch is shown in Figure 7.6. Notice that when stretched horizontally, the stretch sensors on the right, left, and in between the keys are all affected; therefore, the system can differentiate between stretching specific sides of the fabric, stretching between the keys, and stretching the whole fabric.

Another modality we have is to detect electric field strength generated by the mains hum coupled through the player's body. Each of the floating conductive fabric patched each key acts as a sense electrode where it is constantly reading current from our body due to the electromagnetic noise coupling. Since our body acts as a shunt or an antenna, by touching these electrodes with one hand while simultaneously reaching towards a field transmitter with the other (a simple light bulb works reasonably), we could also control the amplitude of the reading as shown in Figure 7.7. Therefore, this electric hum detection could not only detect touch but also other hand's coupling distance to a transmitter. It can be observed in the figure that there is a challenge faced in this approach when dealing with multi-sensing. Touching several keys simultaneously results in an equal voltage level drop on each sensing electrode based on the current sharing principles. However, some offsets still exist and we can calibrate the threshold to the lowest amount when all keys are pressed simultaneously. Detecting electromagnetic noise is thus a challenging process, since the strength of this field varies across different areas and environments; calibrations must then be done regularly. This modality will tend to be used for relative rather than absolute sensing.

Finally, Figure 7.8 provides all of the multi-modal sensor data (proximity, touch, pressure, and stretch) as two fingers strike and stretch two keys (key A and B). All sensors detect our fingers well as they are approaching, floating on the air, touching, pressing, as well as stretching both keys simultaneously.

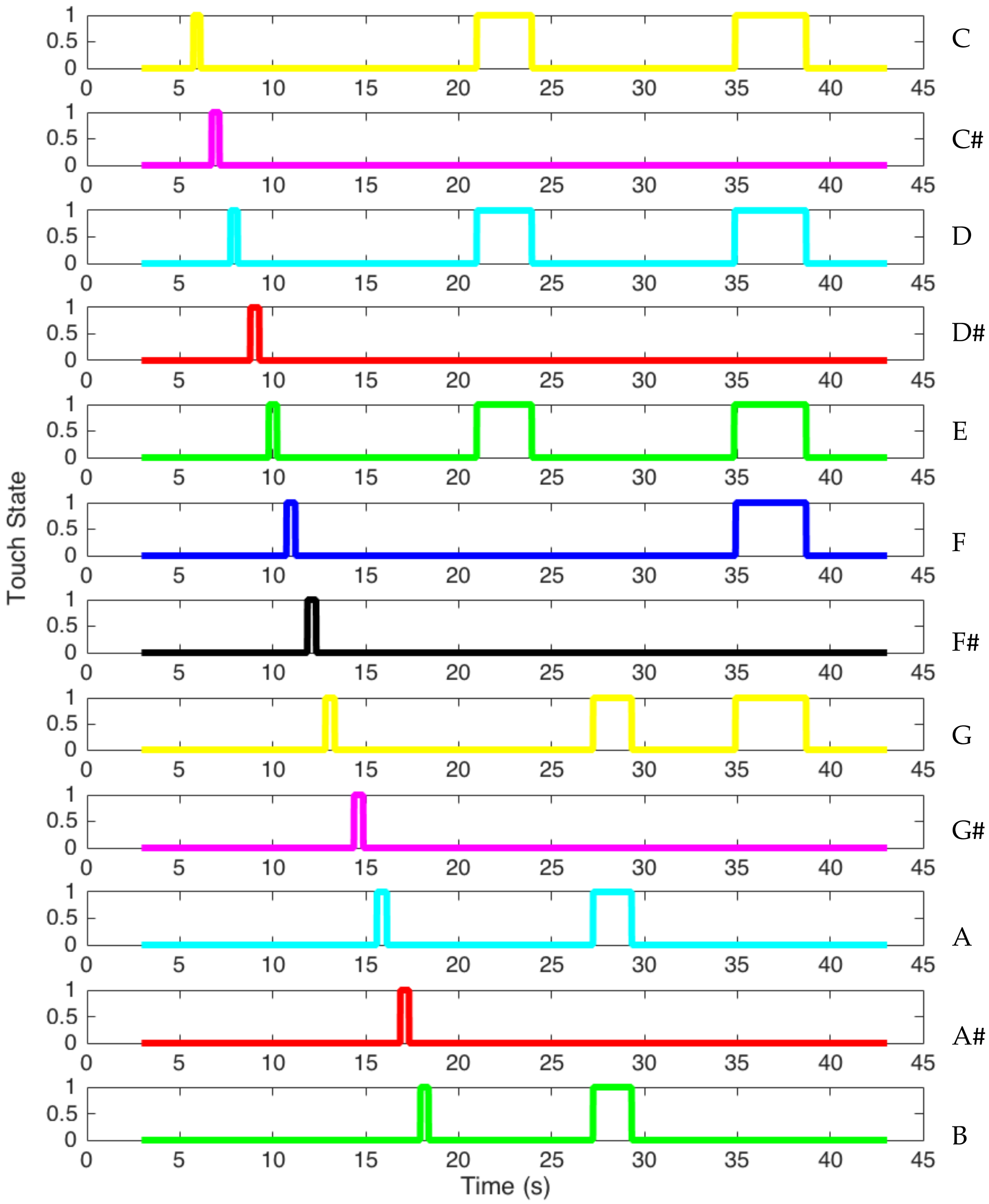

Figure 7.3: Single-touch and multi-touch (poly-touc h) test on all of the keys

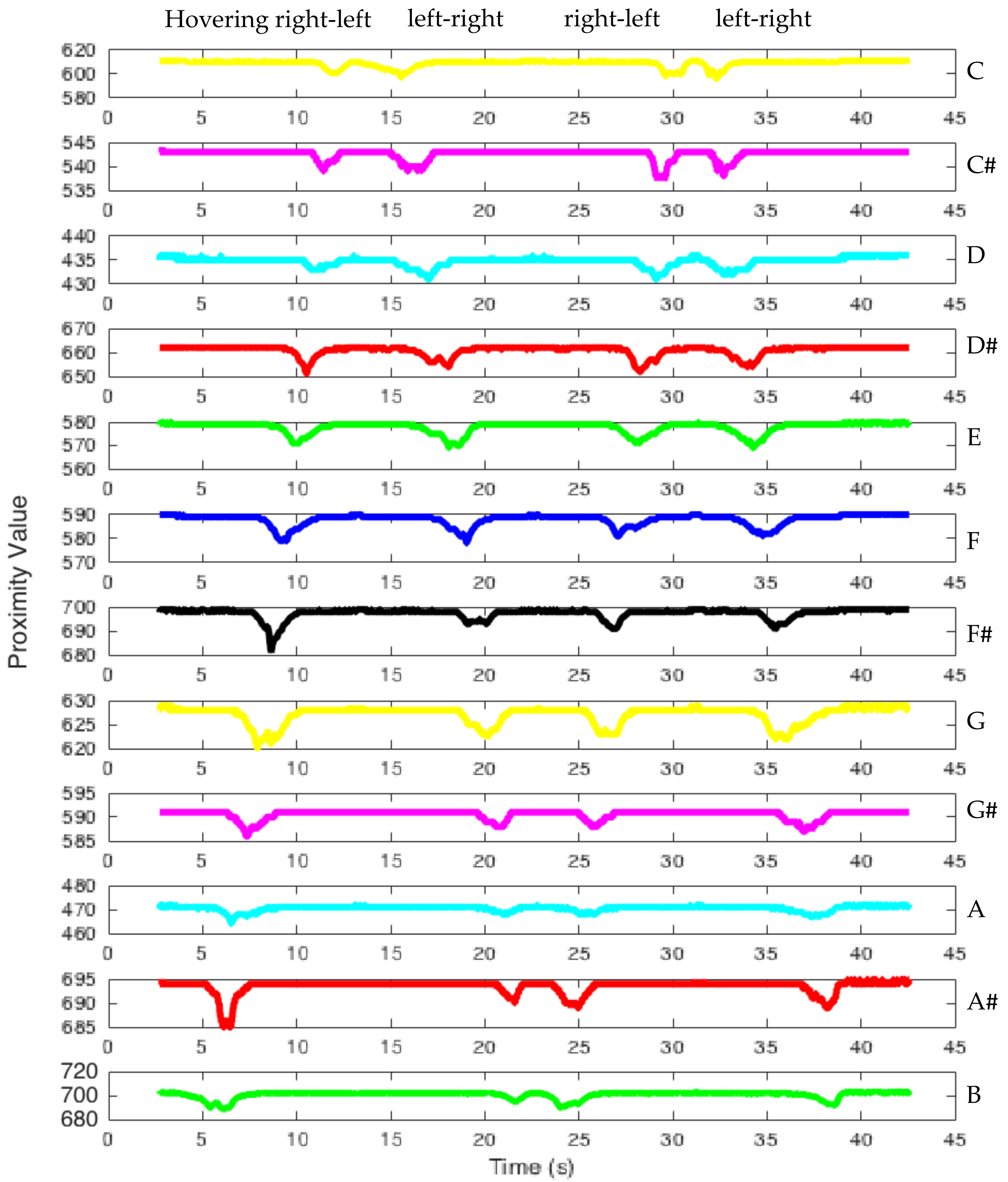

Figure 7.4: Capacitance sensing (proximity) as one hand hovers around the keyboard (~5cm)

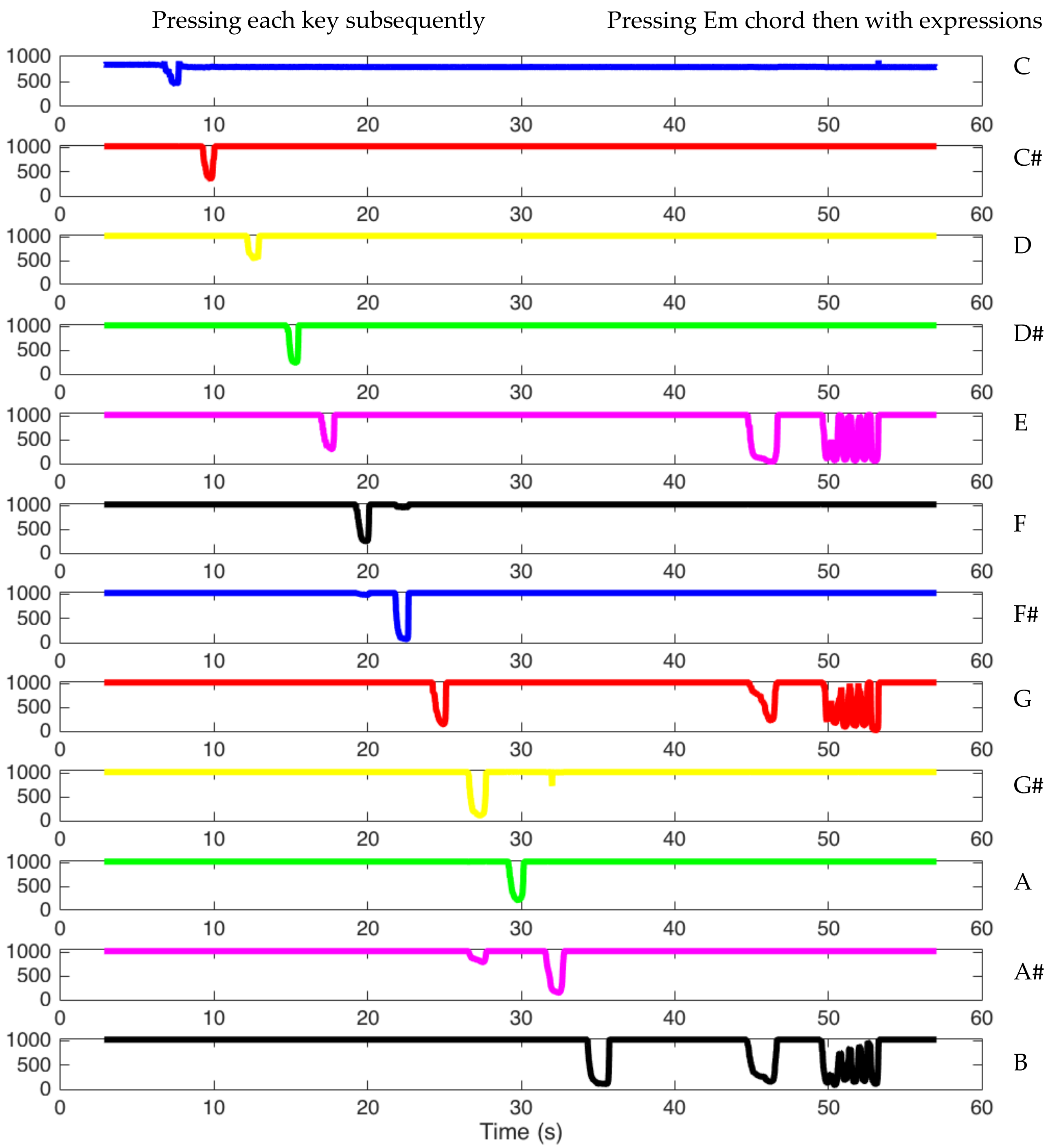

Figure 7.5: Single-pressure and multi-pressure sensing on each key

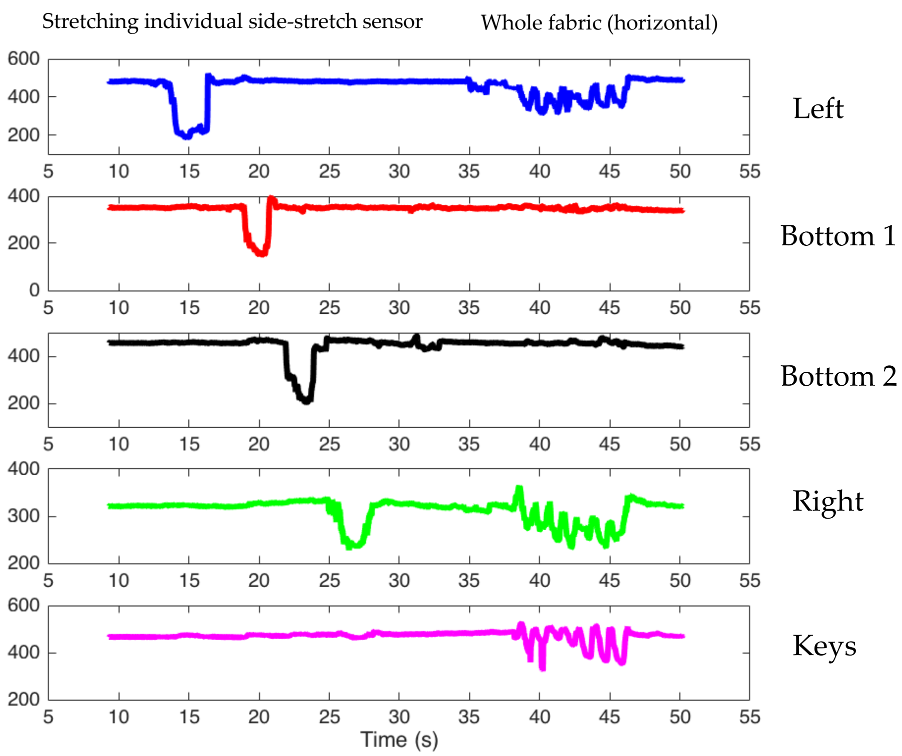

Fgure 7.6: Individual stretch and multi-stretch sensing (stretching the whole fabric)

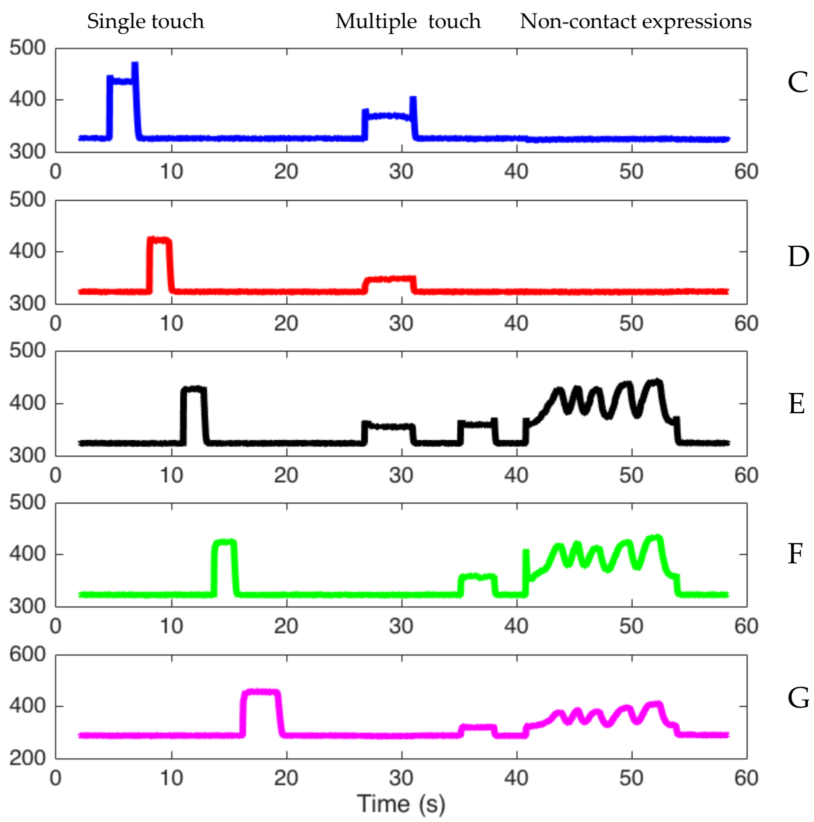

Figure 7.7: Individual and multi-sensing of e-field (with non-contact expressions)

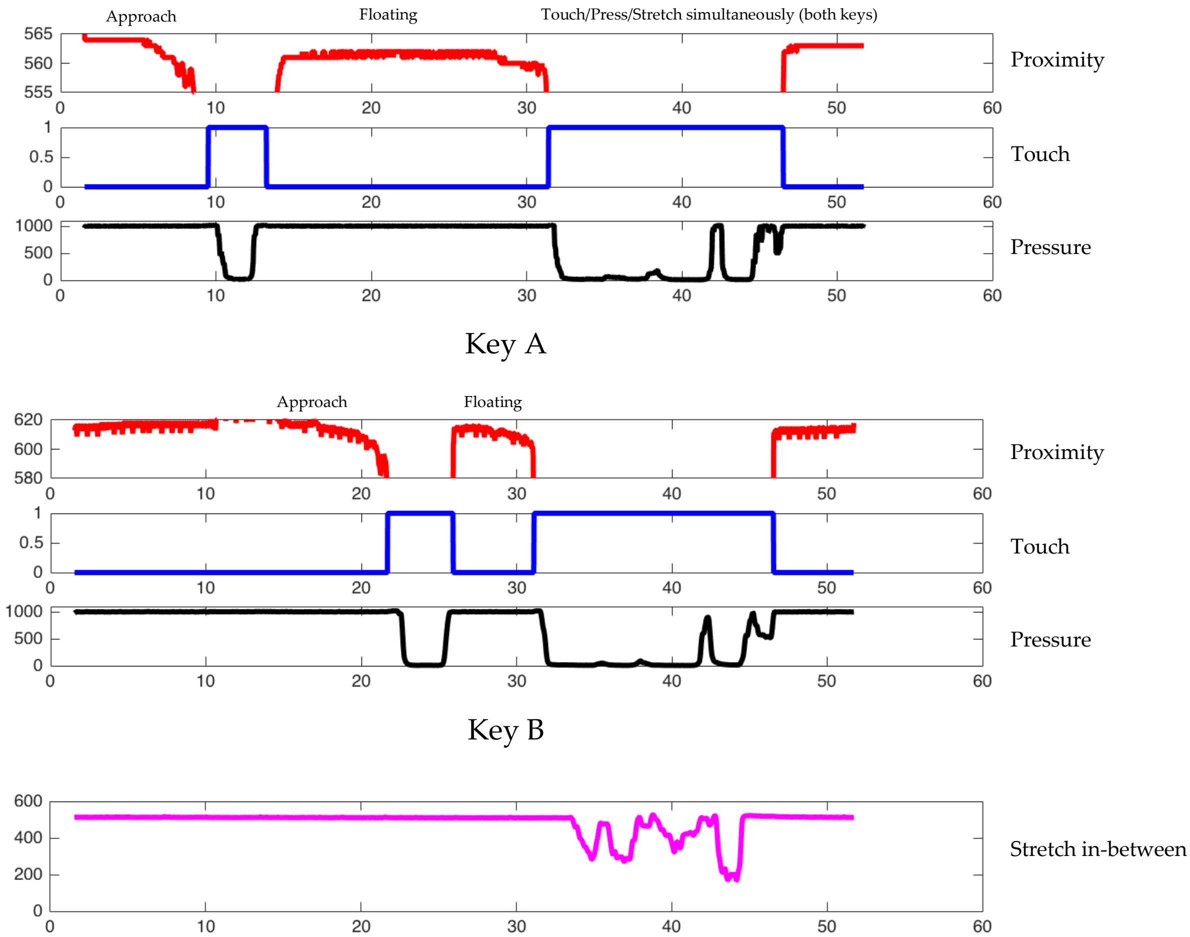

Figure 7.8: Multi-modal sensor data of two keys as two fingers interact with them

We also developed a fabric-based trackpad and ribbon-controller for position sensing as shown in Figure 7.9. We used the combination of conductive, mesh, and resistive fabric inspired by the current resistive touchscreen technology to realise these fabric controllers (Chapter 4.2). Table 7.1 compares the resistive fabric trackpad characteristics with other methods such as capacitive grids. Trackpads based on surface capacitance requires a more complex system and is prone to parasitic capacitive coupling. A projected capacitive trackpad with interpolation gives a very high resolution and sensitivity with multi-touch capability; however, has a high implementation effort [69]. For a single touch purpose with the least amount of complexity, the approach discussed here is the most suitable since it gives a high resolution trackpad (depending on ADC resolution) with the least system complexity (4 interconnects) on any given touch area. However, since our finger has a relatively large contact surface, such a high resolution might not be necessary.

Figure 7.9: The fabric trackpad and ribbon-controller

	Resistive Fabric Trackpad (4-Wire)	Other Fabric Trackpad (Grid)
Resolution	High depending on ADC bits	Medium depending on size of grid, and technique
Area	Could be as large as possible with only 4 connection lines	Larger size requires more grid lines
Complexity	Low (Only 4 interconnects)	High (M + N interconnects)
Single/Multi-touch	Single	Single/ Multi
Sensitivity to touch	Low	High

Table 7.1: Comparison of 4-wire resistive trackpad with grid-based capacitive trackpad

On the hardware side, we built two versions of PCB: one for the multi-touch and proximity sensing with MPR121 (*StretchyKeys*) and the other one for electromagnetic noise sensing with custom analogue circuits (*ThereminKeys*). Both PCBs are integrated with multi-pressure and stretch sensing. The hardware USB data-rates for reading all of the sensor data is 53 Hz and 62 Hz while the maximum latency is 19.33 ms and 16 ms respectively.

7.2 MIDI Fabric Keyboard Controller

After the textile and hardware developments were completed, we then proceeded to the software development, which involves sensor-computer interfacing and sound mapping. We implemented several approaches of data transmission using a Serial UART, MIDI, and OSC (Chapter 6). At the end, we decided to focus on MIDI development while taking into an account its interoperability, throughput, and wide software support. Ableton Live 9 was used to map MIDI messages to instruments and audio effects.

7.2.1 Example Interactions and Mappings

As described in this section, we developed many musical mappings to experiment with this novel controller. Video examples of these performances can be seen at (http://resenv.media.mit.edu/#Projects#StretchyKeyboard)

Figure 7.10 to 7.13 present several interactions that have been developed with this deformable musical interface. Transforming the physically rigid and bulky keyboard into stretchable fabric with multi-sensory capabilities allows discrete, conventional keyboard play with multiple new continuous types of expression. Figure 7.10a shows a finger striking a key; besides the discrete touch sensing, the fabric pressure sensor embedded inside each key can emulate a piano, measuring velocity of key-strike as well as giving after-touch effects such as tremolo or vibrato. The stretch sensor sewn in between the keys (Figure 7.10b) senses how far pressed keys are stretched against each other, enabling a novel expression that combines both discrete and continuous controls in one hand. Several stretch sensors sewn around the edges of the fabric (except the top side) provide additional stretch-mode controls (Figure 7.10c-f). In these figures, one hand is playing the keyboard while another pinching or stretching it in specific direction. Besides mapping them to pitch, which resembles the tactile feedback of the stretch sensors, we also mapped timbral, dynamic, and tempo variations such as filter frequency, resonance, reverb, and distortion to the MIDI CC messages that correspond to these stretch sensors.

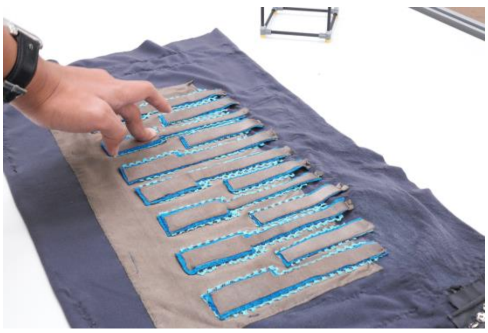

(a)

(b)

(c) (d)

(e) (f)

Figure 7.10: a) pressing a key b) pressing keys and then stretching it sideways c-f) pressing keys while stretching the fabric

We can also pinch the keys or squeeze the fabric after pressing the keys (Figure 7.11a). This would result in a much stronger pressure and possibly a parasitic influence to the stretch sensors embedded between the keys giving two dimensional control to the sound generated. Another potential gesture is stretching the whole fabric, which influences the three stretch sensors horizontal to the fabric (Figure 7.11b); in this case, to modulate an echo. One can also further improvise, by lifting the fabric up before stretching and twisting it (Figure 7.11c-d).

(a) (b)

(c) (d)

Figure 7.11: a) squeezing b) stretching c) lifting and stretching d)twisting the whole fabric

The multi-modal sensing on each key also enables us to explore non-contact gesture sensing. We have two scenarios of non-contact sensing as shown in Figure 7.12 below. The first one is proximity sensing where each key responds to approach; in our implementation, an approach triggers an instrument or an ambient sound. The other non-contact gesture sensing requires EMI source in our vicinity, as it senses the electromagnetic noise generated by it. This modality combines both physical and non-contact gestures, as one of our hands plays the keys and the other modulates the sound by waving towards, against, and around the source (any unshielded appliance will work as a source).

(a) (b)

Figure 7.12: Non-contact gestures a) proximity b) e-field sensing by waving towards a source

The development of modular extensions allows performer to snap other fabric interfaces as they perform; in this case, ribbon-controller and trackpad. Both interfaces can either be independent instruments or keyboard expressions. Ribbon-controllers have been widely used to bend or modulate frequency so we used it as an expression (glissando) while we implemented the trackpad as a complement generating sound and effects with its two dimensional controls (Figure 7.13). There are even more interactions that could be possible with this modular and deformable musical interface; for example, by combining several modalities, combining physical with non-contact gestures, or transforming between them. Developing a fluid interaction between each modality as they transition, however, requires further studies and explorations in HCI.

(a) (b)

Figure 7.13: a) Pitch-bending a sound by sliding through the ribbon controller b) generating two dimensional effects with trackpad as we play the keyboard

7.2.2 User Experience

The fabric keyboard was exhibited and demonstrated at the MIT Media Labs' annual Fall Members Week 2016, where our industrial sponsors and other visitors, some of whom were artists and musicians, could play this controller and give feedbacks. We implemented the discrete touch and all of the stretch sensors during this opportunity. Most of the visitors showed some kind of astonishment when they felt how soft the fabric controller is and that it is also stretchable. Some people who had watched the demo video of this keyboard went straight to play and stretch the fabrics and keys with their hands, but still felt uncomfortable of how they should stretch the fabric, since the stretch sensors are hidden behind. Therefore, some signs or cuts should be added to show where the user can stretch the fabric.

Most people were stretching the fabric to control the sound instead of producing it, which matches our intentions. One interesting observation was to relate the sound as an embodiment of the physical state of the fabric and its sensors. Since all of the fabric sensors are embedded to the fabric substrate, stretching the whole fabric could dampen the response of the pressure sensor by somewhat as the piezo-resistive fabric is also stretchy; this also applies vice versa to the stretch sensors. The initial non-linearity in response of the stretch sensors also gives a unique characteristic to the sound. Moreover, when stretched constantly, especially outside its allowed range, the stretch sensor's response could shift and calibrations are then necessary. This is similar in how we tune our guitars, but instead of physically turning a peg, we digitally calibrate it in software.

Even though physical interaction on deformable interfaces can be detected with cameras, it is still a challenge to simulate a complex gesture and adapt to physical change of the material accurately [74]. The vision sensing setup could also be troublesome for active performances where there are a lot of subtle–but-important movements both on the performer and the instrument that are hard to remotely detect. Self-aware materials should have its receptors and processors in or on itself, mimicking the biological skin. Therefore, the intrinsic electrical and mechanical properties of the fabric sensors and the substrate make this deformable musical interface unique and interesting in its own way.

7.2.3 Qualitative Analysis

There are several things that could have been improved in the development of this fabric-based musical controller. It was experienced that the touch sensing could sometimes get stuck in one state and the hardware needs to recalibrate to solve this issue. This issue happened mostly because of the dense network of interconnects going through the fabric from PCB to each sensor. Since we used bare conductive threads, some of these threads could get "hairy" after they are sewn. They could then form accidental short-circuits to the neighbouring interconnects especially when the fabric is actively moved or worn. The MPR121 controller also suggests keeping minimal length and resistance from the pin to the sensor; some parasitic capacitance from the environments could then easily affect the detection if we use bare conductive threads. Encapsulation might solve this issue, but the most straight forward way is to use insulated conductive threads. There are several conductive yarns produced by winding insulated copper wire with common threads, but they are not accessible and might not be machine-sewable. Using insulated conductive thread, or even better, shielded conductive thread would also improve our proximity sensing as currently, it is most-affected by the bare interconnect lines.

Another thing that could be improved is not related to the technical side, but more to the design. To allow more extension as we stretch the keys, we created a gap in between them; however, these gaps expanded the active surface area of the keyboard making it relatively hard to play chords. Choosing a more stretchable base fabric while reducing the gap distance could possibly keep the keyboard active area manageable.

In terms of latency, our worst-case scenario which is around 20ms is acceptable for electronic musical controllers, as Lago and Kon defines the maximum limit of 30ms [75]. Although for staccato keyboard performance, delays should be on the order of 1ms. The effective latency however could be a little bit higher than this, as we have not considered the latency in the software processing side. To minimize this, further efforts can be done: by reducing the ADC resolution and cycles perhaps, or using a faster microprocessor with more ADC pins to reduce the multiplexing load.

Chapter 8:

Conclusions and Future Work

8.1 Conclusion

With this work, we present *StretchyKeyboard*: a multi-modal fabric sensate surface as a deformable musical interface. Twelve keys comprising a multi-layer of fabric sensors (proximity, touch, electric field, pressure, and stretch) were patterned with a sewing machine on a stretchable fabric surface. To complement this fabric keyboard, other fabric interfaces such as ribbon-controllers and trackpads were developed. These fabric interfaces are modular and can be snapped to the main keyboard controller. Our design separates the soft-circuit portions (smart fabrics) from rigid-circuits (circuit boards) allowing easily customizable hardware. Supported by MIDI protocol, the fabric keyboard can be connected to any audio synthesis or sequencer software and mapped to essentially any instrument, sound, or effects the way we wish with endless possibilities.

StretchyKeyboard is interesting and unusual, since it combines the discrete controls of a keyboard with continuous controls of the embedded fabric sensors. The soft and deformable nature of this fabric-based musical controller gives a new tactile experience to the performer. One can play discrete notes with the keys while performing different gestures such as pressing, stretching, pulling, and twisting simultaneously to expressively shape the sound generated. Indeed, the performer's ability to fully explore this fabric enhances the relationship between the physical interaction and the music, as the fabric deeply embodies the sound it resonates.

The multi-modal characteristics of the fabric sensate surface also enabled other new novel interactions in keyboard interfaces. The multi- and multiplexed- proximity sensing brings non-contact gesture sensing beyond the surface of the keyboard. We also adapted electric field sensing at each key, allowing the combination of physical and non-contact gestures as the performer plays discrete sounds with one hand and waves his or her other hand towards and against a transmitter for a continuous modulation. Furthermore, the keyboard extensions we developed, the fabric ribbon-controller and trackpad, could give more expressive controls to live performance. We believe there are many more new interactions that could be possible with these fabric interfaces as we further reveal mappings that exploit them.

We hope that this work not only inspires new explorations of deformable musical interfaces and keyboard controllers, but also triggers further developments in multi-modal sensate surface in novel substrates, especially in textiles, bringing us closer to the vision of seamless, self-aware, and washable media.

8.2 Future Work

The completion of this project does not stop it from going forward, but it opens more questions, room for improvements, and new possibilities instead. One octave of keyboard, even though was challenging to implement especially with its dense interconnects, it certainly is not enough for most performances. We could then extend the keyboard to two or three octaves. Making the fabric keyboard wearable will also be interesting as it can be used either as a common scarf, by unplugging the hardware, or as a wearable instrument by changing the current hardware to wireless mode. In some cases, the keyboard does not need to be multi-modal, since the touch and proximity sensing only works reliably when the fabric keyboard is played on a surface. As we discovered that the pressure sensors are also sensitive to soft presses or touch, we could use pressure sensing to detect both touch and pressure instead of capacitance for the wearable version; this will reduce the number of interconnects by approximately half. The hardware, which currently is in the form of a rigid PCB, can also be improved in performance (latency) and further miniaturised. It can be fabricated possibly on flex to minimize the total weight of the system.

It is also important to do further reliability testing especially as the fabric encounters multiple uses. All the materials we used are washable; therefore, some tests could also be done to observe the performance of each sensor after multiple washings.

Integration of haptic feedback could also enhance the tactile experience given by this fabric-based musical controller. Some current possibilities are to use electrostatic force or embedding PZT/PVDF materials, although these actuations entail high voltages and associated caveats. There have not been many efforts in seamlessly integrating actuators on textiles besides heating and display, especially in large surfaces. Combining physical sensing and actuation together in one substrate would therefore be a compelling research.

Another area we would like to explore is in the musical mappings. The multi-modal sensing of this fabric-based musical interface gives us rich interaction potentials, both in physical and non-contact gestures. It is therefore interesting to study the relationship between each modality and sound and how we can design a fluid interaction and musical experience as we transition from one modality to another. To support this work, it is recommended to move from audio sequencer to audio synthesis software such as Max/MSP or Pure Data and to continue our work in adopting OSC with SYN dialect. Besides its compatibility with Max/MSP, OSC will give us freedom to define and control our own interface and give better resolution of sensor data. The realization of this will provide a canvas for sound artists to create sonic experiences based on a fabric-based musical interface.

It will also be interesting to add new sensor modalities as we have developed a fabric fur (stroke sensing) but due to the time-constraint, could not incorporate it to our fabric keyboard and include it in this thesis. Finally, we would like to improve the ergonomics of our keyboard, to make it even stretchier as well as to further learn how to best play it.

8.3 Outlook

Mark Weiser (1991) stated that "The most profound technologies are those that disappear. They weave themselves into the fabric of everyday life until they are indistinguishable from it" [76]. This vision has galvanized the area of ubiquitous computing, where abundant information can now be processed in the background as computer processing power allows it. However, to enable a truly ubiquitous experience, efforts should also be done in miniaturizing devices and integrating them seamlessly to common objects, such as fabrics. This project demonstrates the integration of various sensors in textile-form, resulting in a self-aware fabric that can feel, respond, and be treated the same way as conventional fabrics. Our limitations in developing a completely textile-based surface required us to separate the sensory (soft) and the processing (hard) part. We therefore envision that the next generation of smart textiles will contain dense network of multi-modal sensors and actuators (heterogeneous) and will be produced in a large scale. This enables them to conform to any surface, be manufactured into anything (garments, carpets, socks, gloves, bed-sheets, *et cetera*) and most importantly, to be programmable. The fact that most of current smart textiles only have certain functions, and are developed in small quantities restrains it from being widely-used and developed [77].

To conclude, we are looking forward to the future where electronics can be seamlessly integrated into fibres and fabrics instead of separated from them. Where circuits, sensors, and actuators are in nanoscales, harvesting energy, forming a network, working in ambient, and are invisible to us. After all, the vision of ubiquitous computing will not be entirely accomplished without its backbone, ubiquitous electronics.

8.4 Project Management

The initial Gantt chart of the project can be seen in Appendix B, Figure B.1 whereas the actual implementation timeline of this project is shown in Figure B.2. Based on the project proposal (Appendix C), the project main goals have been successfully completed. We even explored further beyond them. We have customized and characterized various textile-based sensors both electrically and mechanically and used them to develop a multi-sensory fabric keyboard. We then fabricated two PCBs for different modalities and characterised their response to several gestural inputs. After that, we implemented MIDI protocol and send the populated sensor data to an audio sequencer (Ableton Live) to generate and control different sound and effects.

In addition, we also showed some efforts in adopting OSC for further developments of this project (a wireless and wearable instrument) and developing other multi-sensory fabric interfaces such as trackpad and ribbon-controller for simultaneous position, pressure, and proximity sensing. At the end of this project, we exhibited this fabric keyboard and performed an elementary user study, by allowing people to perform with it and experience its sonic behaviour.

References

[1] Orth, M., Post, R. and Cooper, E., 1998, April. Fabric computing interfaces. In *CHI 98 Cconference Summary on Human Factors in Computing Systems* (pp. 331-332). ACM.

[2] Paradiso, J., Abler, C., Hsiao, K.Y. and Reynolds, M., 1997, March. The magic carpet: physical sensing for immersive environments. In *CHI'97 Extended Abstracts on Human Factors in Computing Systems* (pp. 277-278). ACM.

[3] Hayafuchi, K. and Suzuki, K., 2008, June. MusicGlove: A Wearable Musical Controller for Massive Media Library. In *NIME* (pp. 241-244).

[4] Chang, A. and Ishii, H., 2007, June. Zstretch: a stretchy fabric music controller. In Proceedings of the 7th international conference on New interfaces for musical expression (pp. 46-49). ACM.

[5] Roh, J.S., Mann, Y., Freed, A. and Wessel, D., 2011. Robust and Reliable Fabric, Piezoresistive Multitouch Sensing Surfaces for Musical Controllers. In *NIME* (pp. 393-398).

[6] Moog, R.A. and Rhea, T.L., 1990. Evolution of the keyboard interface: The Bösendorfer 290 SE recording piano and the Moog multiply-touch-sensitive keyboards. *Computer Music Journal*, *14*(2), pp.52-60.

[7] Grosshauser, T. and Tröster, G., 2013, May. Finger Position and Pressure Sensing Techniques for String and Keyboard Instruments. In *NIME* (Vol. 13, pp. 27-30).

[8] McPherson, A., 2012. TouchKeys: Capacitive Multi-Touch Sensing on a Physical Keyboard. In *NIME*.

[9] Lamb, R. and Robertson, A., 2011. Seaboard: a New Piano Keyboard-related Interface Combining Discrete and Continuous Control. In *NIME* (pp. 503-506).

[10] Paradiso, J.A. and Borque, L. L., A Fabric Keyboard for Composing on the Road. (Unpublished manuscript)

[11] Japanese Textile Maker Gunze Piano http://www.gettyimages.com/detail/news-photo/japans-textile-maker-gunze-employee-displays-a-textile-news-photo/504953886

[12] Miranda, E.R. and Wanderley, M.M., 2006. *New digital musical instruments: control and interaction beyond the keyboard* (Vol. 21). AR Editions, Inc.

[13] Paradiso, J.A., 1997. Electronic music: new ways to play. *IEEE spectrum*, *34*(12), pp.18-30.

[14]Electronic Sackbut: Hugh Le Caine http://www.hughlecaine.com/en/sackbut.html

[15] Campbell, M., Greated, C.A. and Myers, A., 2004. *Musical instruments: history, technology, and performance of instruments of western music*. Oxford University Press on Demand.

[16] Donald Duncan, Key Concepts, the Notebender http://www.bikexprt.com/music/refine.htm

[17] Haken, L., Tellman, E. and Wolfe, P., 1998. An indiscrete music keyboard. *Computer Music Journal*, *22*(1), pp.30-48.

[18] Snyder, J., 2011. Snyderphonics Manta Controller, a Novel USB Touch-Controller. In *NIME* (pp. 413-416).

[19] Singer, E., 2003, May. Sonic banana: a novel bend-sensor-based MIDI controller. In *Proceedings of the 2003 conference on New interfaces for musical expression* (pp. 220-221). National University of Singapore.

[20] Laetitia Sonami's Lady Glove http://www.sonami.net/lady_glove2.htm

[21] Bongers, B., 2000. Physical interfaces in the electronic arts. *Trends in gestural control of music*, pp.41-70.

[22] Paradiso, J.A. 2004. Electronic Controllers for Musical Performance and Interaction. Draft 1.0. MIT Press.

[23] Cherenack, K. and van Pieterson, L., 2012. Smart textiles: challenges and opportunities. *Journal of Applied Physics*, *112*(9), p.091301.

[24] Sinclair, R. ed., 2014. *Textiles and fashion: materials, design and technology*. Elsevier.

[25] McCann, J. and Bryson, D. eds., 2009. *Smart clothes and wearable technology*. Elsevier.

[26] Stoppa, M. and Chiolerio, A., 2014. Wearable electronics and smart textiles: a critical review. *Sensors*, *14*(7), pp.11957-11992.

[27] Poupyrev, I., Gong, N.W., Fukuhara, S., Karagozler, M.E., Schwesig, C. and Robinson, K., 2016. Project Jacquard: Manufacturing Digital Textiles at Scale. In *Proceedings of the 34th Annual ACM Conference on Human Factors in Computing Systems*.

[28] Adrian Freed, Grid Proximity Sensinghttp://adrianfreed.com/content/zoned-proximity-sensing-double-woven-fabric-and-interleaved-conductive-grid

[29] Adafruit Plush Game Controller https://learn.adafruit.com/plush-game-controller/overview

[30] Meyer, J., Lukowicz, P. and Tröster, G., 2006, October. Textile pressure sensor for muscle activity and motion detection. In *2006 10th IEEE International Symposium on Wearable Computers* (pp. 69-72). IEEE.

[31] Enokibori, Y., Suzuki, A., Mizuno, H., Shimakami, Y. and Mase, K., 2013, September. E-textile pressure sensor based on conductive fibre and its structure. In *Proceedings of the 2013 ACM conference on Pervasive and ubiquitous computing adjunct publication* (pp. 207-210). ACM.

[32] Bhattacharjee, T., Jain, A., Vaish, S., Killpack, M.D. and Kemp, C.C., 2013, April. Tactile sensing over articulated joints with stretchable sensors. In *World Haptics Conference (WHC), 2013* (pp. 103-108). IEEE.

[33] De Rossi, D., Carpi, F., Lorussi, F., Mazzoldi, A., Scilingo, E.P. and Tognetti, A., 2002. 5.1: Electroactive Fabrics for Distributed, Conformable and Interactive Systems.

[34] StretchSense, Capacitive Stretch Sensorhttps://stretchsense.com/sensors/stretch/

[35] Wilson, H.P. How to Get What You Want, DIY Smart Textileshttp://www.kobakant.at/

[36] Gioberto, G. and Dunne, L.E., 2013. Overlock-stitched stretch sensors: characterization and effect of fabric property. *Journal of Textile and Apparel, Technology and Management*, *8*(3).

[37] Locher, I., Kirstein, T. and Tröster, G., 2005, September. Temperature profile estimation with smart textiles. In *Proceedings of the International Conference on Intelligent textiles, Smart clothing, Well-being, and Design, Tampere, Finland* (pp. 19-20).

[38] Husain, M.D., Atalay, O. and Kennon, R., 2013. Effect of strain and humidity on the performance of temperature sensing fabric. *International Journal of Textile Science*, *2*(4), pp.105-112.

[39] Pereira, T., Silva, P., Carvalho, H. and Carvalho, M., 2011, April. Textile moisture sensor matrix for monitoring of disabled and bed-rest patients. In *EUROCON-International Conference on Computer as a Tool (EUROCON), 2011 IEEE* (pp. 1-4). IEEE.

[40] Nocke, A., Schröter, A., Cherif, C. and Gerlach, G., 2012. Miniaturized textile-based multi-layer ph-sensor for wound monitoring applications. *Autex Research Journal*, *12*(1), pp.20-22.

[41] Seesaard, T., Lorwongtragool, P. and Kerdcharoen, T., 2015. Development of fabric-based chemical gas sensors for use as wearable electronic noses. *Sensors*, *15*(1), pp.1885-1902.

[42] Kinkeldei, T., Zysset, C., Münzenrieder, N. and Tröster, G., 2012. An electronic nose on flexible substrates integrated into a smart textile. *Sensors and Actuators B: Chemical*, *174*, pp.81-86.

[43] Post, E. Rehmi, *et al.* "E-broidery: Design and fabrication of textile-based computing." *IBM Systems journal* 39.3.4 (2000): 840-860.

[44] Linz, T., Kallmayer, C., Aschenbrenner, R. and Reichl, H., 2006, April. Fully untegrated EKG shirt based on embroidered electrical interconnections with conductive yarn and miniaturized flexible electronics. In *International Workshop on Wearable and Implantable Body Sensor Networks (BSN'06)* (pp. 4-pp). IEEE.

[45] Locher, I., Kirstein, T. and Tröster, G., 2004, November. Routing methods adapted to e-textiles. In *Proceedings of 37th international symposium on microelectronics (IMAPS), Long Beach*.

[46] Buechley, L. and Eisenberg, M., 2009. Fabric PCBs, electronic sequins, and socket buttons: techniques for e-textile craft. *Personal and Ubiquitous Computing*, *13*(2), pp.133-150.

[47] Lee, S., Kim, B., Roh, T., Hong, S. and Yoo, H.J., 2010, October. Arm-band type textile-MP3 player with multi-layer Planar Fashionable Circuit Board (P-FCB) techniques. In *International Symposium on Wearable Computers (ISWC) 2010* (pp. 1-7). IEEE.

[48] Cherenack, K., Zysset, C., Kinkeldei, T., Münzenrieder, N. and Tröster, G., 2010. Woven electronic fibres with sensing and display functions for smart textiles. *Advanced materials*, *22*(45), pp.5178-5182.

[49] Hamedi, M., Forchheimer, R. and Inganäs, O., 2007. Towards woven logic from organic electronic fibres. *Nature materials*, *6*(5), pp.357-362.

[50] Mattmann, C., Clemens, F. and Tröster, G., 2008. Sensor for measuring strain in textile. *Sensors*, *8*(6), pp.3719-3732.

[51] Kan, V., Fujii, K., Amores, J., Zhu Jin, C.L., Maes, P. and Ishii, H., 2015, January. Social textiles: Social affordances and icebreaking interactions through wearable social messaging. In *Proceedings of the Ninth International Conference on Tangible, Embedded, and Embodied Interaction* (pp. 619-624). ACM.

[52] Orth, M. http://www.maggieorth.com/art_100EAYears.html

[53] Paradiso, J.A., Lifton, J. and Broxton, M., 2004. Sensate media—multimodal electronic skins as dense sensor networks. *BT Technology Journal*, *22*(4), pp.32-44.

[54] Kim, D.H., Lu, N., Ma, R., Kim, Y.S., Kim, R.H., Wang, S., Wu, J., Won, S.M., Tao, H., Islam, A. and Yu, K.J., 2011. Epidermal electronics. *science*, *333*(6044), pp.838-843.

[55] Son, D., Lee, J., Qiao, S., Ghaffari, R., Kim, J., Lee, J.E., Song, C., Kim, S.J., Lee, D.J., Jun, S.W. and Yang, S., 2014. Multifunctional wearable devices for diagnosis and therapy of movement disorders. *Nature Nanotechnology*, *9*(5), pp.397-404.

[56] Gong, N.W., Steimle, J., Olberding, S., Hodges, S., Gillian, N.E., Kawahara, Y. and Paradiso, J.A., 2014, April. PrintSense: a versatile sensing technique to support multimodal flexible surface interaction. In *Proceedings of the 32nd annual ACM conference on Human factors in computing systems* (pp. 1407-1410). ACM.

[57] Verplank, W., 2009. Interaction Design Sketchbook by Frameworks for designing interactive products and systems. *Last accessed*, *18*(2), p.2014.

[58] McPherson, A., 2015. Buttons, handles, and keys: advances in continuous-control keyboard instruments. *Computer Music Journal*.

[59] Paradiso, J.A., 2003, May. Dual-use technologies for electronic music controllers: a personal perspective. In *Proceedings of the 2003 conference on New interfaces for musical expression* (pp. 228-234). National University of Singapore.

[60] **Sculpted Computational Objects, with Smart and Active Computing Materials** Orth, M. Thesis for the Degree of Doctor of Philosophy, at the Massachusetts Institute of Technology, Cambridge, MA, (May, 2001).

[61] Hocheng, H. and Chen, C.M., 2014. Design, fabrication and failure analysis of stretchable electrical routings. *Sensors*, *14*(7), pp.11855-11877.

[62] Bekinox, Bekaert Thread https://www.sparkfun.com/datasheets/E-Textiles/thread1.pdf

[63] Dupont, Stretchable Electronic Materials http://www.dupont.com/content/dam/dupont/products-and-services/electronic-and-electrical-materials/documents/prodlib/DuPont-Electronic-Inks-for-the-Wearable-World.pdf

[64] Li, Y., Cheng, X.Y., Leung, M.Y., Tsang, J., Tao, X.M. and Yuen, M.C.W., 2005. A flexible strain sensor from polypyrrole-coated fabrics. *Synthetic Metals*, *155*(1), pp.89-94.

[65] Zimmerman, T.G., Smith, J.R., Paradiso, J.A., Allport, D. and Gershenfeld, N., 1995, May. Applying electric field sensing to human-computer interfaces. In *Proceedings of the SIGCHI conference on Human factors in computing systems* (pp. 280-287). ACM Press/Addison-Wesley Publishing Co..

[66] Kinoshita, H., Furuya, S., Aoki, T. and Altenmüller, E., 2007. Loudness control in pianists as exemplified in keystroke force measurements on different touches. *The Journal of the Acoustical Society of America*, *121*(5), pp.2959-2969.

[67] Capineri, L., 2015. Piezoresistive Sensors Fabricated with Conductive Textiles for Monitoring the Step Rate with Read-Out Electronics and Wireless Connection to a Smart Watch. J Fashion Technol Textile Eng 3: 3. *of*, *6*, p.2.

[68] Wang, J., Xue, P., Tao, X. and Yu, T. (2014), Strain Sensing Behavior and Its Mechanisms of Electrically Conductive PPy-Coated Fabric. Adv. Eng. Mater., 16: 565–570. doi:10.1002/adem.201300407

[69] Bhalla, M.R. and Bhalla, A.V., 2010. Comparative study of various touchscreen technologies. *International Journal of Computer Applications*, *6*(8), pp.12-18.

[70] Resistive Touch Screen Technology http://www.atmel.com/Images/doc8091.pdf

[71] MPR121 Touch Proximity Controllerhttp://www.nxp.com/pages/proximity-capacitive-touch-sensor-controller:MPR121

[72] SAMD21 Data Sheet. *atmel.force.com/support/servlet/fileField?id=0BEG0000000HT19*

[73] Musical Instrument Digital Interface https://learn.sparkfun.com/tutorials/midi-tutorial/all

[74] Smith, R.T., Thomas, B.H. and Piekarski, W., 2008, October. Digital foam interaction techniques for 3D modeling. In *Proceedings of the 2008 ACM symposium on Virtual reality software and technology* (pp. 61-68). ACM.

[75] Lago, N.P. and Kon, F., 2004, November. The quest for low latency. In *Proceedings of the International Computer Music Conference* (pp. 33-36).

[76] Weiser, M., 1991. The computer for the 21st century. *Scientific american*, *265*(3), pp.94-104.

[77] Tröster, G., 2011. Smart Clothes—The Unfulfilled Pledge?. *IEEE Pervasive Computing*, *10*(2), pp.87-89.

[78] Troiano, G.M., Pedersen, E.W. and Hornbæk, K., 2015, April. Deformable interfaces for performing music. In *Proceedings of the 33rd Annual ACM Conference on Human Factors in Computing Systems* (pp. 377-386). ACM.

[79] Open Sound Control. http://opensoundcontrol.org/

[80] SYN.A Standardized Dialect for OSC https://github.com/fabb/SynOSCopy/wiki

[81] Paradiso, J.A. American Innovations in Electronic Musical Instrument http://www.newmusicbox.org/articles/american-innovations-in-electronic-musical-instruments/

[82] Baxter, L.K., 2000. Capacitive sensors. *Ann Arbor*, *1001*, p.48109.

[83] Paradiso, J.A. and Gershenfeld, N., 1997. Musical applications of electric field sensing. *Computer music journal*, *21*(22), pp.69-89.

Appendix A: PCB Design

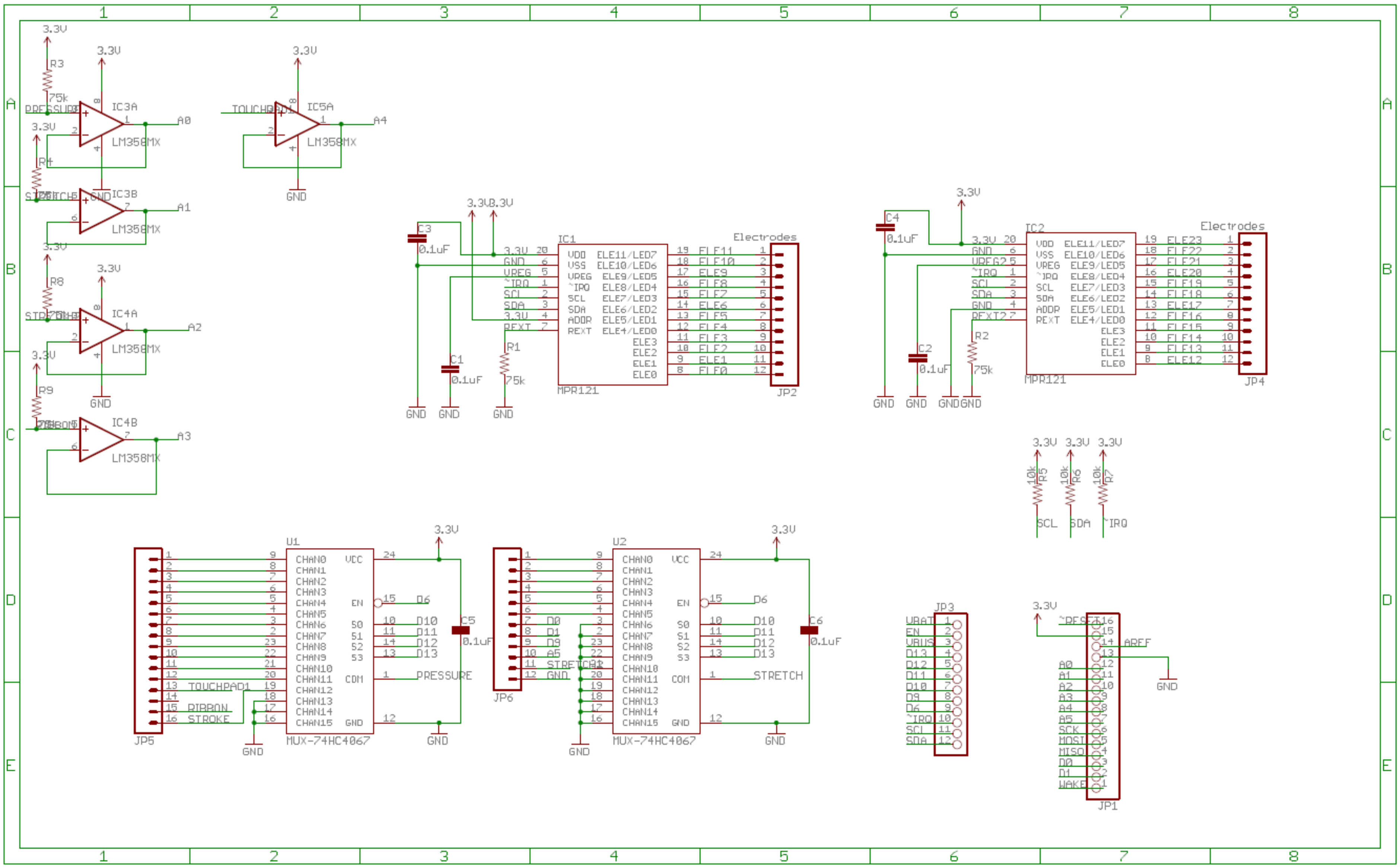

Figure A.1: Circuit Schematic of *"StretchyKeys"*

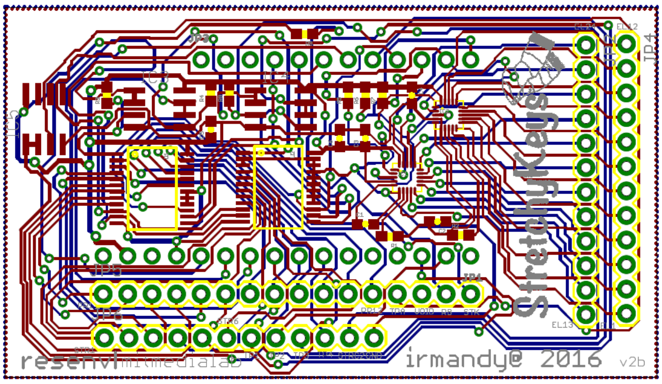

Figure A.2: PCB Layout of "*StretchyKeys*"

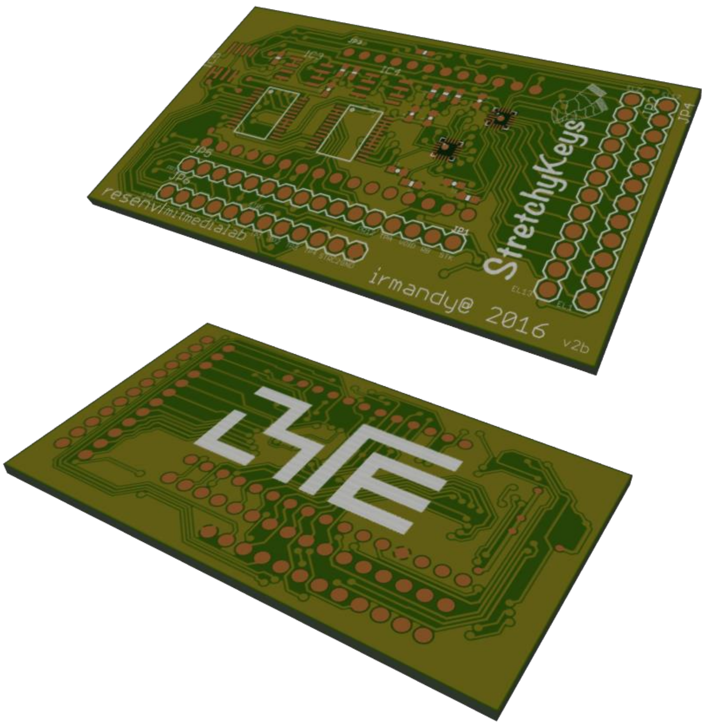

Figure A.3: 3D Visualizations of "*StretchyKeys*"

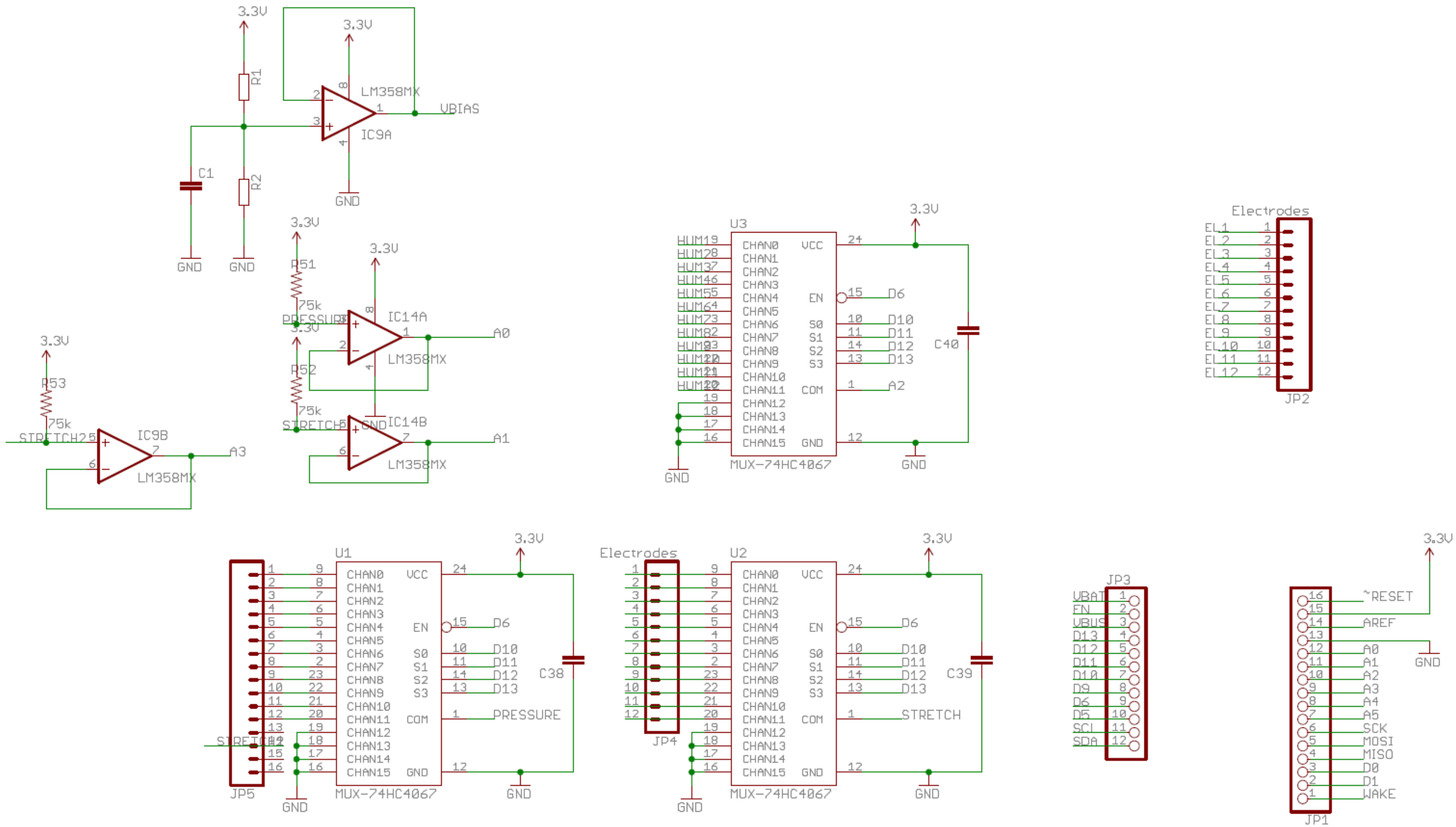

Figure A.4: Circuit Schematic of *"ThereminKeys"* part 1

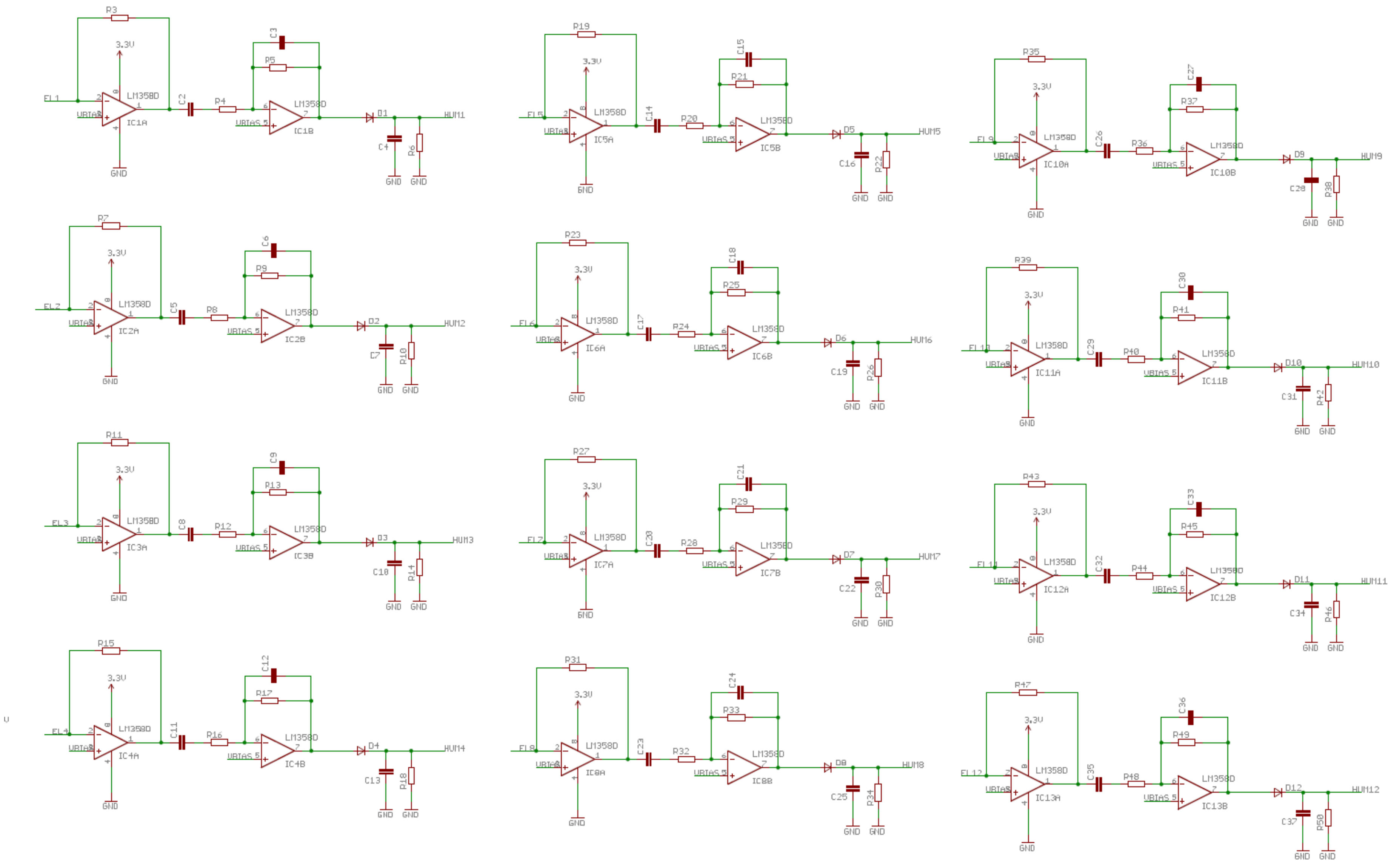

Figure A.5: Circuit Schematic of *"ThereminKeys"* part 2

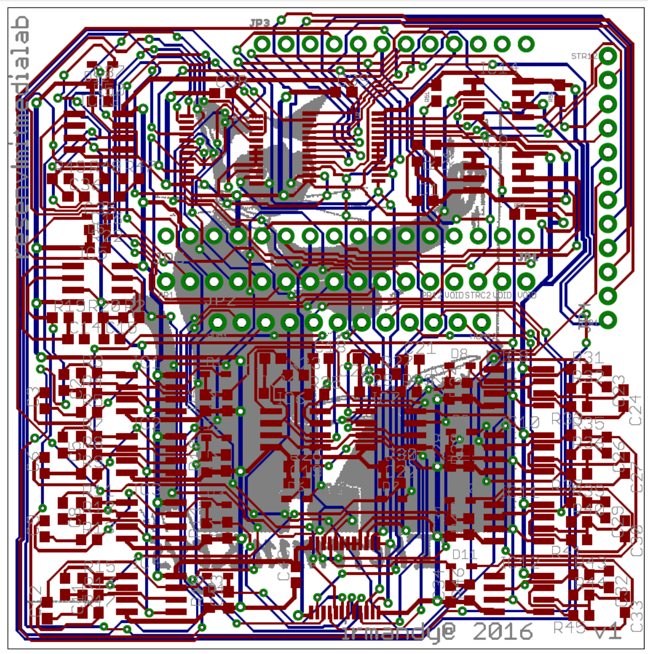

Figure A.6: PCB Layout of “*ThereminKeys*”

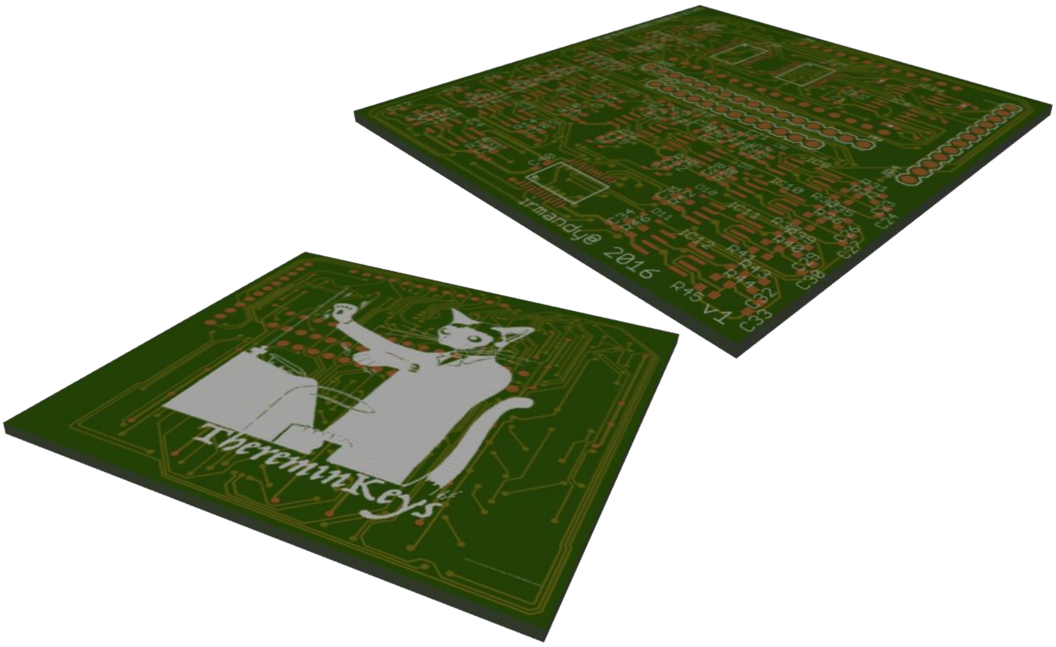

Figure A.7: 3D Visualisations of “*ThereminKeys*”

Appendix B: Project Management

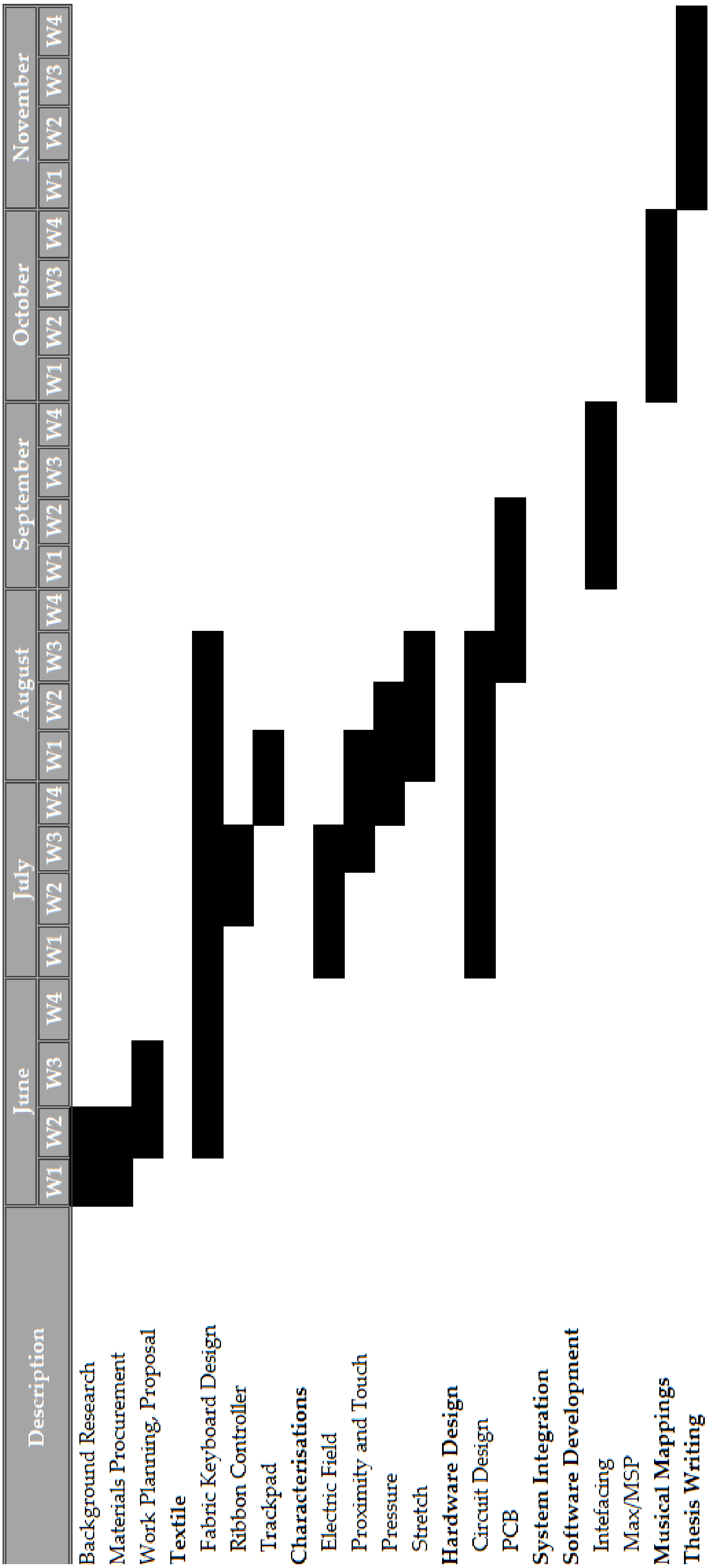

Figure B.1: Gantt chart of initial plan of the project

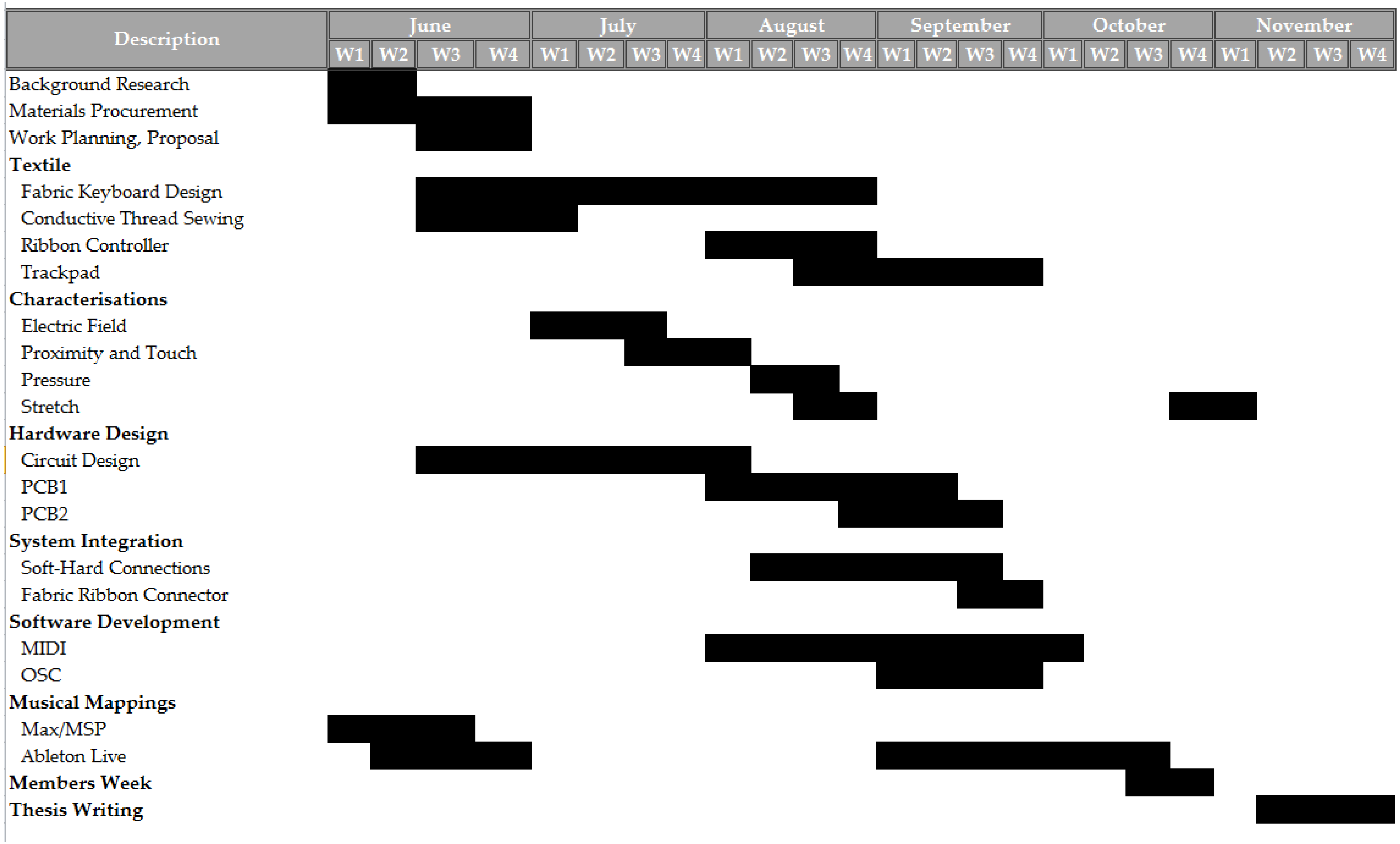

Figure B.2: Gantt chart of actual project progress

ETH

Eidgenössische Technische Hochschule Zürich
Swiss Federal Institute of Technology Zurich

Declaration of originality

The signed declaration of originality is a component of every semester paper, Bachelor's thesis, Master's thesis and any other degree paper undertaken during the course of studies, including the respective electronic versions.

Lecturers may also require a declaration of originality for other written papers compiled for their courses.

I hereby confirm that I am the sole author of the written work here enclosed and that I have compiled it in my own words. Parts excepted are corrections of form and content by the supervisor.

Title of work (in block letters):

DESIGN AND IMPLEMENTATION OF MULTI-SENSORY FABRIC AS DEFORMABLE MUSICAL INTERFACE

Authored by (in block letters):
For papers written by groups the names of all authors are required.

Name(s):	First name(s):
WICAKSONO	IRMANDY

With my signature I confirm that
- I have committed none of the forms of plagiarism described in the 'Citation etiquette' information sheet.
- I have documented all methods, data and processes truthfully.
- I have not manipulated any data.
- I have mentioned all persons who were significant facilitators of the work.

I am aware that the work may be screened electronically for plagiarism.

Place, date

CAMBRIDGE, 26/11/2016

Signature(s)

signature redacted

For papers written by groups the names of all authors are required. Their signatures collectively guarantee the entire content of the written paper.